Thesis for the Master's degree in chemistry

Wycliffe Omondi Ojwando

Monitoring of phosphorous fractions – Understanding the hydrogeochemical processes governing mobilization and transfer of phosphorous in an agricultural watershed in north-eastern China

60 study points

DEPARTMENT OF CHEMISTRY

Faculty of mathematics and natural sciences

UNIVERSITY OF OSLO 05/2014

Dedication

To my late Dad, who passed on a month into this study

Acknowledgements

This master thesis has been carried out at the Department of Chemistry, University of Oslo, Norway between August 2012 and May 2014. This study is part of SinoTropia project, a joint collabaration between China and Norway. I would like to thank the following people for their help, support, guidance and positive critism during this study.

First, acknowledgement thanks goes to the Lord GOD Almighty for the gift of life and grace. Secondly, I would like to thank my supervisor and mentor, Profesor Rolf D. Vogt for giving me the opportunity to be involved in this study. In addition, I want to thank him for being there for me, for his support and guidance during the entire study. I would also want to thank Research Coumncil of Norway (RCN) for funding of this project.

Special regards and appreciation to my co-supervisors Professor Grethe Wibetoe and PhD candidate, Christian Wilhem Mohr for guidance and sharing your knowledge and experince which were handy in making this study a success. My gratitude also goes to PhD candidate Zhou Bin for his knowledge and help during the DGT sampling and the trip to China and also for acting as a link between project staff in China and Norway.

I would also want to thank Anne-Marie Skramstad for her help and patience during the microwave digestion, David Wragg for his technical expertise in the use of XRD machine, Agaje Bedomo Beyene for assisting me with the ICP-MS analysis. I wish also to thank my departmental collegues and classmates for ideas shared and for making my stay in Norway comfortable and enjoyable.

Finaly, I would like to express my deep gratitude to my lovely wife, my Mum and my siblings for their support and love. I would have not made it it it were not for your moral support and prayers.

Abstract

Eutrophication is known to be one of the most common impairment of surface water. It is a worldwide problem with lakes throughout the world undergoing the process of eutrophication. Phosphorous is believed to be the main limiting nutrient in aquatic environment causing eutrophication. Eutrophication remains one of the most critical problems of lakes and reservoirs in China today hence necessary and effective abatement action must be put in place. This cannot be achieved with the understanding of hydro-geochemical processes governing mobility and transport of phosphorous fractions in the environment.

Investigation of Yuqiao reservoir, a eutrophic reservoir in an agricultural catchment in north – eastern China reveal several hydro-geochemical process governing phosphorous mobility and transport. Monitory of the phosphorous fraction in the watershed was done through investigation of stream water chemistry and Diffusion Gradient in Thin films (DGT) with emphasis on the most bioavailable fractions.

The result reveal that the pH of the rivers is between 7-7.5 hence Ca is expected to precipitate P. Ca is also the dominant cation in the river water and parent rock material. The cationic composition of the rivers is fairly constant though there is high discrepancy in ionic charge of anions. TP in the river water is between 60-350µg P/L with particulate matter being relating to the particulate P. DIP is the major fraction in the river with expectation of Mixed 1catchement. TDP measured by DGT is low (2-250µg P/L). DGT-DIP and water DIP is quite close and comparable, while DGT-DOP and water-DOP shows lots of variation which is mainly due to uncertainties in DGT calculations.

Al and Ca dominate the cationic composition of the suspended particulate matter. The mineralogy of the particulate matter is fairly the same under different flow regimes and land use. It is mainly composed of 1:1 clay which is likely to play a major role in P mobilization and transport through increases surface area and sorption of Al and Fe oxides and hydroxides.

List of abbreviations

BAP – Bioavailable Phosphorous

CSA's – Critical Source Area's

DBL – Diffusion Boundary Layer

DGT – Diffusion Gradient in Thin films

DOM – Dissolve Organic Matter

DOP – Dissolved Organic Phosphorous

DPS – Degree of Phosphorous Saturation

EPA – Tianjin Enviromental Protection Bureau

FAO – Food and Agriculture Organization of the United Nations

LMWOP – Low Molecular Weight Organic Phosphorous

LOI – Loss of Ignition

MBM – Molybdate Blue Method

OECD – Organization of Economic Co-operation and Development

Orthophosphates – The sum of H_3PO_4, $H_2PO_4^-$, HPO_4^{2-}, PO_4^{3-}

P – Phosphorous

PIP – Particulate Inorganic Phosphate

POP – Particulate Organic Phosphorous

PSC – Phosphorous Sorption Capacity

PSI – Phosphorous Sorption Index

RCN – Research Council of Norway

RCEES – Research Centre for Eco-Environmental Sciences Chinese Academy of Sciences

List of figures

List of tables

Table of Contents

1.0 INTRODUCTION

Like air, water is one of the essentials that support all forms of plant and animal life. It is used for drinking, irrigation, industry, transportation, recreation, fishing and support of diversity (Carpenter et al. 1998). It also plays a fundamental role in climate regulation cycle. However of all the global water only 3 % is available as fresh water and out of which only 0.4% is accessible as surface water (vanLoon and Duffy 2011). This limited accessible surface water is under constant pollution and overharvesting pressure from anthropogenic activities. These pressures come as a result of increased population, urbanization and increased individual consumption. Therefore, there is need to protect this essential yet limited resource. In view of this, Millennium development goals and EU Water Framework directives were adopted by member states to ensure accessibility and good water quality in sufficient quantities for all legitimate uses. Millennium Development Goal 7 targets to halve by 2015 the proportion of people without sustainable access to safe drinking water and basic sanitation (WHO 2011) while Water Framework Directive (WFD) is a European Union directive which commits members states to achieve qualitative and quantitative status of all water bodies by 2015 (EU 2013). Despite these directives, water scarcity and lack of quality drinking water are still common in many countries.

Lack of water to meet daily needs is a reality today for one in three people around the world. This translates to about 1.2 billion of world's population with no access to clean drinking water (www.WHO.org). Water pollution is one of the main reasons faulted as the cause of this problem. Water pollution has increased in the recent decades resulting into degradation of surface waters such as rivers and lakes as well as ground water (Carpenter et al. 1998). Water pollution leads to water scarcity and increased cost of water purification. Therefore, preventing pollution is paramount to cost effective means of increasing water supplies (Carpenter et al. 1998).

Out of the several causes of water pollution, eutrophication caused by excess nutrient loads (Phosphorous and Nitrogen) is known to be one of the most common impairment of surface water. Eutrophication is a worldwide problem with lakes throughout the world undergoing the process of eutrophication. Phosphorous is believed to be the main limiting nutrient in aquatic environment causing eutrophication (Maher 1998).

Phosphorous fluxes into surface waters can be both from point and non-point sources. Point sources are mainly sewage and industrial effluent while non-point sources are generally as a result of runoffs from agricultural fields and urban canters. Over the last decades, the contribution of nutrients to surface waters from point sources has been reduced in many developed countries mainly because these sources are well known and relatively easy to control (Sharpley et al. 2001, Schoumans and Chardon 2003). However this is not the case in many developing countries and emerging economies like China, due to inadequate infrastructure and lack of strict enforcement of environmental laws.

Even though great strides has been made in western countries in control of phosphorous point sources, such as sewage and effluent treatment, phosphorous fluxes has continued to increased due to enhanced contribution from non-point source (Delgado and Scalenghe 2008). In the past the attention directed in controlling these non-point sources of phosphorous has been low, mainly due to the difficulty in their source identification and control (Sharpley et al. 2001). Due to the magnitude of the problem, non-point phosphorous flux especially from agricultural lands has therefore attracted increased attention in the last decade (Haygarth et al. 2005).

Agriculture is regarded as an important pressure on phosphorous flux to surface through the application of inorganic fertilizers and/or manure to the fields (Haygarth et al. 2005). The exponential increase in human population and even greater increase in consumption has been vitally supported by commensurate increase in the agricultural production of foodstuffs. This has involved both rapid expansion in the global land under food production and also a great increase in the intensity of area-specific yields. Neither could have been achieved without the widespread application of inorganic fertilizers to offset the natural deficiencies in the bioavailable phosphorus in most soils (Reynolds and Davies 2001).

Application of fertilizers in excess of crop needs creates surpluses of phosphorous that accumulation as phosphorous pools in the soil. This phosphorous may be mobilized through overland flow, erosion and leaching and thereby cause increased flux of phosphorous fractions from land to water (Sharpley et al. 2001).

In the environment, phosphorous is present in both inorganic and organic forms and partitions among dissolved, colloidal and particulate phases (Reynolds and Davies 2001). The main transport mechanism of phosphorous to surface waters is as particle bound, mainly as a result

of soil erosion. From land with perennial vegetation, limiting the erosion, the main loss of phosphorous is usually as organically bound to dissolve natural organic matter. Bioavailable phosphate is mainly free aqueous ortho-phosphate as well as some small organic phosphate compounds. These bioavailable phosphorous compounds are relatively immobile in most natural soils since they are rapidly assimilated or sorb to the soil. Elevated fluxes of bioavailable phosphorous is therefore only found downstream of diffuse and point phosphorous sources. However, the mobility and transport of phosphorous from soil to surface waters, and the dynamic transformation of phosphorous between dissolved, colloidal, and particulate fractions in the water remains poorly understood (Lin et al. 2012). Furthermore, it is not adequately clear to what extent the different phosphorous fractions are biologically available or become bioavailable through transformations. The answers to the above are vital in the design of strategies to control and manage eutrophication successfully (Reynolds and Davies 2001).

Data on phosphorus concentration and fluxes of phosphorous fractions is a prerequisite for any impact assessment as their bioavailability (Van Moorleghem et al. 2011). Thus their environmental impact is critically dependent on their physicochemical form (Worsfold et al. 2005). Knowledge regarding the impact of bioavailable phosphorous is important in understanding the effects of eutrophication. The potential impact of nutrient inputs to surface waters can therefore not be assessed without obtaining detailed information about the flux of the nutrient fractions and the biogeochemical reactivity of nutrients bound to different chemical compounds constituting these fractions (Pacini and Gachter 1999).

To effectively manage eutrophication, we therefore need to understand the chemistry governing mobilization, transport, fate and impact of phosphorous fractions in the environment. We also need to understand the phosphorous cycling, speciation and bioavailability to primary biomass producers and thus, of its precise role in promoting eutrophication (Reynolds and Davies 2001).

1.1 Cultural Eutrophication

Eutrophication is an accelerated growth of algae caused by the enrichment of water by nutrients, especially nitrogen and phosphorus, thereby inducing an undesirable disturbance to the balance of organisms present in the water and to the quality of the water concerned (WHO and EC 2002). Eutrophication causes algae blooms and increased growth of aquatic weeds. It also causes aquatic oxygen shortage, as a result of decomposition of dead plants, and thereby loss of habitat and aquatic biodiversity (Carpenter et al. 1998).

Agriculture is regarded as an important non-point source of phosphorous in the environment. Phosphorous is introduced into agricultural soils through application of inorganic fertilizers and animal manure (Sharpley et al. 2001). Inorganic fertilizers and animal manure are applied to the agricultural fields in order to sustain productivity, but this addition is inefficiently replenishment, as only 5-10% of phosphorous which is added to soil is taken up by crops (Haygarth and Jarvis 1999). Over time therefore, an accumulation of phosphorous in these agricultural soils occurs. For example, Withers et al. (2001), found out that the annual phosphorous surplus in UK over the last 65 years amounted to an average cumulative phosphorous loading of 1000 kg P ha^{-1} over the productive grassland and arable area. This amounted to a 50% increase in average native soil total and exchangeable P levels (Withers et al. 2001).

Intense use of inorganic fertilizers in agricultural land has resulted in significantly accelerated phosphorous loss to water. Recent catchment studies have demonstrated that areas of established intensive agriculture have increased loss of both dissolved and particulate phosphorous fractions (Reynolds and Davies 2001). Total phosphorous loss in dissolved and partculate forms to surface water are in the order of 1kg ha^{-1} $year^{-1}$ whereas fertilizers and manure input is typically between 20 and 50 kg P ha^{-1} $year^{-1}$. Though this loss is trivial in agronomic terms, the concern is the increased flux of bioavailable phosphorous to surface waters (Haygarth and Jarvis 1999, Haygarth et al. 2005).

The global demand for phosphorous fertilizers is increasing with 90% of global consumption for phosphorus being for food production. The demand for phosphorus is predicted to increase by 50–100% by 2050 as a result of population increase and increased meat consumption (Cordell et al. 2009). FAO, estimated the world demand for total fertilizers nutrients growth to

be 2.6% per annum between 2010 and 2014 while demand for phosphate fertilizers to be 2.9% during the same period (FAO 2010).

1.2 Classification of Eutrophication states

According to old eutrophication classification methods, eutrophication state classification was based on parameters such as Total-P concentration, Chlorophyll a and water transparency. This was however misleading as lakes nutrient values vary across the globe. For example Organization of Economic Co-operation and Development (OECD) regarded a lake with a total-P concentration between 35-100μg/L to be eutrophic. However this concentration does not necessary mean that the system is experiencing algae bloom.

Due to the above limitations, Water Framework Directive (WFD) was adopted by member states as a guideline in maintaining good ecological status of surface water. The guidelines only allow for minor disturbances as long these disturbances results into no or only very minor ecological effects. WFD classify eutrophication states based on biological, hydro-morphological and physico-chemical quality of elements of the surface water. Classification is based on ecological ratios which are derived from biological quality values. Using this criterion, eutrophication status is categorized into high, good, moderate, poor and bad status with high and low status represented by quality ratios of 1 and 0 respectively. High status refers to no or very minor deviation from the undisturbed conditions while low status refers to large deviations from undisturbed conditions (EC 2003).

In China, surface water quality of a lake is classified according to the concentration of Total-N, Total-P, Chlorophyll a and transparency among others parameters. The lakes are divided into five main classes as shown in the Table 1 below (Yang et al. 2008).

Table 1: Criteria of surface water quality for lakes and reservoirs in China (Yang et al. 2008)

Item	Surface water quality classification				
	Class I	**Class II**	**Class III**	**Class IV**	**Class V**
Total-N (mg/L)	≤0.2	≤0.5	≤1.0	≤1.5	≤2.0
Total-P (mg/L)	≤0.01	≤0.025	≤0.05	≤0.1	≤0.2
Chlorophyll a (mg/L)	≤0.001	≤0.004	≤0.01	≤0.03	≤0.065
Transparency (m)	≥15	≥4	≥2.5	≥1.5	≥0.5

1.3 Current state of Eutrophication in China

China is extremely short of natural resources, given its enormous population. It ranks sixth in the world in terms of total water resources, but is almost the lowest in terms of per capita water resource availability. China has lost 23.0% of its freshwater swamps, 16.1% of lakes, 15.3% of rivers, and 51.2% of coastal wetlands over the past 60 years (Gao and Zhang 2010).Therefore, chronic water stress in China is a widely recognized crisis in Northern China (Gao and Zhang 2010). Increased water extraction for agriculture and climate change have been suggested as the main reasons for this drastic reduction in lake surface area in the region.

Moreover, the surface water quality has deteriorated significantly in China during the nation's rapid economic growth over the past 30 years (Qu and Fan 2010). Within only two decades, China has evolved into one of the largest economies, with an annual GDP growth rate of nearly 10% (Pernet et al. 2012). This high growth rate in addition to the population increase, urbanization, rising living standards, local agriculture, and industrial development have all contributed to increased water consumption. As a consequence, water pollution and water shortage have now become major environmental problems in Northern China (Chen et al. 2003), with both surface and groundwater supplies suffering serious levels of impairment. Because of pollution, the quality of many drinking water sources has been significantly degraded thereby reducing the availability of potable fresh water (Qu and Fan 2010). These problems have become an obstacle to sustainable development, which depends heavily on water resources (Liu and Qiu 2007).

Eutrophication remains one of the most critical problems of lakes and reservoirs in China today. The common stressors include heavy point and non-point pollution from sewage flows, industrial wastes, and agricultural fertilizers which results into high concentrations of nitrogen and phosphorous substances in these water bodies (Qu and Fan 2010). Eutrophication has become one of the most important factors in the derailing of Chinese economic growth while at the same time pushing China away from its desired sustainable development goals (Liu and Qiu 2007).

According to the study by Chai et al. (2006), eutrophic and hypertrophic lakes account for 57.5% of lakes in China. However, (Le et al. 2010) pointed out that 80 % of the 67 investigated lakes around the country have been polluted to a level of being unhealthy for

human contact with only the remaining 20% having relatively good quality. Furthermore, the study indicates that the percentage of eutrophic lakes rapidly increased to 84.5% in 2001–2005 (Le et al. 2010).

1.4 Factors driving Eutrophication in China

China is strongly committed to restoring its environmental quality since the advent of the new millennium, and eutrophication control is among the top priorities of governments (Gao and Zhang 2010). In spite of the ascending efforts in eutrophication control upward trends of algal blooms have been observed in Chinese freshwaters for the past two decades. This is partly due to the huge knowledge gaps that still exist in the understanding of the sources and pathways of nutrient losses to aquatic ecosystems (Orderud and Vogt 2013). Many environmental problems in China are unique due to its huge population and their environmental values and attitudes, as well as the indigenous social and political setting, set by their exceptional history. Furthermore, China's fast economic development and rapid urbanization is changing the lifestyle of the Chinese into increased food consumption, especially of meat. More intensive horticulture and increased husbandry spur the loss of nutrients from agriculture. Finally, the environmental setting, with climate change on top of the impact of monsoon climate, coupled with soils that have poor water drainage due to high content of non-swelling clays, is causing an increased non-point source nutrient loss to surface waters (Gao and Zhang 2010).

Fuelled by rapid economic growth, urbanization has greatly accelerated in the last three years in China. However, water infrastructure and treatment has lagged behind, as most cities are underserved by sewer network and wastewater treatment plants (Gao and Zhang 2010). In 2001 only 30% of the sewage was treated in sewage plants. This increased to 45% in 2005, and optimistic estimates are that the treatment will reach 60% by 2030. Still, huge amounts of untreated sewage will then be discharged into surface water resources. If control measures remain at their current pace, all urban lakes in China may reach Class IV or V (Table 1) status by 2030 (Liu and Qiu 2007). In rural China human excreta are typically collected in household tanks where fermentation takes place, increasing the relative percentage and availability of phosphorous. This sewage is subsequently distributed onto farmlands along with manure and inorganic fertilizers. This practice, though very efficient way for nutrient

recycling may lead nutrient discharge from these farmlands (Gao and Zhang 2010). Recently, with the introduction of water closets, the sewage waste is instead increasingly dumped onto wasteland or directly into drainage channels.

Historically, Chinese farmers successfully managed to maintain a modest soil fertility and agricultural productivity by efficient recycling of nutrients within agro-ecosystems. Nutrient inputs originated almost entirely from organic sources (Gao and Zhang 2010). However, since the agriculture reforms of the 1980s, horticulture intensified in order to feed the increasing population using less available land due to rapid urbanization. The agricultural intensified through intense use of high-yield crop varieties combined with increased tillage and irrigation, as well as high application of industrially produced fertilizers and manure (Zhang and Shan 2008). China has experienced rapid increases in chemical fertilizer use, from 12.69 million tons in 1980 to 41.46 million tons in 2000, accounting for about 30% of global fertilizer consumption at present (Gao and Zhang 2010). With increased fertilizer application causing nutrient accumulation in cultivated soils, contribution of nutrients from non-point agricultural sources is predicted to increase. Rapid development of livestock husbandry and aquaculture is another reason for increased nutrient discharge into aquatic ecosystems. The increasing food demand and changing diet preferences not only increase the production of livestock and poultry products but also lead to an increased production of manure. Excessive application of animal manure on agricultural fields cause increased nutrient flux through drainage. Moreover, deliberate spills of livestock wastes, because of poor on-farm management practices and lack of appropriate reception centers, results in increased nutrient discharge.

China is the world's largest producer of aquaculture grown food, with a steep increase in freshwater aquaculture taking place over the last 20 years. Fish farmers increase their production through application of organic and inorganic fertilizers directly into the ponds to stimulate plankton growth. Discharge of effluent from these fish farms may thus cause eutrophication of the water surrounding rearing ponds or the rivers receiving aquaculture effluent (Gao and Zhang 2010).

A large part of China's territory is characterized by a monsoon climate with 60% of total annual precipitation occurring between April–August. The region might also experience either prolonged periods of low rainfall, causing droughts, or periods of extreme precipitation

generating floods that typically flush out nutrients resulting into heavy non-point source pollution (Domagalski et al. 2007). The agricultural practices in China are dominated by harvesting multiple yearly crops, with most intense harvesting, tilling, sowing, transplanting, fertilization, and other agronomic activities during monsoon season. This renders the lands more susceptible to soil erosion and nutrient losses during this period, since the land surfaces are often left barely or partially covered by vegetation, especially between previous and follow-up crops and also at early seedling stages (Gao and Zhang 2010).

Wetlands play a vital role in maintaining environmental stability through nutrient retention. However, natural wetlands in China have undergone great loss and degradation since the early 1950s mainly due to reclamation, pollution, desertification, hydrologic modification, and climatic change. China has lost 23.0% of its freshwater swamps over the past 60 years (Gao and Zhang 2010). Heavy pollution of river systems by other toxic substances is also suggested as an important factor for the decreasing nutrient assimilation capacity of natural ecosystems (Gao and Zhang 2010).

The most densely populated areas in China lie typically in the relatively flat lowlands. In these areas the lakes are naturally shallow (≥7 m mean depth) or have become shallow through siltation. These lakes are more susceptible to human influence, such as eutrophication, because of heavy nutrient loadings from their relatively large catchment areas which are very densely populated and land resources intensively used for agriculture. These lakes are also subjected to profound human influence through construction and management of dams and reservoirs for flood control, power generation, navigation, irrigation, and drinking water supply. Shallow lakes are known to be slow to recover following considerable reductions in external nutrient loading. This is because wind-generated currents can cause frequent re-suspension of nutrient-enriched bottom sediments and thereby a continued release of nutrients into the photic zone.

1.5 Eutrophication remedies in China

Typical abatement actions in western countries target external nutrient load through reduction of phosphate fertilizers, reduction in fall tilling, especially in erosion exposed areas, construction of buffer strips along waterways and wetlands to sediment particles and assimilate bioavailable phosphorous. In China a large range of abatement actions have been employed targeting both external and internal nutrient loads, as well as a focus on ecosystem recoveries.

Control of external nutrient loads is achieved through control of both point and non-point pollution. Point source is decreased by development of sewage treatment plants while non-point through limiting traditional flooding and seeping irrigation. Flooding and poor drainage are the principal reasons for serious soil erosion and the low utilization rate of fertilizers in China. The Chinese government has made an effort to enhance best management practices of farmland in the watersheds of nutrient sensitive lakes. A common abatement action is the construction of shelter forest belt, functioning as a buffer zone, along the shore around nutrient exposed lakes (Liu and Qiu 2007).

Control of internal loads is achieved through removal of upper layer of sediment that contain high phosphorous level to reduce release if phosphorous from the sediments (Zorica et al. 2008). Another method is mixing and oxygenation procedures through either a deoxygenated hypolimon or the entire waterbody to achieve destartification of the lake, and decrease pH to shift from blue-green algae to less noxious green algae (Zorica et al. 2008). Keeping an aerobic environment in the water also limit the mobility of P out of the sediments since the reduced Fe^{2+} , that is the counter ion for phosphate is oxidized and co-precipitates the phosphate.

Biomanupulation has also been employed, that is the laterantion of a food web to restore ecosystem health. This is achieved through removal of secondary consumers to control algae growth or planting and harveting of aquatic/submerged macrophages thereby restraining the algae growth by competing for nutrients and sunlight. The harvested plants are used as organic manure (Liu and Qiu 2007).

1.6 SinoTropia Project

SinoTropia is a Sino-Norwegian trans-disciplinary project addressing eutrophication problem in China by assessing the impact of changes in environmental pressures on mobilization, transport, fate and impact of nutrient fractions to the Yuqiao reservoir in Tianjin, China, and the societal response to abatement actions. It is a four year project funded by Research Council of Norway (no. 209687/E40) and Chinese Academy of Science with partners institutes that includes University of Oslo (UiO), Norwegian Institute of Water Research (NIVA), Norwegian Institute of Urban and Regional Research (NIBR), Research Centre for Eco-Environmental Sciences Chinese Academy of Sciences (RCEES), Tianjin Academy of Environmental Sciences (TAES) and Institute of Urban and Environmental Studies Chinese Academy of Social Sciences.

This thesis is integral part of the SinoTropia project and focuses on the hydro-geochemical processes that govern the mobility and transport of phosphorous fractions into the Yuqiao reservoir. The study aims at determining the temporal and spatial variation in the concentration of phosphorous fractions thereby providing information on phosphorous sources, as well as their mobilization and transport mechanisms. This was achieved through fractionation and determination of phosphorous in water samples collected during synoptic and episodes studies. In addition passive sampling using Diffusion Gradient in Thin films (DGTs) were used to determine time average concentration of assumed bioavailable and low molecular weight phosphorous.

2.0 THEORY

2.1 Terrestrial phosphorous cycling

Phosphorus (P) is an essential nutrient for plants and animals (Sharpley et al. 2001) and plays a crucial role in regulating the primary production and biogeochemical cycling of other bioactive elements in surface waters (Lin et al. 2012). A variety of natural and anthropogenic phosphorous inputs contribute phosphorous to the aqueous environment via a number of different mechanisms (Figure 1). These sources differ with respect to their phase (solid or dissolved), composition (speciation and bioavailability), mode of transport and time of delivery (continuous or episodic discharge, seasonality) (Withers and Jarvie 2008).

Natural inputs of phosphorous to the biosphere are through the weathering of phosphorous containing parent material (Withers and Jarvie 2008). Under natural conditions, it is assumed that apatites are the primary P-containing mineral from which various P fractions are derived though other common minerals contain trace amounts of phosphate (Reynolds and Davies 2001). Phosphorous is commonly contained in the crystalline apatite as Hydroxyl, Chloro and Fluor $Ca_5(PO_4,CO_3,OH)_3(OH,F)$ (Manning 2008), with as much as 95% occurring as fluorapetite (Holtan et al. 1988). Phosphorous is liberated from these minerals during weathering. The dissolved and thus bioavailable phosphorous fraction is then rapidly assimilated into the biosphere through uptake by plants. The weathering is increased by that plants roots that produce organic acids, such as citric acid (Manning 2008). However, these natural sources of phosphorous are very minimal as compared to anthropogenic sources (Withers and Jarvie 2008) such as production of fertilizers and effluent/sewage discharges.

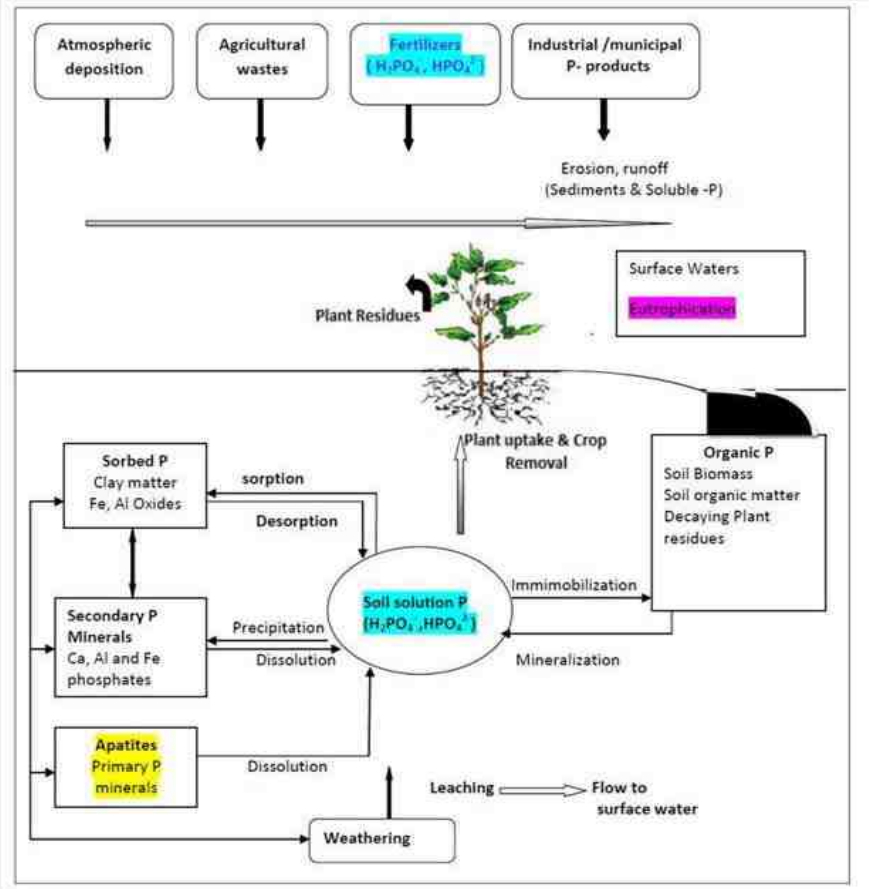

Figure 1: Phosphorous pathways (Adapted from Mullins 2009)

2.2 Phosphorous in the environment

Phosphorous occurs in the environment either as organic or inorganic and either as dissolved forms or bound to particles (Robards et al. 1994). Particle bound phosphate is a product of direct precipitation or sorption to other precipitates (Broberg and Persson 1988). Orthophosphates (H_3PO_4, $H_2PO_4^-$, HPO_4^{2-} and PO_4^{3}) mostly complexes with Ca, Fe, Al and silicates minerals (Reynolds and Davies 2001) forms the major component of soluble reactive phosphorous (SRP).

In most agricultuaral soils, 50-70% of total P is inorganic P (IP), though this might vary considerably. The inorganic P form are dominated by Ca in alkaline and calcerous soils (figure 2), wheras sesquioxides, amorphous and crystalline Al and Fe phosphates compounds dominate acidic and non-calcareous soils (Anna 2000).

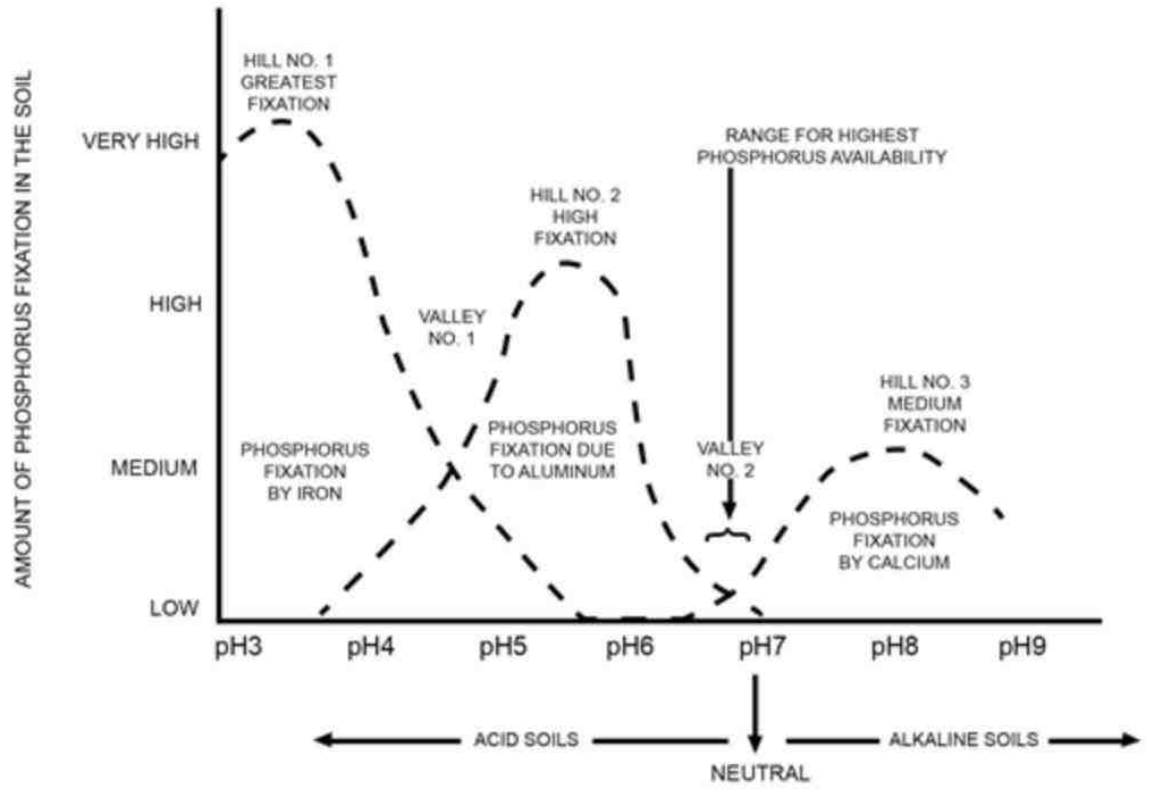

Figure 2: Degree of phosphorous fixation in soils (Adapted from Lajos 2008)

P in solution is the soils appear to be in equilibrium with quantity of labile inorganic P. Phosphorous in solution is governed by sorption processes. Sorption can be either through adsorption or adsorption reactions. Sorption of P in the soils is governed by Ca, Al and Fe ions (Reynolds and Davies 2001). In acid soils may contain elevated concentrations of labile Al and Fe ions, which then may form insoluble Fe and Al phosphates. The sorption of phosphate may also be a result of sorbed Al^{3+} and Fe^{3+} binding both to the negative charges on the soil and to the phosphate, thereby creating a binding bridge for phosphate to be bound to the negatively charged soil surfaces (Pratt 2006).

The above process can be explained by use of Fe, phosphate can be sorbed to Fe both through monodented and bidented bridging complexes (Figure 3 a & b). Only the monodented fraction is considered to be labile, thus it achieves rapid equilibrium with the soil solution P. By contrast, the bidented fraction is very strongly adsorbed and hence considered to be unlabile

form. Since Al is smaller ion, it is more likely that a binuclear complex will form between phosphate and Al, which may be stable (Anna 2000).

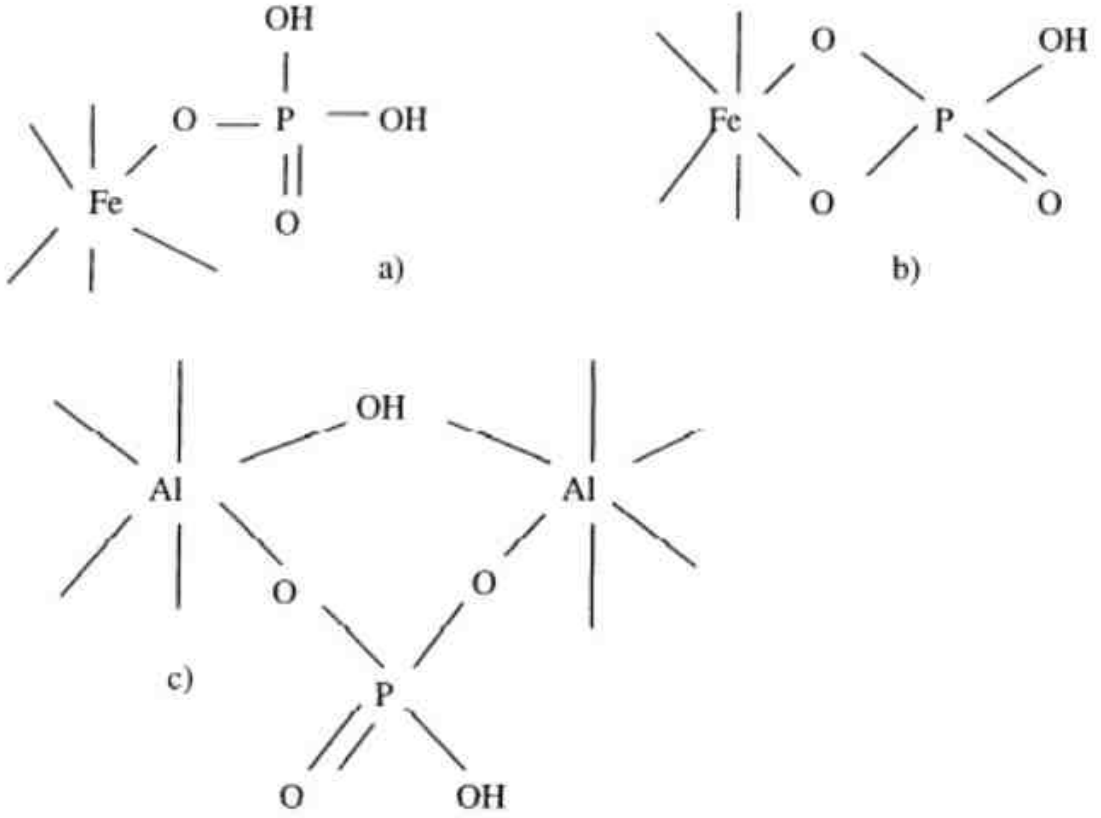

Figure 3: P sorption by Fe, a) Monodented complex, b) Bidented complex and c) Binuclear complex (Anna 2000).

Carbonates are also known to be sorbers of P. Soils with circum neutral and alkaline pH are usually buffered by carbonate dissolution and the soil solution and are therefore typically rich in Ca ions which may then precipitate out the phosphate as calcium phosphates (Mullins 2009).

Desorption process occur through chemical and biological processes. Significant pools of organically bound phosphorous exist in mineral soils characterized by high soil organic matter content. The organic matter contains inherently some phosphate, but this does usually constitute a large fraction. Humus is negatively charged and so does not retain much phosphate, however substantial amounts of phosphates can be sorbed onto it through association with complexed positive multivalent ions such as Fe^{3+} and Al^{3+}. This is important

in soils even with low organic content due to that coating organic material on the surface of mineral particles. On the other hand, high concentrations of dissolved organic chelating agents, as found in manure and sewage, may replace phosphate by competing for the adsorption sites with Fe or Al, and thereby increase phosphorous mobility. Therefore, organic anions like oxalate ion (RCOO-) may increase the mobility of phosphate ion by anion exchange or block sorption sites on mineral sites and thereby reduce the sorption of phosphorous (Holtan et al. 1988).

Mineralization of organic matter releases IP into soil solution through formation of H_2CO_3 or cleaving of IP from organic compounds. Humates produced during decompostion may form protective surface over colloidal sesquioxides, thereby reducing P fixation. Furthermore, low molecular organic carboxylic acids can chelate Fe and Al to form $AlPO_4$ and $FePO_4$ where Ip is rendered soluble (Anna 2000). Desorption can also be influneced by pH, as the pH is raised, $HCO3^-$ are able to exchange with adsorbed P and release it into soil solution. P is most soluble in very acidic and very alkaline soil. A pH of range of 6-7 is considered to being sutable for both phosphates of Fe and Al and phosphates of Ca (Figure 4) will be moderately soluble at these pH (Anna 2000).

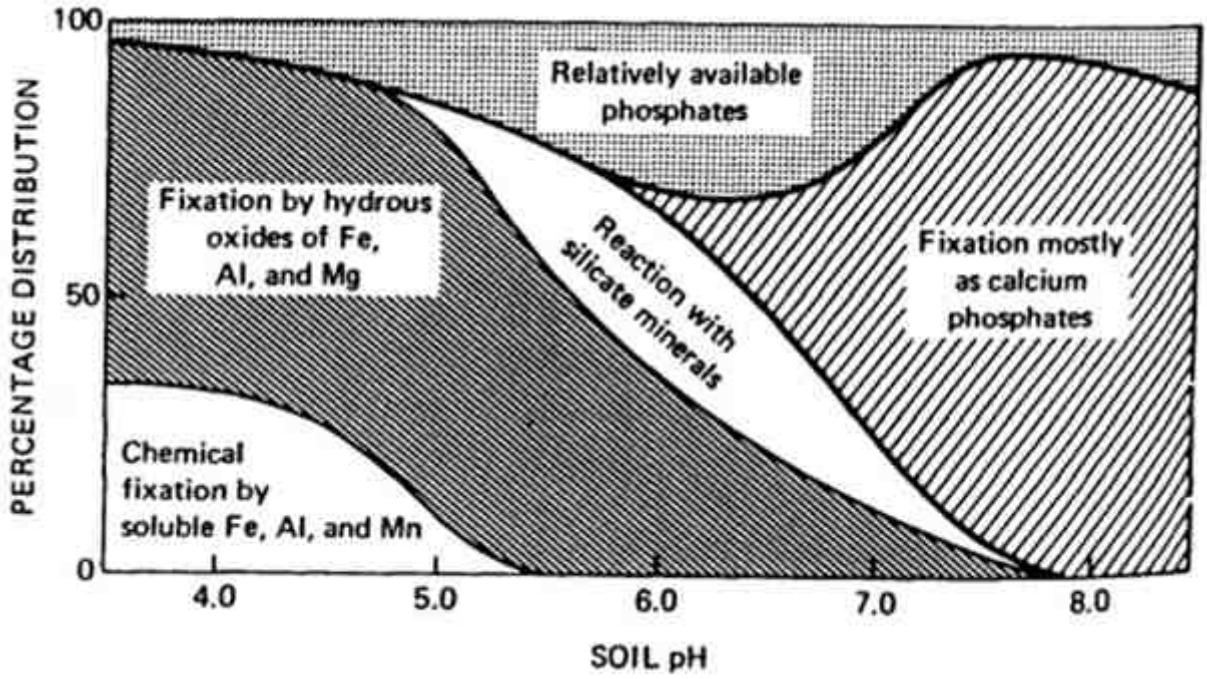

Figure 4: Inorganic fixation of added phosphates at various pH values (Adapted from Brady, 1966).

Phosphorus sorption capacity in soil is also regulated by the content of the soil's finest particle size fractions, silt and clay. The reason is that the active surface area increases with decreasing particle size. Because of this, a positive correlation is often found between phosphate sorption and clay content despite the net negative charge on 1:1 clays at soil pH > 4.6. This correlation can mainly be explained by iron and aluminium on the surface of the clay minerals constituting a charge bridge (Holtan et al. 1988).

2.3 Phosphorous speciation and fractionation

The concentrations of phosphorus fractions and species in environmental matrices are essential data for assessing the health of ecosystems and monitoring environmental compliance with legislation. Furthermore, these data are needed in order to assess the hydro-biogeochemical processes governing mobilization, transport, fate and impact of phosphorous as these processes are critically dependent on the prevailing physiochemical forms of phosphorous (Worsfold et al. 2005).

Improved knowledge regarding the hydro-biogeochemistry of these fractions is required in order to understand the transformations, fate and effects of the phosphorous compounds in soil, water and aquatic environment. Free inorganic orthophosphate ions are generally the main bioavailable form of phosphorus in water, and are readily sorbed and rapidly assimilated. Decomposition and mineralization of complex organic P molecules to the small bioavailable orthophosphate ions is thus an important process (Oddvar et al. 2013). Generally, four fractions can be separated through filtration process. Table 2 indicate the bioavailability and susceptibility for mineralization/degradation to orthophosphate of each fraction.

Table 2: Phosphorous fractions, bioavailability and mineralization (Oddvar et al. 2013)

Total fraction	Total P (TP) by digestion			
Filtration (0.45µm)	Particulate P (PP) (on filter)		Dissolved P (TDP) (filtrate)	
Fractions	Particulate Inorganic P	Particulate Organic P	Dissolved Organic P	Dissolved Inorganic P
Denotation	PIP	POP	DOP	DIP
Compounds	Inorganic particu-late matter, clays, hydroxides, etc	Organic particu-late matter, algae, bacteria, etc	Fytines, Nucleo-tides,,P-sugars, P-lipids, humics	Free ortho-phosphate ions
Bioavailability	Low	Low	Medium	High
Mineralization to DIP	Slow	Slow	Medium	Instant

Monitoring of bioavailable fractions of phosphorus compounds in water represents several analytical challenges as the concentration of the free orthophosphate fraction is usually low or below the detection limit (typically 1 µg P/L for common methods). In addition, analytical challenges related to fraction separation, especially the differentiation of colloid and suspended particles need to be overcome (Oddvar et al. 2013).

Particulate and dissolved phosphorous components have been separated and characterized mainly on the basis of their physical and chemical properties through filtration. The use of 0.45µm membrane filter for the separation of phosphorous into total dissolved P (TDP) and particulate P (PP) is widely accepted as a standard procedure. However this separation method does not distinguish colloids fraction which can be in both the dissolved and particulate fractions. Deviation from this method is the use of 0.2 µm GF/F membrane to retain all aquatic bacteria and the also use of GF/C (approx. 0.7 and 1.2 µm) glass fibre filters (Broberg and Persson 1988). In this study the 0.7 µm GF/F membrane is used to distinguish between organic and inorganic particles. The rationale for this was the need to non-combustible filter material in order to determine the mass of particles on the filters by loss on ignition.

Total phosphorous (TP) is determined on the unfiltered water sample while total dissolved fractions (TDP) are determined on the filtrate after digestion. Particulate (PP) is determined by the difference between the total P (TP) and dissolved fractions (TDP) (Robards et al. 1994). Dissolved inorganic fraction (DIP) is determined in the filtrate solution without digestion (Table 2). The dissolved organic fraction (DOP) is arbitrary estimated as the difference between TDP and the DIP. TP, TDP and DIP are measured using the widely employed ammonium molybdate blue spectrometric method. It is based on the reaction of phosphate in an acidified molybdate reagent to yield phosphomolybdate heteropolyacid, which is then reduced with acid to produce an intensely coloured blue compound that is determined spectrophotometrically (ISO 6878:2004). According to this method DIP is determined as Dissolved Reactive Phosphorous (DRP) while TP and TDP are determined as TP. The intensity of the blue colour correlated to the concentration of phosphate in the solution. TP can also be measured by other analytical methods and instruments such as the use of ICP-MS. The instrument offers better measurements due to its low limit of detection.

2.4 Phosphorous cycle in the watershed

Phosphorous cycling in the watershed encompasses many phosphorous transformations governed by a range of dynamic biotic and abiotic processes. Balances of uptake/release, adsorption/desorption and precipitation/dissolution control the concentration of dissolved phosphorous, while erosion/sedimentation and advection/diffusion processes determines phosphorous transport. These processes play therefore an important role in modifying phosphorous fluxes (Withers and Jarvie 2008).

Studies have shown that phosphorous fluxes entering rivers do not add up to what is measured at the watercourse outlet (Withers and Jarvie 2008). Depending on the period, phosphorous can either be retained or stored in the river system or mobilized from within the system. Retention is mainly observed during low flow periods. This corresponds usually to the summer, which is time of greatest eutrophication risk. During low flow, phosphorous is retained in the system through sorption to sediments or sedimentation of the particulate P. During rainstorm, phosphorous can be remobilized through re-suspension of fine sediments or mobilization of materials from the river beds or marginalized zones of the river (House 2003). In addition, phosphorous inputs delivered to streams under very high flows are likely to be

flushed through without entering the stream biogeochemical pathways (Withers and Jarvie 2008).

Not all phosphorous fractions entering a stream plays equal role in the biochemical cycle within the watercourse as this depends on its bioavailability, reactivity and the water residence time. Phosphorous retention results in changes to the amount and timing of phosphorous fluxes downstream. Moreover, river processes may also alter the form and thereby the fractionation of phosphorous transported downstream, with implications for phosphorous bioavailability. For example, through sorption to sediment or by uptake by biota highly bioavailable low molecular weight dissolved phosphate may be converted into less-bioavailable particulate and large molecular weight organic fractions. This leads to an increase in the phosphorous content of the (re)-suspended particulate (Gebreslasse 2012).

2.5 Mobilization of soil phosphorous pools

Mobilization of phosphorous from soil pools to soil water is a function of solubility, desorption and detachment processes. Solubilization and desorption is a result of chemical non-equilibrium while detachment is the removal of PP attached to soil particles or colloids by erosion, where the driving force is exerted by moving water. Solubility and desorption generates TDP while detachment is responsible for PP (Gburek et al. 2005).

In addition to the size of P pools the contact time between the phosphorous and soil particles is important in explaining the temporal and spatial variation in TDP. Established soil P relates to the phosphorous that has had sufficient contact time with the soil to become strongly bound. This occurs within days/weeks after fertilizer and manure application. Recently applied P is more easily bound and thus becomes more readily mobilized. Recently applied fertilizers/manure may therefore substantial increase phosphorous losses, especially when these applications coincide with heavy rainfall before contact with sorbing soil is achieved. Also, catastrophic phosphorous losses may occur if fertilizers/manure is applied to already saturated or frozen soil (Gburek et al. 2005, Heathwaite et al. 2005). In addition, the accumulation of P in topsoil make it more susceptible to losses through fast flow processes that are mainly event based.

An increase in soil phosphorous status results in a disproportionately increased in P losses. This may however differ between soils since the amount of P released into the solution is a function of the amount of phosphorous already adsorbed and the sorption capacity of each soil. Therefore, to predict amount of P available for transport, soil test such as degree of P sorption saturation (DPSS) or sorption index (PSI) needs to be determined. PSI of soils has been found to be a good indicator of P mobility. Mobilization can also be influenced by ionic strength of the solution. During high discharges, the low ionic strength of the rapid infiltrating solution allows for little exchange between drainage water and soil water leading to extraction of more phosphorous from the soil. Variations in ionic strength may therefore influence the phosphorous concentration of surface runoff, and thereby partially explain the temporal variation of phosphorous concentrations in runoff water (Gburek et al. 2005, Heathwaite et al. 2005).

To understand the processes governing detachment of PP, both the amount of phosphorous associated with different size fractions and dispensability of soil particles as a function of soil properties and management practices must be looked into. Concentration of phosphorous on the eroded particle is controlled by the PSI and specific physiochemical and biochemical reactions of the soil, while the absolute flux of phosphorous loss is regulated by physical forces which are exerted by flowing water for larger particles and dispersion/flocculation behaviour colloids particles. Particulate size distribution in the flowing water is therefore mainly a function of soils erosion, which is a size selective process that show preference for smaller size sized particles, as well as flocculation processes. Total P in sand is relatively low because the absorption capacity is slow. Total phosphorous increases therefore with decrease in particle size. Most of the P found in the sand fraction is bound to the organic coating (likely through Al and Fe bridging), sorb as calcium phosphate or in its primary mineral form. P in the clay fractions is largely of secondary origin, mainly Fe-bound, and is a result of adsorption of both organic and inorganic P due to the greater surface area and thereby P retention capacity of clay (Gburek et al. 2005, Heathwaite et al. 2005).

Total P and organic content of finer soil particles are higher in the surface horizon than those at depth in well drained soils. This enrichment is mainly due to internal biocycling in natural systems and due to fertilizing in agricultural systems. These surface layers are more prone to be leached through sub-lateral flow and eroded by surface runoff. Cultivation tends to

increase the amount of phosphorous especially in the clay fraction, and thus, potential for P detachment, not only under fertilization but also when no fertilizers are added (Gburek et al. 2005).

2.6 Transport of phosphorous along water flow-paths

Phosphorous fluxes to a surface water resource are mainly associated with critical source areas (CSAs). CSA are specific and identifiable areas within the catchment that have close proximity to the surface water and are most susceptible to P loss. These CSAs are thus dependent on both source factors (soil, crop and management practices) and transport factors (surface runoff, erosion, subsurface flow and channel processes). The source factor is a function of soil and catchment characteristics rendering a high potential to contribute to P export. These are relatively well defined and reflect pattern of land-use as this relates to soil P status, as well as fertilizers and manure inputs. The source factor is usually determined by the amount of P pools in the soils, though the mobility of P present is determined by the PSI as well as the characteristics of the fertilizers/manure and the methodology of application in the soil as well as the timing relative to rainfall. The transport factors are more a function of the interaction between landscape and climate mediated by advective transport through water flow-paths (Gburek et al. 2005, Heathwaite et al. 2005).

Hydrology is driven principally by precipitation (rainfall) that ranges in intensity, duration and interval. These factors are important in influencing discharges and may have differing impact on transport of phosphorous. Therefore understanding these rainfall phenomena is important in understanding P discharges from the watershed. In addition, the rise, peak and recession of a storm hydrograph can be effectively simulated to help understand P transfer (Haygarth and Jarvis 1999).

Rainfall drives phosphorous transported through various water flow-paths through the soils such as overland flow, sub-lateral flow, preferential flow and matrix flow. Overland flow (surface runoff) is generated when the rate of surface accretion of water exceeds the rate of its removal by percolation. Surface runoff is mainly responsible for particulate P losses thus it's closely linked to soil erosion. Overland flow increases with intensity of precipitation and with relative saturation of the soil but decreases with porosity. Runoffs are prevalent in agricultural

land due to the loose soil particles. It results in both soluble and particulate P and provide a cocktail of organic and inorganic P, from which solution and desorption may increase the bioavailable P content (Reynolds and Davies 2001).

Preferential is the rapid and direct transfer through fissures, macropores, worm holes and cracks (in clay soil). Preferential flow is important in removing surface P especially those found in excreta, manure or fertilizers (Haygarth and Jarvis 1999). Sub-surface run off (interflow) is the fraction of total runoff that infiltrates the ground by moving downwards and laterally in response to gravity. The water in this flow is open to modification through solution, concentration and uptake by plants. Therefore the dissolved P in soil can removed efficiently through sub-surface flow. Therefore, soil P solution due to saturating fertilization may be transport onwards and over distances as determined by the next soil horizon encountered. If P is abundant P-binding capacity exist a little deeper down, then P can be immobilized there. Therefore, shallow or sandy soils with steep hillsides are more likely to yield SRP through interflow (Reynolds and Davies 2001).

2.7 Interaction of soil P pools with the water flow-paths

The product of the source and transport factor gives the potential for actual P losses. The dynamics of P export form a catchment is thus a result of the interaction between a variety of P pools and transport mechanism. In order to understand the spatial and temporal variation in P export it is necessary to understand how hydrological conditions vary with time and how major P pools vary in space. Most investigations have shown that interaction of the flow of water with the soil is depth limited and occurs within a very thin surface layer which is in the order of millimetres to centimetres at most (Gburek et al. 2005). Therefore, accumulation of P in top soils makes it more susceptible to interaction with the flow resulting in P loss.

Temporal dynamics also plays an important role in P mobilization and transport processes. The anthropogenically derived soil P pools are characterized by rapid depletion rates (days/week), while other P pools may exhibit longer depletion time. These anthropogenic pools will thus be flushed out during the onset of a rainfall period. It is therefore important to evaluate both short and long term trends in a watershed. Long term trends reflect the

cumulative effect of land management whereas short term effects relate to P balance in the system (Gburek et al. 2005).

Seasonal variations has also been shown to influence inorganic P concentrations with higher inorganic P concentration being observed in winter on fine textured soils than in summer and the reverse for coarser soils. Organic P is also affected by seasonal fluctuations as detachment of organic particles is influenced by processes acting at different time scales. Since soil cover is the most dominant factor, mobilization by soil erosion is strongly influenced by the seasonality of the different crops. Other management practices such as leaving crop residue on the field also have immediate effect on the risk of detachment and transport as aggregate stability is affected by the content of organic material. Soil organic material composition undergoes long-term changes due to different management practices paths (Gburek et al. 2005, Heathwaite et al. 2005).

3.0 MATERIALS AND METHODS

3.1 Site description

3.1.1 Yuqiao Reservoir

Yuqiao reservoir is the primary source of drinking water for the people living in Tianjin City. Tianjin, with a population of more than 10 million, is the fourth largest city and a major industrial centre in the People's Republic of China (PRC). The reservoir is located at the northern part of Tianjin at border of the lowland and uplands constituted by the foothills of Yanshan Mountain (figure 5). Apart from being the primary source of drinking water, it is also a source of water for the numerous industries in the area, used for fishing and some restricted recreational activities.

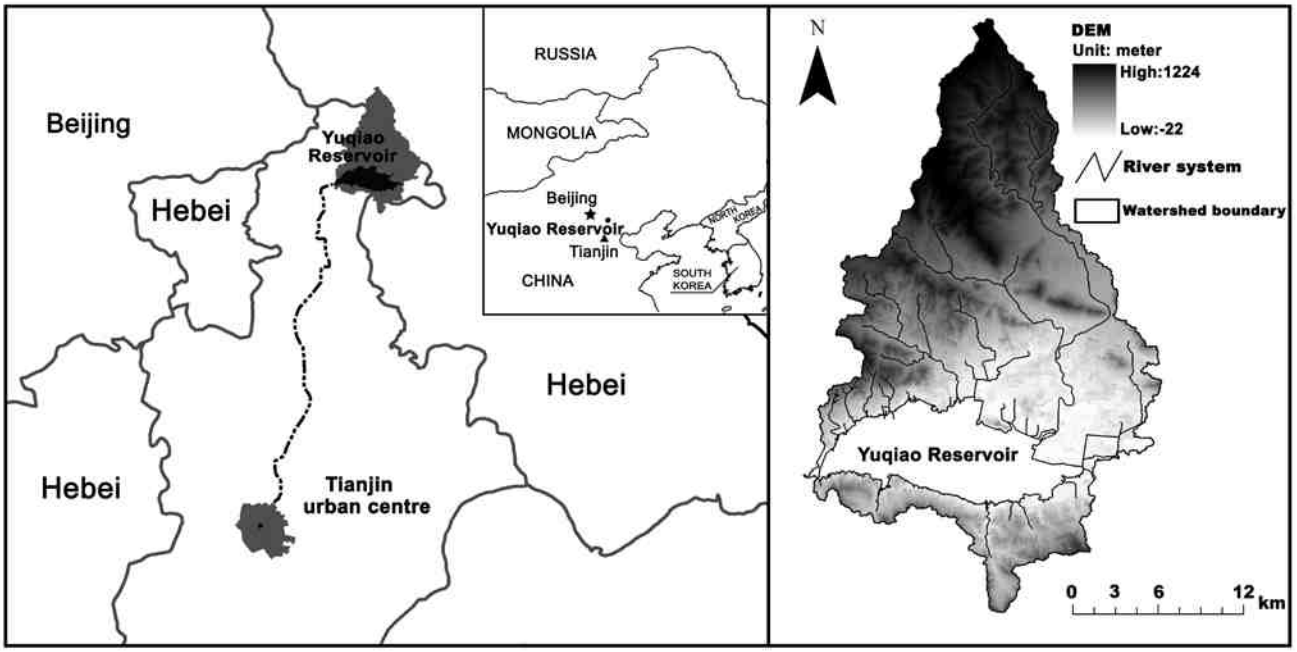

Figure 5: Location of Yuquiao reservoir and its surrounding boundaries (Map: Courtesy of Zhou Bin)

The construction of the reservoir began in 1959 for the purposes of flood protection and agricultural irrigation. But, due to increasing population, economic expansion and increased demand for water from the reservoir, a major project was undertaken in the late 1970's to divert water from the adjacent Luan He watershed to the reservoir. Water commenced flowing through the diversion in 1983 and has since served as the main inflow of water to reservoir.

During dry years the diversion accounts for up to nearly 90% of the annual inflow to the reservoir and around 30 % during wet years (EPA et al. 2003, TAES 2012).

The reservoir covers an area of approximately 250km^2. It is shallow with average depth of 4.3 meters, average surface elevation of 21.6 m a.s.l average area of 86.8 km^2 and average volume of 385 million m^3. These dimensions are highly variable from year-to-year, depending on the amount of rainfall. The maximum recorded dimension are length of 30km, width of 8km, depth of 12km and capacity of 1560 million m^3 and elevation of 27.72m (EPA et al. 2003, TAES 2012).

3.1.2 Yuqiao reservoir watershed

The reservoir has a watershed that covers 2060 km^2 comprising of mountains and low land region. There are three (3) main rivers that flow into the reservoir: Sha river, Li river and Lin river (figure 6). Sha river has a catchment area of 887km^2, Li river with 448km^2 and Lin river with 252km^2 and the rest being covered by the other smaller streams. Li and Sha rivers confluence to form Guo river at about 10km before draining into the reservoir. There are three dams on the watershed, two on Sha river and one on Lin river which harvest water for the city of Zunhau in Hebei province, Sha and Lin rivers have low flow during the dry winter season of the year but experience high flow during the rainy summer seasons (EPA et al. 2003, TAES 2012).

Flow of Li river is modified through diversion from Panjiakau and Luan river thereby ensuring a steady flow throughout the year. Water is diverted from the Luan He between October and May and constitutes almost all of the flow in the Li river and the inflow into the reservoir during this period. There are no obvious temporal patterns in the diversions from the Luan He. The relative inflow contributions into the reservoir follows wet and dry seasonal variations and vary also between wet and dry years. The peak flows through the local watershed occur during the wet season between June and September, with the highest flows occurring in July and August (EPA et al. 2003, EPA and TEPB 2005).

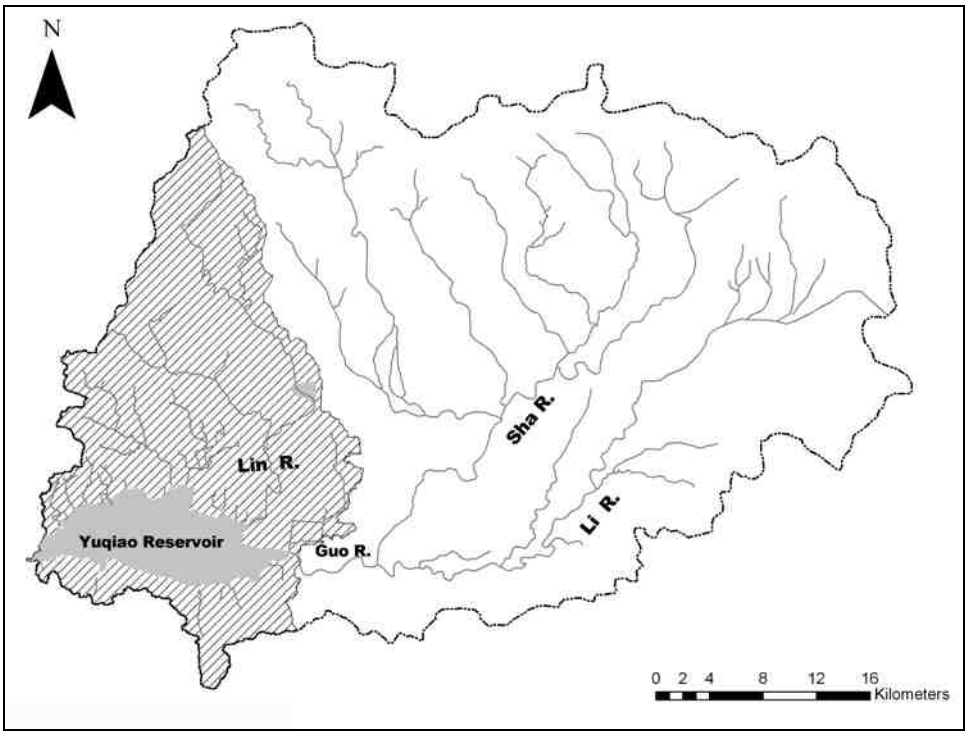

Figure 6: Yuquiao reservoir internal watershed (Map: Courtesy of Zhou Bin)

3.1.3 Climate

The watershed lies in the temperate zone within the steppe climate region(FAO 1978) and experiencing typical monsoonal seasonal fluctuations . Mean annual temperature is around 11°C with a high temperature mean of 29 °C in July and low temperature mean of –7 °C in January (Figure 7). The annual mean rainfall is 590 mm, with lowest of 390 mm. Out of the total rainfall received in the area, about 66% falls during the wet months of July and August. Winter is the driest season, with about 2% of the annual precipitation. The prevailing wind is northwest in winter and southwest in summer, with an average wind velocity of 3.3 m/s (EPA et al. 2003).

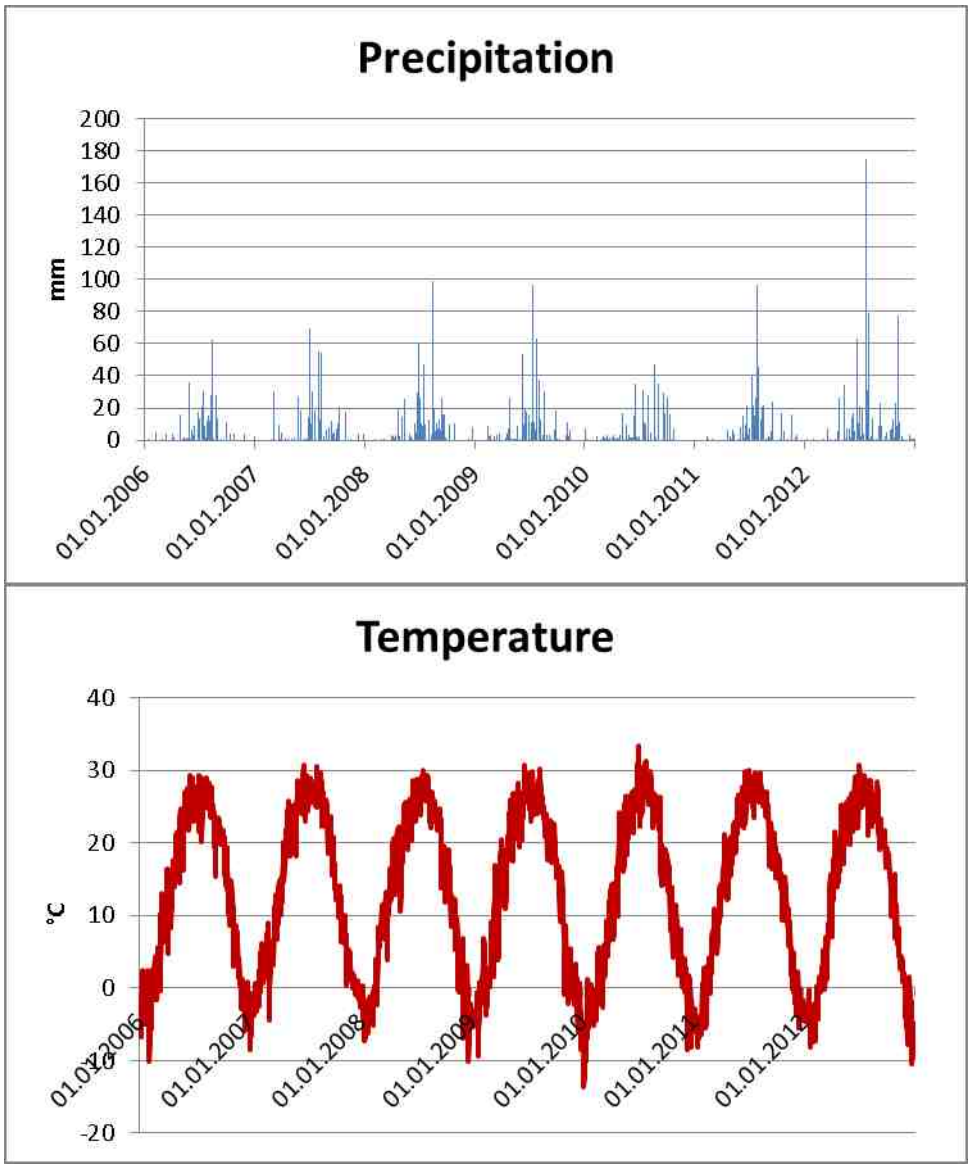

Figure 7: Precipitation and temperature pattern (2006-2012)

3.1.4 Demographics

The human population in the watershed is estimated to be between 120,000 – 140, 000 living in the 153 villages in the watershed (Figure 8). The villages are found in the area close and around the reservoir although some villages are also found in the northern mountain region of the reservoir. The economic activities practised by the villagers are agriculture (both for domestic and commercial purposes), animal husbandry, fishing, aquaculture and small scale business in food, hospitality and manufacturing industries (EPA et al. 2003). The management practises in the agricultural fields are extensive application of inorganic

fertilizers and manure to improve yields. This may suggest the influence of agriculture and managemnt practises in the nutrient enrichments in the watershed.

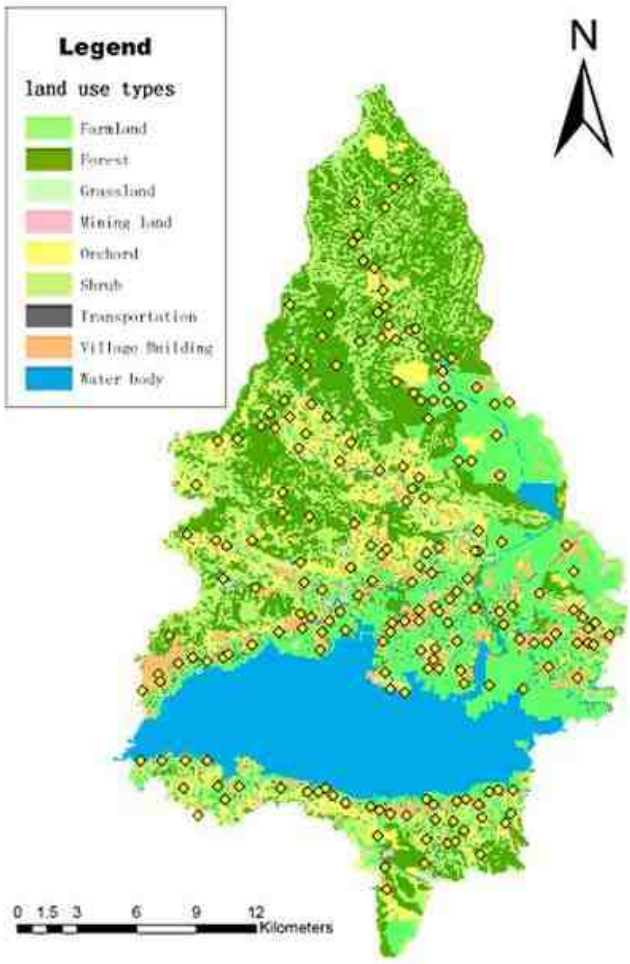

Figure 8: The distribution of land-use practices and villages (Villages with yellow dots**)** (Map: Courtesy of Zhou Bin)

3.1.5 Land Use

The land-uses within the local catchment include agricultural lands (farmland), orchards, shrubs, forests, fish farms, industries and settlements (Figure 9). Over 30% of the land is under forest while cultivated land (farmland and orchards) accounts for 37% of the total land use. Dominant management practices within the farmlands are crop rotation, application of fertilizers, irrigation and tilling (EPA et al. 2003).

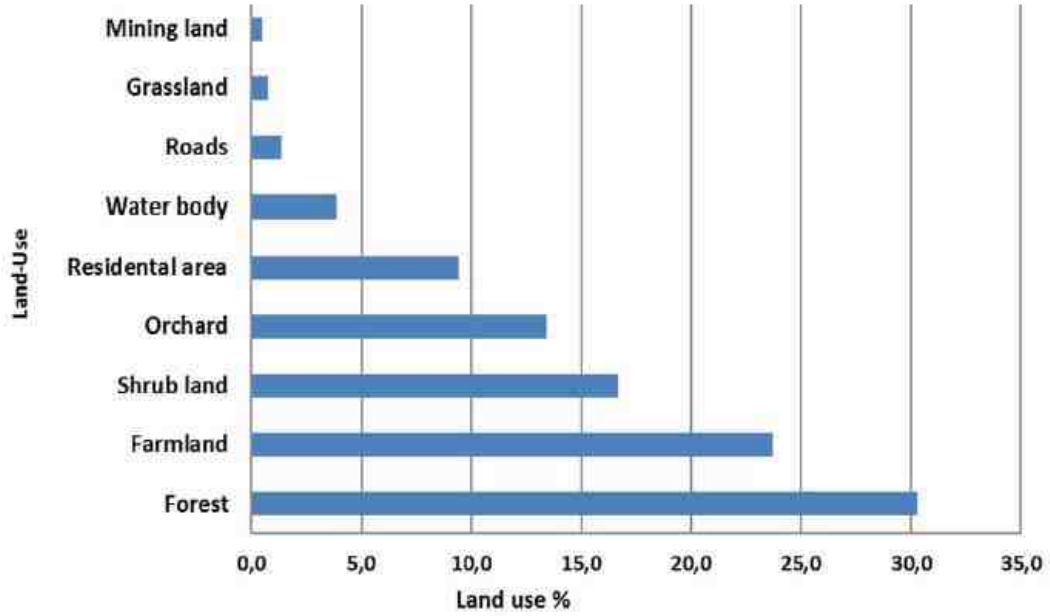

Figure 9: Land use percentage within the internal watershed of Yuqiao reservoir (EPA 2000)

The distribution land use within the local watershed is as per figure 10 below. Forest dominates the northern mountain part of the watershed while farmland and orchards are found eastern and northern parts. Fish pond dots the eastern part of the reservoir where Guo River enters the reservoir.

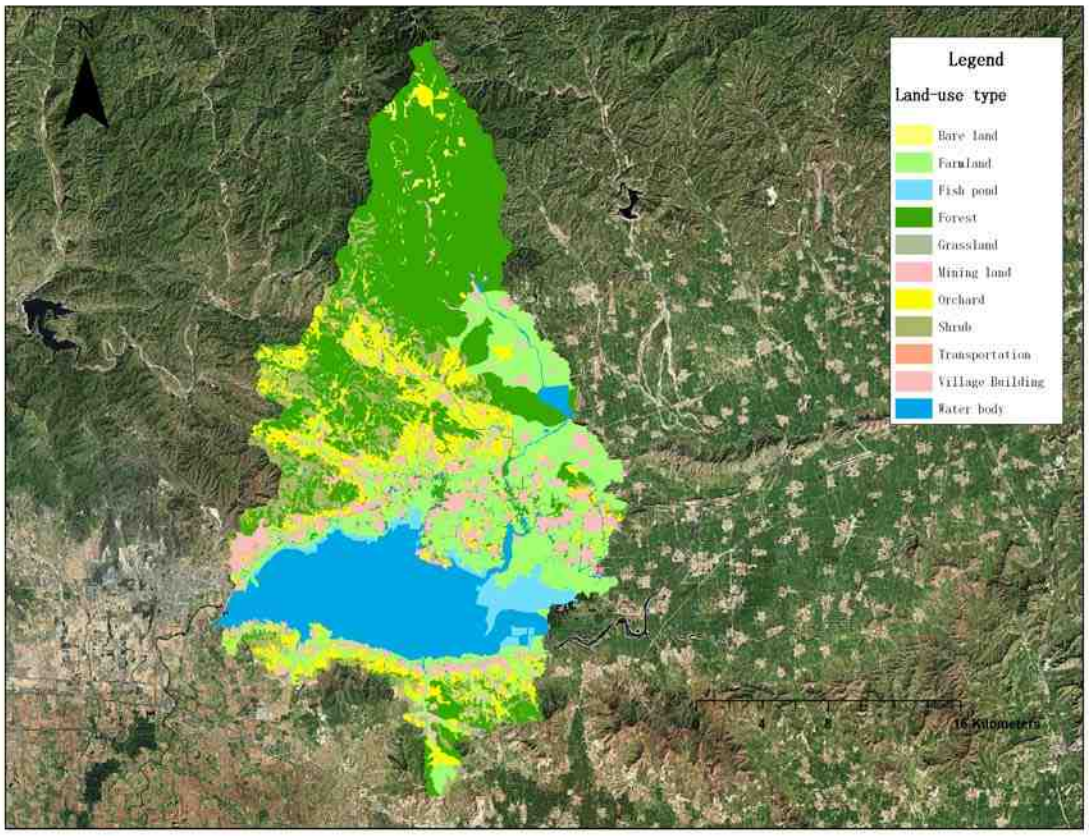

Figure 10: Land use distribution within the local catchemt of Yuqiao reservoir (Map: Courtesy of Zhou Bin)

3.1.6 Soil types

The soils in the watershed was developed through weathering of the parent sedimentary bedrock (FAO 2000), consisting of sandstone and limestone. Most of the soil material, especially in the lowland area, is deltaic alluvial sediments. Soil types in the catchment according to FAO classification system includes calceric cambisols, calceric flovisols, calceric luvisols, butric cambisols, butric cambisols, gleyic luvisols and haplic luvisols. Their distribution in the watershed is a shown in Figure 11. The soil is predominately clay with agricultural soils having a typically a plough layer (Ap) thickness of 30-40cm. Below the Ap layer in the lowland soils, surrounding the reservoir, there is an impermeable clay layer. The Ap layer therefore becomes easily saturated during rainfall resulting into a predominant overland flow.

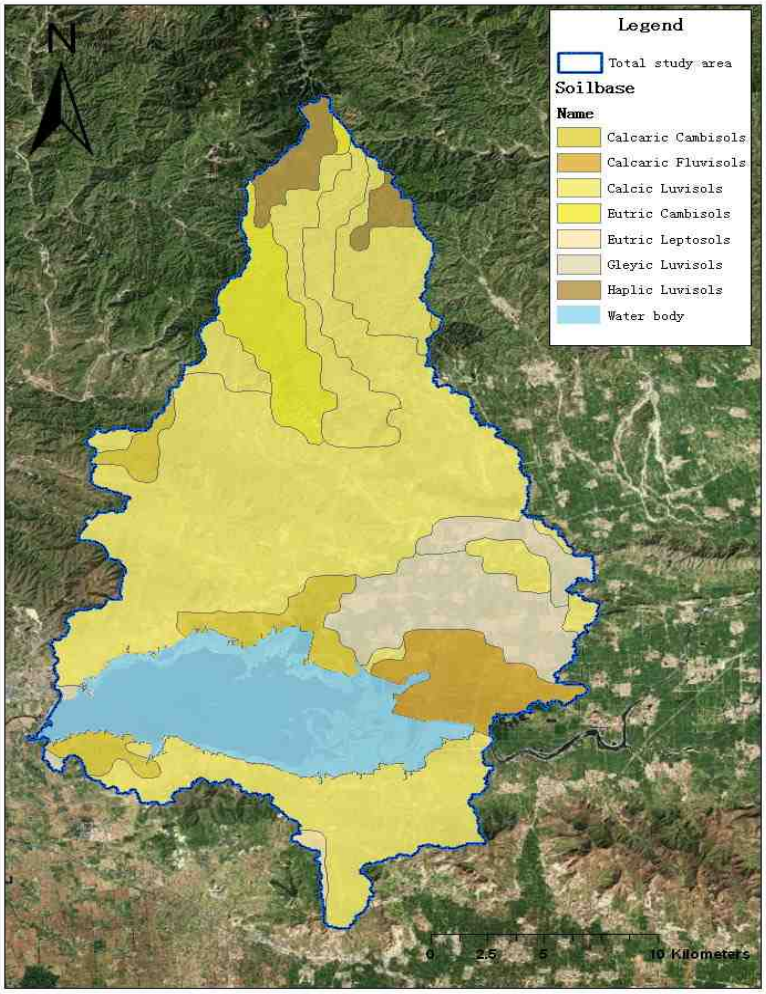

Figure 11: Soil types in the local catchment (Map: Courtesy of Zhou Bin)

3.1.7 Nutrient level and water quality

Monitoring data from the local EPB shows that the reservoir has high nutrient level and is highly productive during the warmer months of summer and fall seasons. The pollutant concentrations in the reservoir are mainly associated with total phosphorous (TP), total nitrogen (TN) and chemical oxygen demand (COD). Total P and Chlorophyll shows seasonal variation with high concentrations during the warm summer months. This is believed to be the cause of the summer algae blooms which is consistent with increased productivity fuelled by high nutrient levels (EPA et al. 2003).

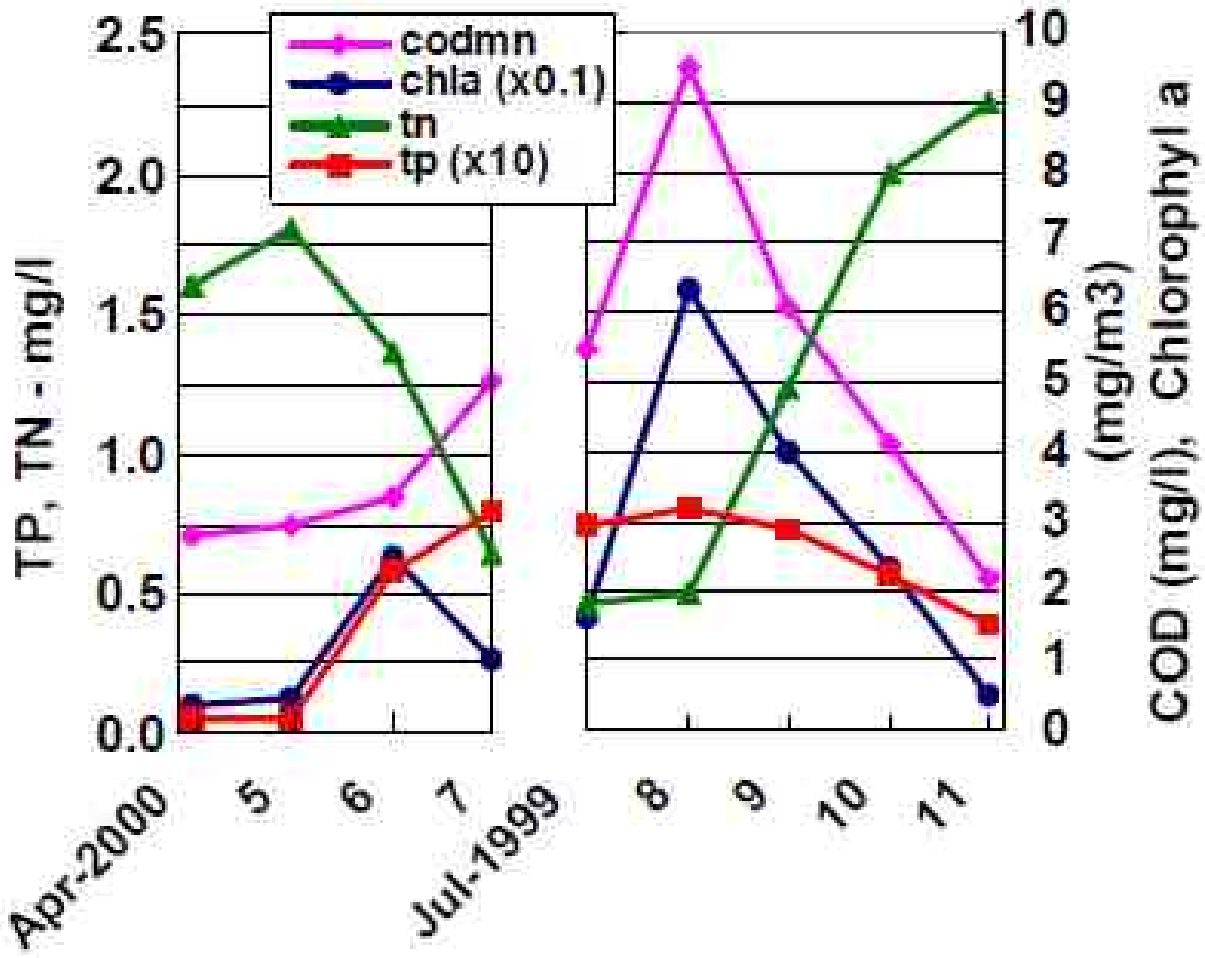

Figure 12: Seasonal patterns of select pollutants in the middle of Yuqiao reservoir, late spring – summer 2000 and summer - fall 1999 (EPA et al. 2003).

The pattern associated with TP concentration is consistent with the pattern of precipitation in the watershed (Figure 12). TP concentration increases during the wet season due to polluted surface runoff from the local catchment and decreases during periods when the inflow to the reservoir is low and mainly through diverted water from Luan He as well as ground water seepage. This is an indication of the significance of surface runoff on water quality in the reservoir.

The seasonal pattern of TN however is the reverse of TP, rising when TP declines and declines when TP rises. This trend could be attributed to the main water source during the dry season is from the diverted water.

According to the monitoring data from Tianjin Water authority **(**Ji Country EPB and Yuqiao Reservoir Management**),** most of the phosphorous is mainly derived from the internal watershed while the main reactive nitrogen loads are from the rest of the watershed and from input of the diverted water: The contribution of phosphorous from the local watershed is 62% and contribution of reactive nitrogen from the rest of the watershed along with diverted water is 93% (Figure 13)

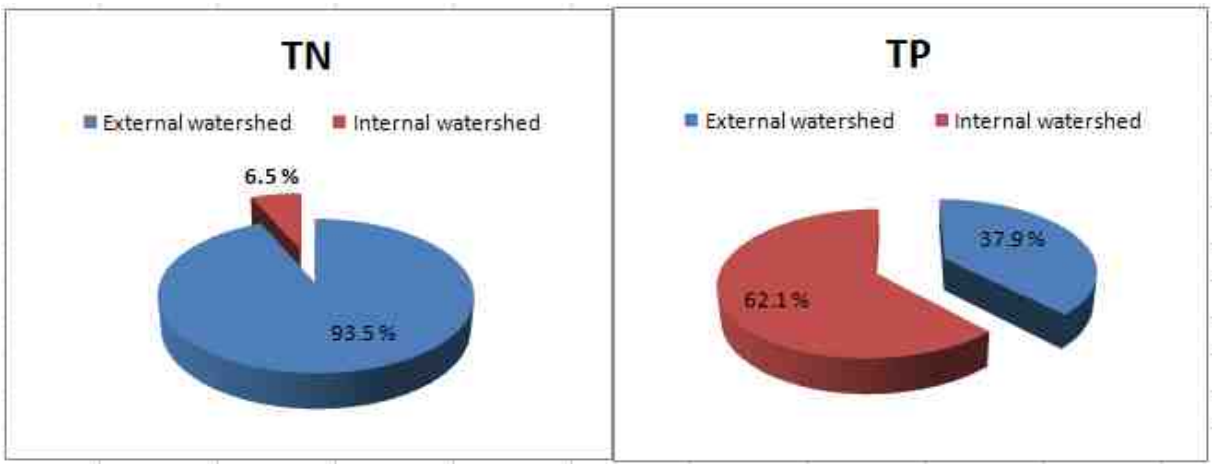

Figure 13: Yuqiao reservoir TN and TP watershed contribution **(Data: Tianjin Water Authority, 2010)**

Annual nutrient contributions from the three rivers show a strong increasing trend for TN and large inter annual variations for TP (Figure 14). The annual pattern from 2004 to 2008 show that major P contributor was Sha river which drains the largest catchment areas of all the rivers. However over the sampling period, the P flux from Sha river shown considerable reduction in P concentration but a rise in P concentration in Lin river. In 2008, the highest total P concentration came from Lin River. The catchments of Lin River and its tributaries are therefore believed to be major source of P flux to the Yuqiao Reservoir. It against the backdrop of the above information that sampling of P was done in Lin river and the surrounding smaller streams.

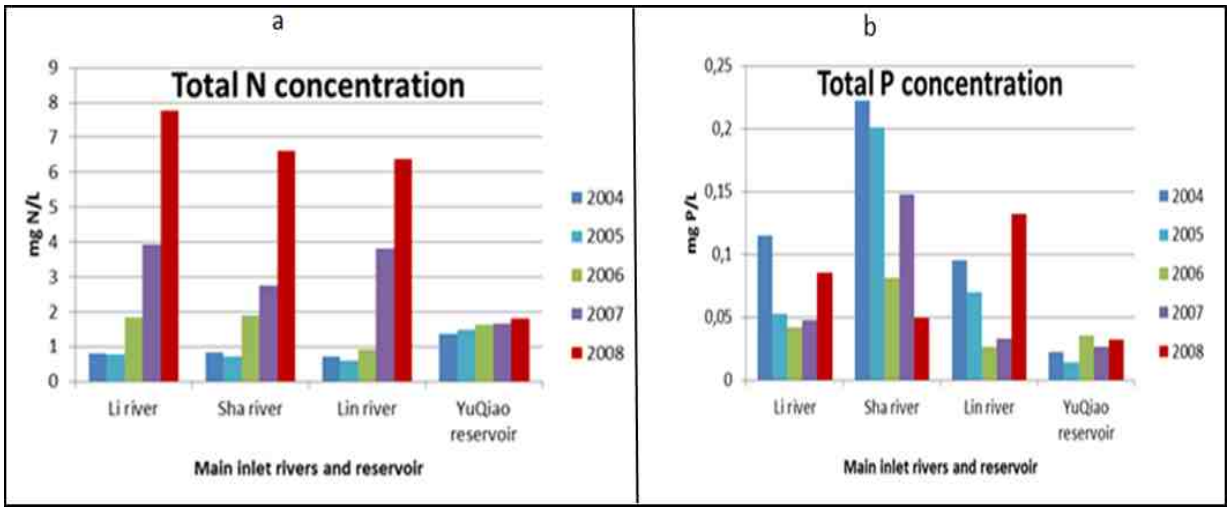

Figure 14: Yearly Total Nitrogen (a) and Total Phosphorous (b) concentrations from 2004 to 2008 in the main tributaries and the reservoir (Data: Ji Country EPB and Yuqiao Resevoir Management)

In order to understand the relative contribution of P flux from the rivers, it is important to look at the water chemistry. As noted earlier (Chapter 3.1.2), 90% of the reservoir water is from diversion from Luan He through Guo river and 30% during wet period. Therefore considering that 62% of P is from the internal watershed, it is probable to state that Lin river and the smaller surrounding streams contribute the major fraction of the P into the reservoir during wet periods. During wet period, 30% of the reservoir water is from Luan He and the remaining 70% is from Lin river and other surrounding streams.

3.2 Diffusion Theory in Thin Films (DGT)

An accurate and precise measurement of phosphorous fractions is a prerequisite in order to gain a better understanding of the biogeochemistry of phosphorous in the environment. There are three main problems related to the determination of phosphorous fractions in water: P is labile and the fractionation may thus change during storage; large temporal fluctuations render phosphorous fractionation on grab samples merely snapshots of their chemistry; and the detection limit of phosphorous is poor relative to what is significant levels of the bioavailable phosphorous fraction in the environment. Ideally P fractionation should therefore be made in situ, accumulating the phosphorous over time. This would produce a time averaged in situ measure that represents no/minimal detection limit problems. A technique

that can be employed for *in-situ* sampling is the use of Diffuse Gradients in Thin films, or just DGTs (figure 15) (Zhang et al. 1998).

The DGT technique, developed by Zhang and Davison (1993), is commonly used to measure in situ labile metals, metalloids and phosphates in water. This is a simple passive device that accumulates dissolved low molecular weight substances, and thus the bioavailable fraction, in a controlled manner. DGT's enable continuous monitoring of water bodies in which the fluctuating levels of contaminants are captured at ambient ionic strength and pH without storage of sampled water. Conventional analysis of the sampled low-molecular weight analyte provides thus an *in-situ* time averaged concentration of the bioavailable fractions over the deployment period (Zhang and Davison 1995). The average concentration may be relevant as threshold value to predict algae blooming. Furthermore, the ability to *in-situ* capture the very labile low molecular weight fraction is especially important for phosphorous since no changes in phosphorous speciation are expected to be introduced during storage and handling (Uher et al. 2012). This opens the possibility to distinguish between inorganic, mainly free aqueous ortho-phosphate determined as DRP, and the low molecular weight organic compounds that are found by the difference between TP and DRP.

Figure 15: The DGT device used for this study

The binding agent in the resin gel is selective to the target ion in solution. Ferrihydrite is a commonly used sorbent in the DGT to capture phosphorous (figure 15). It is a hydrous ferric oxyhydroxide ($(Fe^{3+})_2O_3 \bullet 0.5H_2O$) that has a large capacity to bind phosphates. The DGT with

Ferihydrite is a tested and proved device for phosphates measurement (Zhang et al. 1998).The phosphorous is completely eluted out of the absorbent by dissolving it completely using H_2SO_4.

The DGT has a base of 2.5cm in diameter and a 2.0cm diameter window (figure 16). It is designed to accommodate a 0.4mm resin layer. Overlying the resin layer is a diffusion gel of 0.8mm and above it is the 0.135mm membrane filter with pore sizes of only 5 – 10nm (Zhang et al. 1998).

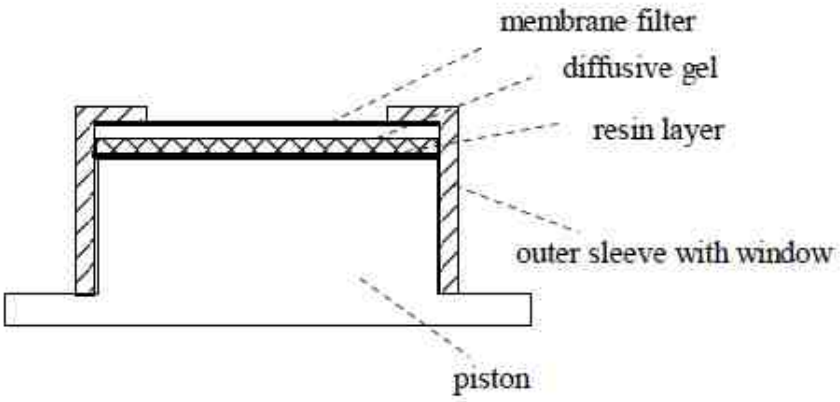

Figure 16: DGT cross section (Zhang et al. 1998)

The DGT principle is based on the diffusion theory as the ions have to diffuse through the filter and diffusive gel to reach the resin layer. That is, phosphates diffuse through the membrane filter and diffusion gel into the Fe-oxide gel resin. The adsorbed phosphorous is then measured after elution of the oxide resin, from which the concentration in solution is calculated. It is therefore the determination of the diffusion coefficient, describing the diffusion gradient that forms the basis for allowing an estimation of the phosphates in solution based on the amount of phosphate determined in the resin (Van Moorleghem et al. 2011). Formula used in DGT calculations are given in appendix A-1.

Within a few minutes of immersion, a steady state linear concentration gradient is established between the solution and the resin gel. By exploiting this simple steady state condition, the DGT technique can be used to measure concentrations *in-situ*. The flux of the ion that diffuses through the diffusive gel is given by the diffusion coefficient that is determined using Ficks's first law of motion. In addition there is an important size cut-off due to the pore size of 5 – 10 nm, as well as a exclusion due to charge and membrane resistance (Oddvar et al. 2013).

Interference with DGT measurements

Resin capacity and other factors influencing and linear uptake: It is essential that the adsorbent capacity is not exceeded during deployment time. The adsorption capacity of the Ferrihydrite DGTs is approximately 6.7 µg P of ortho-phosphate. To avoid back diffusion from the DGT, it is recommended that the DGTs are deployed no longer than a time which would result in accumulation of 50% of this adsorption capacity. The maximum deployment time depends on diffusion flux rate, which is dependent on the concentration of low molecular weight phosphorous in solution and the temperatures of the solution.

In addition, the linear uptake rate may be affected by fluctuation water flow past the membrane. In consideration of the above factors, monitoring data rather than theoretical estimates was used to calculate the maximum deployment time that would results in 50% capacity. In addition, DGTs were deployed in the free flowing water in the middle of the streams to optimize linear water flow.

Biofilm development: Biofilm may accumulate on the surface of the filter membrane of DGT samplers during long deployment periods. This may affect the thickness of the diffusion layer and/or modify the diffusion coefficient (Pichette et al. 2009). Use of toxic metals (copper or silver iodide), physical barrier or coating has been used to try to solve this problem. These techniques have shown success to a certain level but do not fully eliminate the problem (Uher et al. 2012)..

In a biofilm development study in fresh water aquaculture, Pichette et al. (2009), observed that biofilms development was more pronounced on the DGTs deployed for 14 and 21 days than those deployed for 7 days and less. They therefore recommended field deployment of a maximum of 14 days (Pichette et al. 2009). In consideration of the above discussion, DGTs were deployment in the rivers for 7 days and in the reservoir for 10 days both due to capacity limitation and also to avoid the development of biofilms.

3.3 Sampling

3.3.1 Sampling the catchments

DGT sampling was limited to the local watershed since this was believed to be the main source of phosphorous to the reservoir according to (Chapter 3.1.6). Focus was therefore given to the streams and rivers that drain into the reservoir from the local catchment. Nine sites (3 main rivers, 2 headwater streams, two fish ponds and 1 site on the reservoir) were identified as the most interesting points for sampling as based on Chapter 3.1.6 and also based on land use.

Figure 17: DGT sampling

Table 3 lists the sampling points in the rivers and headwater streams, with information regarding the land-use composition in their respective catchments. The selection of the rivers and streams was aimed at capturing runoff draining catchments with different land-use, as this is considered to be the main explanatory factor governing differences in nutrient contribution to the reservoir. The sites were sampled 2-3 times using three parallel DGTs that were immersed at the same depth to obtain representative sample. Sampling deployment duration was 7 days for the rivers and 10 days for the reservoir. The calculation for the deployed period is given in appendix A-2.

Table 3: Sampling sites and their respective land-use

Catchment	**Site name**	**Dominant Land-use**		**Land-use composition (%)**	
Xiaogugezhuan river catchment (Basin 1)	Xiaojugezhuang bridge (#1)	Mountain and lowland	Forest and shrubs	Forest-Deciduous	37
				Shrubs	23
				Orchard	22
				Farm Land	8
				Other	10
Beixinzhuang river catchment (Basin 2)	Mashen (Yumaqiao Bridge) (#2)	Strongly influenced Lowland	Farmland and villages	Farm Land	44
				Residential land	19
				Other	37
	Beixinzhuang bridge (#3)	Large basin Mainly lowland	Orchard	Orchard	44
				Farm Land	11
				Residential land	11
				Other	34
Lin River catchment (Basin 3)	Baxianshan river bridge (#4)	Mountain background	Deciduous forest	Forest-Deciduous	62
				Orchard	17
				Other	21
	Lin river bridge (#5)	Large basin	Deciduous forest	Forest - Deciduous	40
				Shrubs	20
				Farm Land	20
				Other	20
Yuqiao Reservoir	YQ01			N/A	N/A

In addition to the DGT sampling, the rivers in the watershed were sampled by TAES throughout the year from 2012 to 2013 during the synoptic studies. A total of 348water samples were collected and analyzed by TAES. Synoptic water sampling was done both during dry periods (Fall, Winter and Spring) and during the wet season (During the 1st storm flow peak and after a prolonged wet period). Episodes were captured through intense sampling capturing a sampling during heavy rainfall/storm flow periods.

The land use of the sampling sites are given in the figure 18 below, Xiaogugezhuan catchment is dominated by forest, shrubs, farmland and orchards and therefore can be categorised into a

mixed land use. Mashen (Yumaqiao) is predominately agricultural catchment with some settlements/residential. Beixinzhuang catchment is agricultural land which is mainly under orchards. Baxianshan is purely a forest catchment though some orchards can also be found. Lin catchment comprises of forest, shrubs, farmland in almost equally proportion, therefore it can be viewed as a mixed catchment though it composition varies from Xiaogugezhuan.

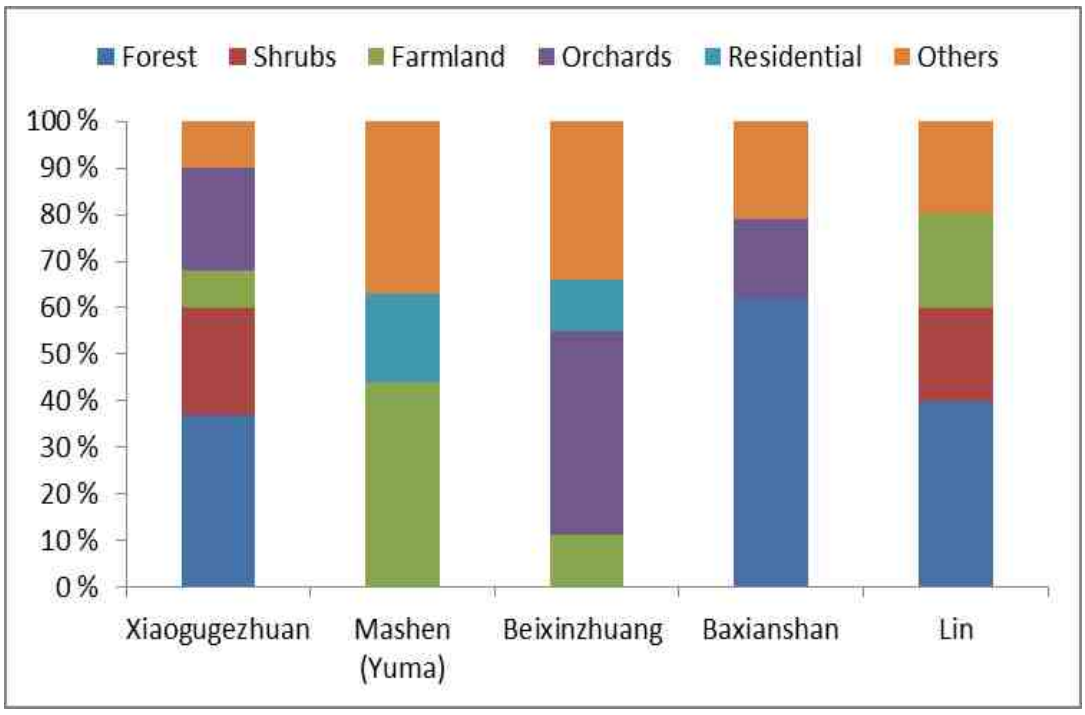

Figure 18: Land use of the DGT sampling sites

3.3.1.1 Main drainage basins

The local watershed consists of three major drainage basins drained by three rivers: Xiaogugezhuan river, Beixinzhuang river and Lin river. These rivers were monitored in order to determine the differences in P fractions between each stream as dictated by the land use and farm practises, as well as temporal fluctuation in P fractions due to seasonal variation in runoff. The two small headwater sub-catchments, represented mainly by 1st order streams, were selected within these basins (figure 19)

Figure 19: DGT river sampling points (Map: Courtesy of Zhou Bin)

3.3.1.2 Xiaogugezhuan river basin

Xiaogugezhuang basin is considered a mixed land-use catchment with mainly mountain forest (37 %) and some shrubs (23 %). Less than a third of the land is managed, manly as orchard (22 %) and some agriculture (8%). This sampling point is represented by point #1 in the figure 19. (Data: TAES, 2013)

Monitoring data from TAES shows increased P fluxes between the month of July and September mainly as a result of precipitation (See figure 20)

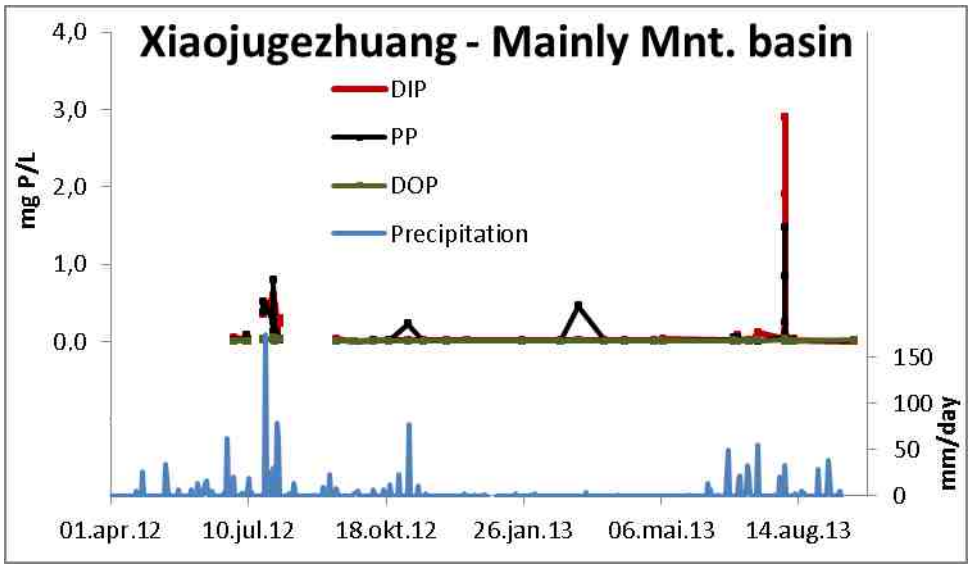

Figure 20: Concentrations of Phosphorus fractions in Xiaojugezhuang River (Data: TAES 2013**)** along with daily amounts of precipitation

3.3.1.3 Beixinzhuang river basin

In order to better capture the differences in land-use the Beixinzhuang river basin (marked as Basin 2 in Fig. 15) was divided into two sub-catchments, Mashen/Yumaqiao bridge (Point #2 in figure 19) and Beixinzhuang bridge (Point #3 in figure 19). Yumaqiao bridge sampling point represents runoff from a lowland watershed dominated by agricultural land (44 %) and residential area (19 %) (Data: TAES, 2013). The nutrient load from this sampling point was interpreted to represent the effect of agricultural practises and probably the sewage that is applied to the fields.

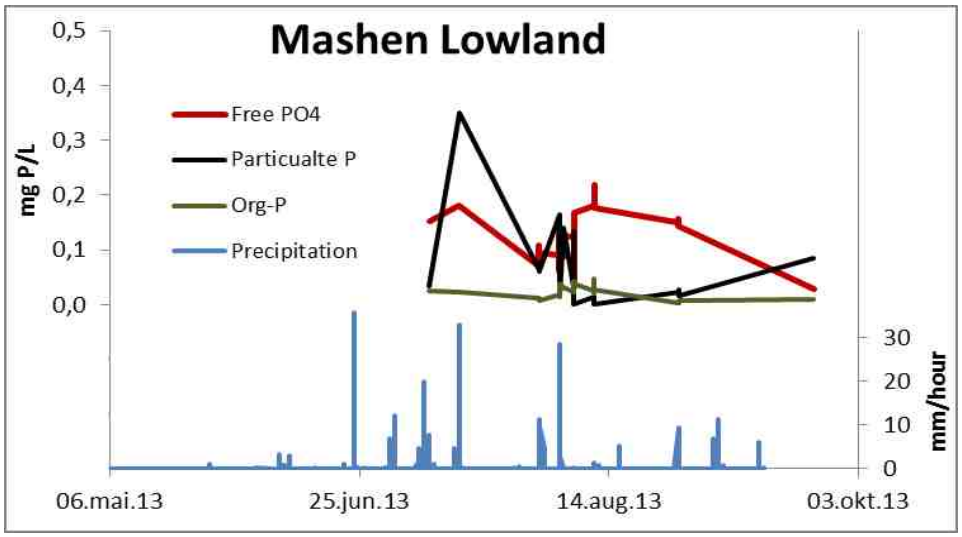

Figure 21: Concentrations of Phosphorous fractions from Yumaqiao bridge (Data: TAES 2013) along with daily precipitation

Beixinzhuang bridge sub catchment was chosen to represent the total outlet load from Beixinzhuang river basin. It basically drains managed land and some settlements. Most land is used for orchards (44 %) and 11 % is used for agricultural practises. The residential area constitutes 11 % of the sub-catchment (Data: TAES, 2013**)** Monitoring data from TAES shows increased P fluxes between the month of July and September mainly as a result of precipitation **(See Figure 22)**

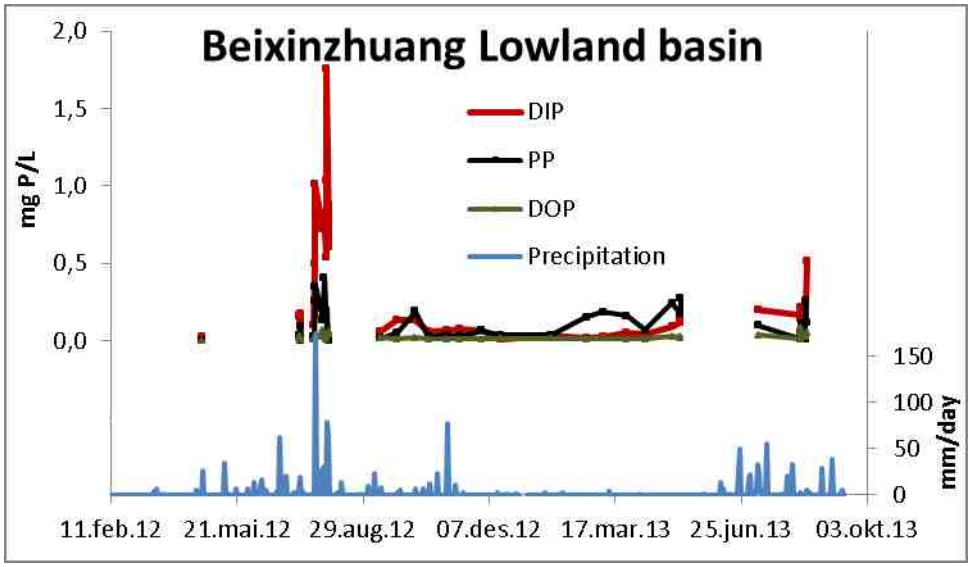

Fig 22: Concentrations of Phosphorous fractions from Yumaqiao bridge and Beizinzhuang river catchment (Data: TAES 2013) along with daily precipitation

3.3.1.4 Lin river basin

To appropriately investigate P contribution of this catchment, two sub catchment were sampled, Baxianshan river sub-catchment and Lin river bridge sub catchment. Baxianshan river sub-catchment which is represented by point #4 in figure 19 is basically a mountainous catchment with natural forest. Of this catchment, 63 % is under natural forest cover with only 17 % under orchards. This catchment was selected to give the background load which is basically attributed from the natural forest. This was important as it acts a baseline for the other loads which are more influenced by the human activities such as agriculture and settlements.

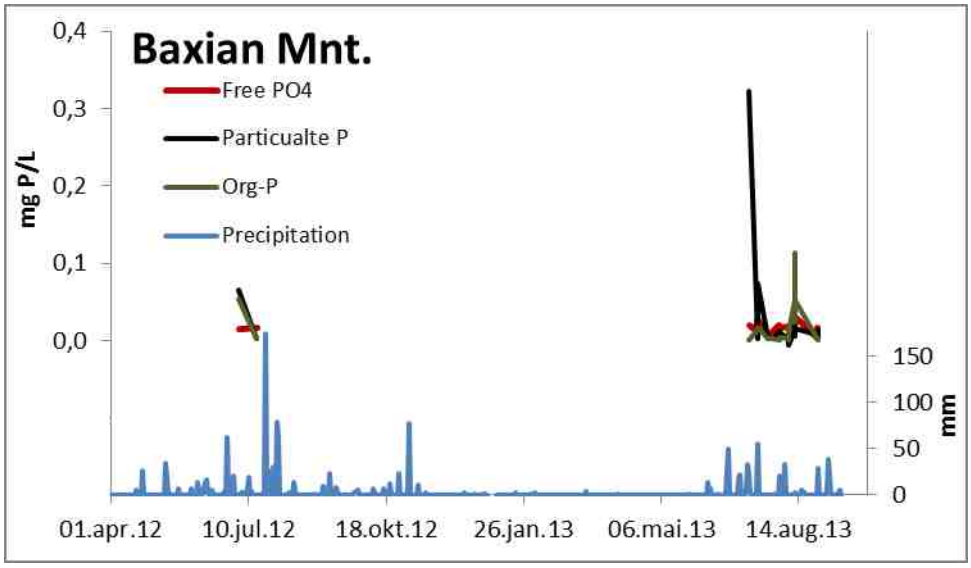

Fig 23: Concentrations of Phosphorous fractions from Yumaqiao bridge and Beizinzhuang river catchment (TAES 2013) along with daily precipitation

The total outlet of the Lin river catchment was also sampled to determine the total load from this river basin. Sampling was done at the Lin river bridge which is represented by point #5 in figure 19. The catchment is mainly comprised of forest with 40 % of the land under forest and additional 20 % under shrubs with only 20 % under agriculture

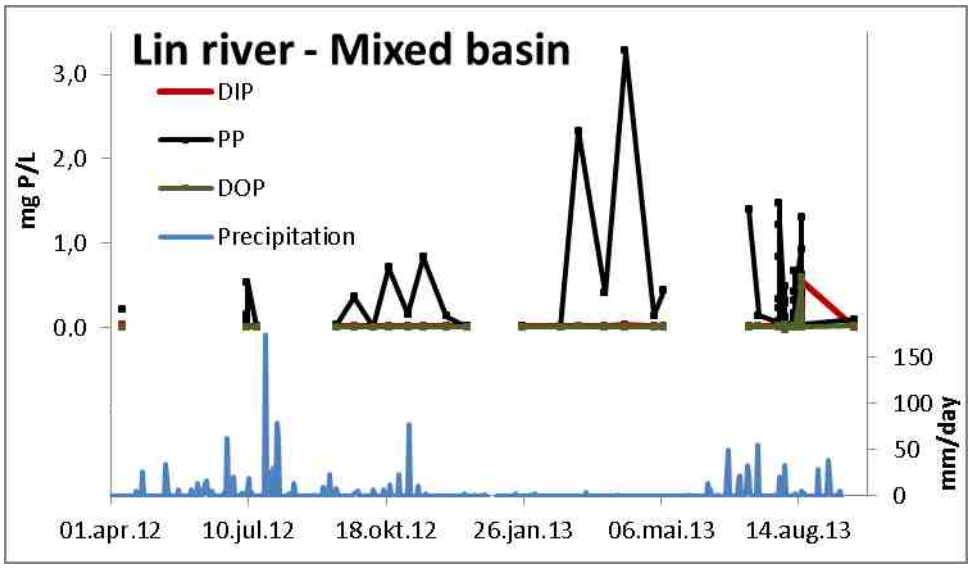

Fig 24: Concentration of Phosphorous fractions in Lin river catchment (TAES 2013) along with daily precipitation amount

3.3.1.5 Yuqiao Reservoir

Yuqiao reservoir has 15 sampling point that are routinely monitored by RCEES for nutrients. Sampling using DGT was done at Sampling point YQ01, which is the point at which the water exits the reservoir to Tianjin City (figure 25).

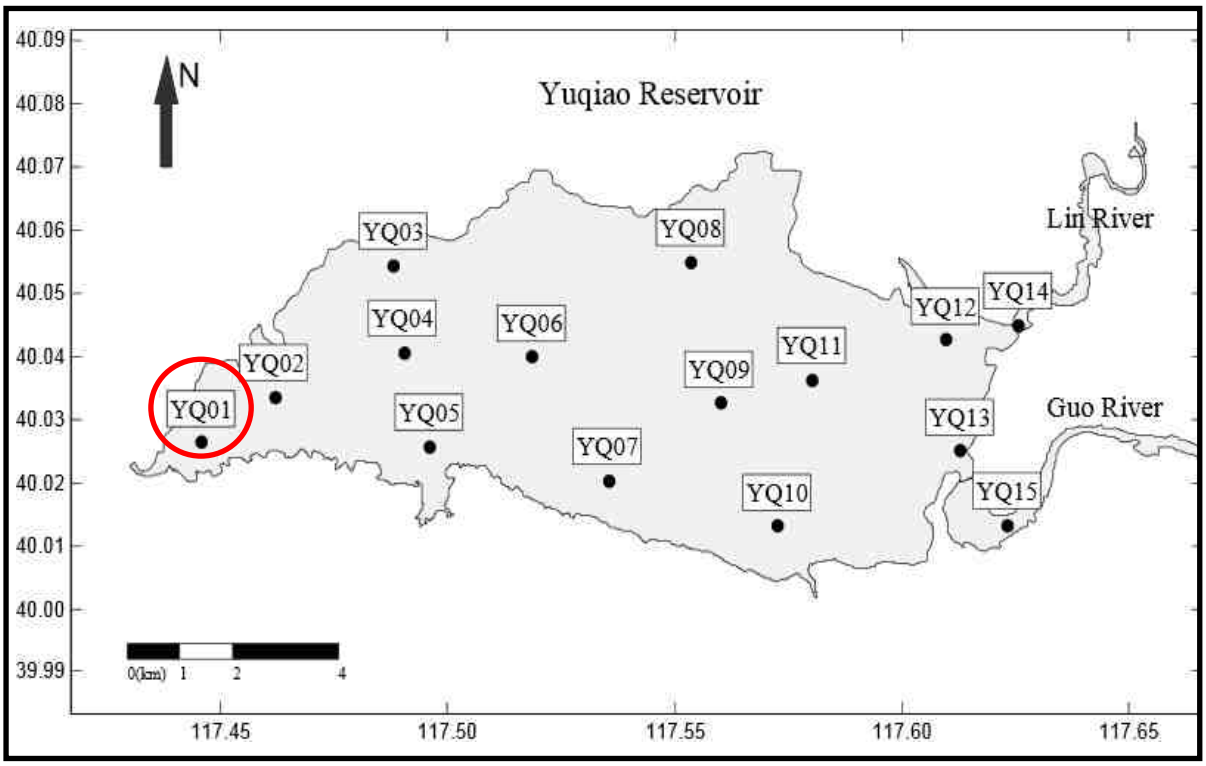

Figure 25: Sampling point using DGT at Yaquiao Reservoir (RCEES, 2013)

3.3.1.6 Fish Ponds

There are about 340 fish ponds around Yuqiao reservoir that covers an area of 11.2 km^2 breeding fish species such as carps, crucian, grass fish, chubs, etc (EPA and TEPB 2005). The fish are fed on food left overs or livestock waste at least once a day. Fingerlings are introduced in the ponds in spring (April) and the mature fish is harvested in October. Water supply is either from direct pumping from the reservoir, seepage or shallow wells which are supplied by the reservoir. Water is aerated through electric pumps and discharged through movement to another pond or preserved in other ponds. However the movement of water is not 100% sufficient with the lost nutrient rich water ending up in the reservoir (EPA and TEPB 2005).

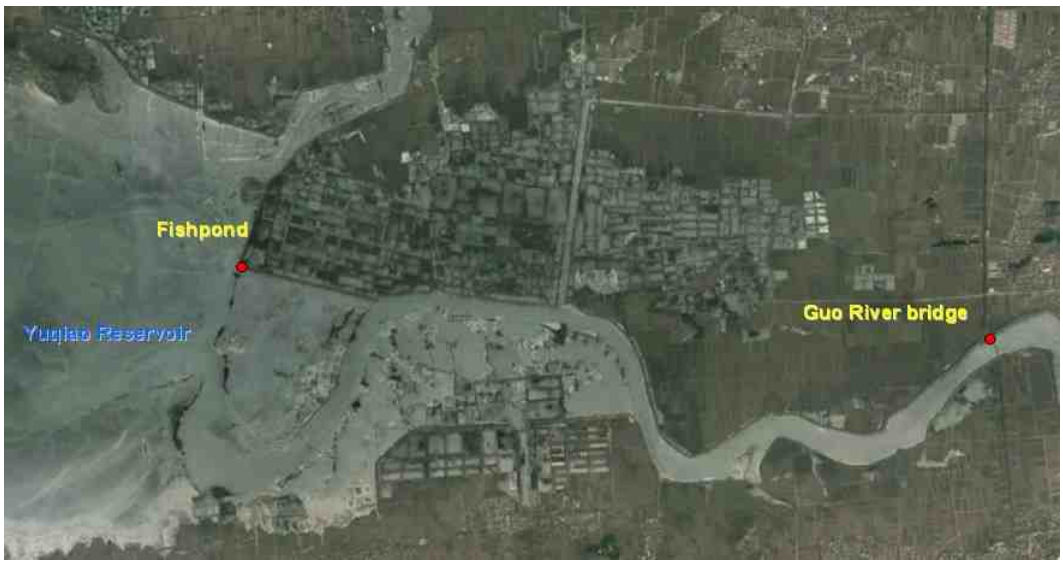

Figure 26: Location of the sampled fish ponds

Two fish ponds were sampled (figure 26), one of which is currently in use and the other which has been abandoned and decommissioned but is still filled with water. The sampled fish pond in use represents one of the numerous fish ponds along the shores of the reservoir. The abandoned fish pond was located near Lin river bridge. During flooding, these fish ponds overflows and the excess water drain into Lin River. This might be contributing to the P loads into the Lin river hence the sampling done is to determine the significance of this source of P flux to the reservoir.

3.3.2 DGT Sampling

Handling: The DGTs were stored in a refrigerator prior to use and were not removed from their original plastic bag until immediately prior to deployment. This was done in order to keep the DGT moist and minimize contamination.

Deployment: The deployment of the DGTs was achieved by placing the DGTs in a sealed polypropylene net tube, anchored by a stone at one end and tied on the other with a rope to a branch or tree (figure 27). Only one depth of sampling was used for the rivers while three depths (0.2M, 3.0M and 7.0M) were sampled in the reservoir to carter for the reservoir stratification during summer. The DGTs were placed at the middle of each layer of each sampling site to ensure representative samples. In the rivers the DGTs was deployed in flowing water but care was taken to avoid excess turbulence as this might interfere with the diffusion gradient due to fluctuation in DBL layer.

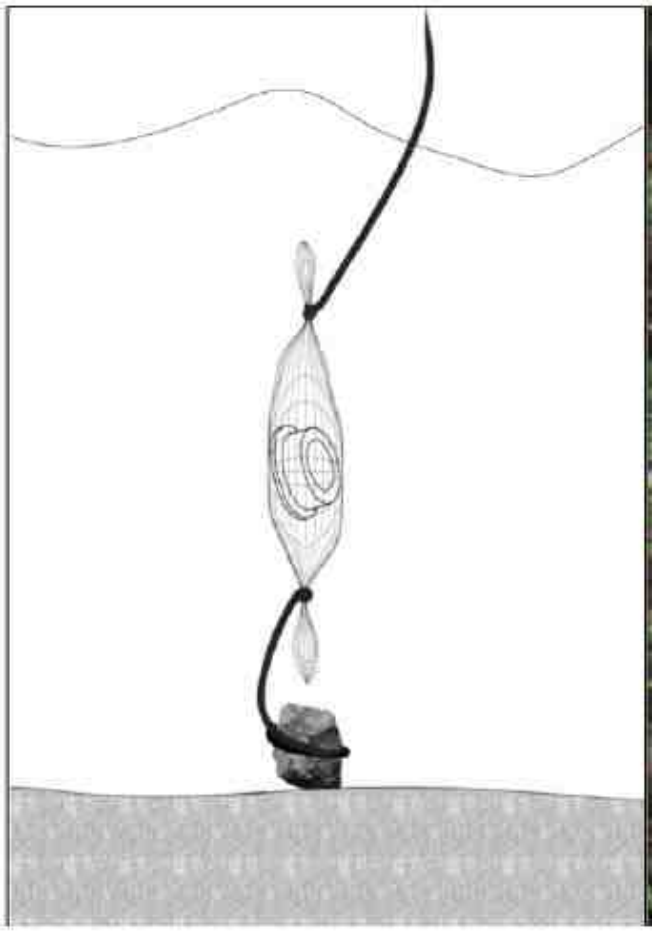

Figure 27: Illustration on how DGTs were deployed in the field (Mohr 2010) **(Mohr 2012)**

Retrieval: After the completion of the sampling period, the sealed polypropylene net tube that contains DGTs was retrieved taking care not to touch the filter face. The DGTs unit was then rinsed with water from the sampling site and the excess water was allowed to drain off, though ensuring that the DGTs did not dry out. The DGTs units were then put in a clean plastic bag and sealed with minimum air space. The samples were marked appropriately (date of installation, end of deployment date, sampling point, depth, DGT no, etc.) and then stored in a refrigerator till shipment to the Department of Chemistry, UiO, for analysis. A total of 57 DGTs samples were collected during the sampling period and the summary is given in the Table 4 below.

Table 4: Summary of DGT sampling exercise

Site	Frequency	Parallel	Total
Xiaojugezhuang bridge	2	3	6
Mashen (Yuma) bridge	3	3	9
Beixinzhuang bridge	3	3	9
Baxianshan bridge	2	3	6
Lin river bridge	2	3	6
Fish pond	2	3	6
Abandoned fish pond	2	3	6
Reservoir – Upper depth	1	3	3
Reservoir – Middle depth	1	3	3
Reservoir – Deep depth	1	3	3
Grand Total			**57**

3.4 Analysis methods

Analysis of the DGTs and filtered particles were done at the department of Chemistry, UiO while water parameters were done in China by TAES. Water sampling and analyses were carried out according to the scheme shown in figure 28. TAES was responsible for sampling and analyses of river water and soil water, RCEES for reservoir water and UiO for particle characterization.

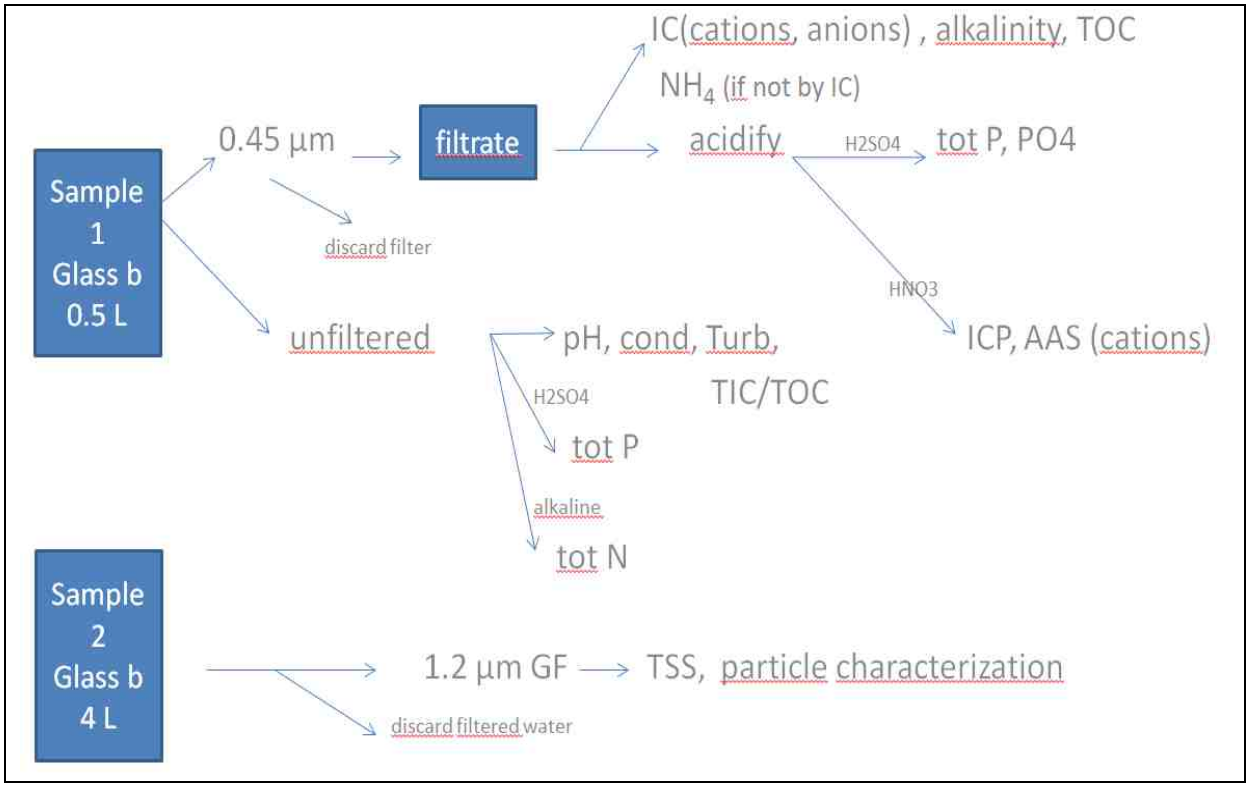

Figure 28: Flow scheme for water sampling and analyses

3.4.1 Water filtration and determination of Loss of Ignition (LOI)

Loss of ignition (LOI) is done to determine the organic matter of the particulate P. All river and stream water samples were filtered and analysed for different PP pools. Filter paper of 0.7µm GF/C was used for filtration in order to determine the organic and inorganic matter content of the particles. Details of the analysis procedure is given in appendix A-2

3.4.2 Filter paper selection

Filter papers were selected to represent rivers during low flow and also following complete episodes for each of the site. Selection was done to correspond to the main sampling period and sites. Episodes were selected based on the concentration of TDP and Particulate P as represented by the monitoring data from TAES (See figure 29). This was done for all the five sites. A total of 67 filters papers were selected from a total of 348 filters collected between 2012 and 2013.

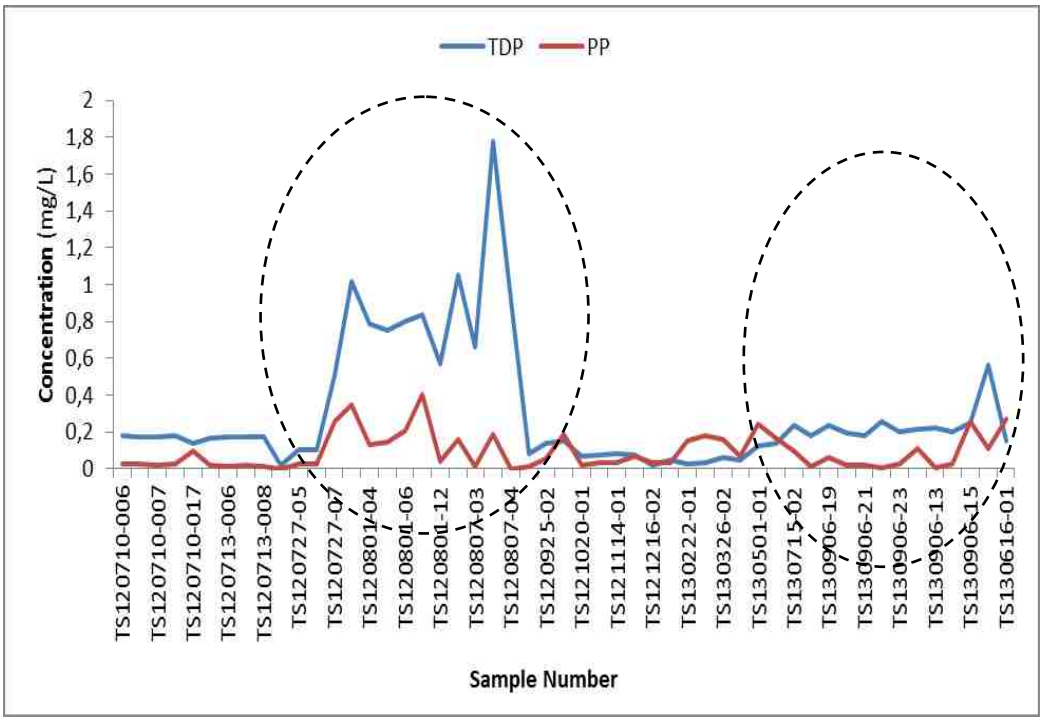

Figure 29: Filter paper sample selection criteria

4.4.3 Analysis of particle on the filter paper

Upon arrival in Norway the burned filter papers were stored at 4^0C till the time of analysis. **Five** blanks filters were prepared through the same procedure as the real samples, through filtration of 1.5L of Type II in place of the river water.

Several procedures were tested to separate the particles from the filter as the filter paper would create interference in analysis and also make the analysis difficult in many types of equipment. Therefore, a separation method with microwave digestion was employed that was able to digest all the inorganic particles without dissolving the glass fibre filter. This was achieved through the use of nitric acid as the other acids and acid mixture resulted into partial digestion of filter paper. Qualitative and quantitative analysis were conducted to provide information on the mineral composition of the particle on the filters. Mineralogy of the crystalline particles was determined by use of X-Ray diffraction and the composition of total cations (Na, Mg, Al, K, Ca, Mn, Fe and Si and P) was determined by ICP-OES on the digested sample

4.4.3.1 X-Ray Diffraction (XRD)

XRD stands for X-ray diffraction, an instrument used for qualitative and quantitative analysis of solid crystalline samples. When X-ray passes through a sample matter the radiation interacts with the electrons in the atoms of the crystalline matter to produce scattering. Scattering can results in both constructive and destructive interference of the rays. This is because the distance between the scattering centres are of the same order of magnitude as the wavelength of the radiation. When an X-ray beam strikes a crystal surface at some angle θ, part of the beam is scattered by the layer of atoms at the surface. The un-scattered part of the beam penetrates a second, third and the other subsequent atoms layers in the crystal. The cumulative effect of the scattering from the regularly spaced centres of the crystal is measured as the diffraction of the beam. The condition for constructive interference of the beam at an angle θ is given by the *Bragg equation* below (Equation 1)

$$n\lambda = 2d \sin \theta \qquad \text{Equation 1}$$

Where d is the inter-planar distance of the crystal, θ is the angle of incident ray, n is an integer of the order of diffraction and λ is the wavelength of the X-ray. The identification and quantification of the identified minerals can then be done using computer programs (EVA and TOPAS).

Each filter paper sample containing particles and blank filters were mounted on the XRD machine sample holder and the edges attached by a thin tape to fix it still in place for the reading done at angle range 2 – 70 degrees. Blanks readings were used for base correction of the filters so as to eliminate the effect of the filter paper.

4.4.3.2 Microwave digestion of particles on filter

In order to accurately analyse the content and composition of a given sample, it is a practice to convert the solids into aqueous homogenous solution by oxidation, reduction or complexion reactions. This can be achieved through open system or closed system, such as microwave oven. Microwave oven digestion in a closed system has proved to be the most suitable method for the digestion of complex matrices such as soil, suspended solid matter and sediments. Some of the advantages of this method are that it reduces digestion times, it reduces the risk of external contamination and requires smaller quantities of acids, thereby improving detection limits and the overall accuracy of the analytical method.
The microwave oven used for digestion was the Milestone ETHOS 1600 microwave oven equipped with ten 100mL high pressure PFA Teflon vessels.

A third of each sample filter papers and blanks were cut using a clean scalpel, accurately weighed and transferred into the microwave Teflon vessels and marked appropriately. Digestion was achieved through the use of 10mL of 65% Nitric acid (HNO_3), v/v of super pure analysis quality (Merck Darmstadt, Germany). Microwave blanks were also prepared by having acid only in the Teflon vessel. The instruments settings were as per appendix B-3.

4.4.3.3 Analysis of elemental composition of the particles on the filters

The analysis of the major cations (Na, Mg, Al, K, Ca, Mn, Fe, Si) and P in the digested particulate samples was done by ICP-OES using ISO 22036 (2008) as a guide line. The ICP-OES functions by measuring the light that is emitted after the analyte has been excited in the high temperature plasma (6000-10000K). The wavelength of the emitted light is specie-specific, and by using the plasma, both atom and ion lines can be obtained. The analysis was performed using Varian (Australia) Vista AX CCD simultaneous axial view ICP–OES equipped with V-groove nebulizer with Sturman-Masters spray chamber. Auto sampler sample introduction method was used and the instrumentation parameters set as per appendix B-4.

4.4.4 Phosphorous analysis

From the cold room, the DGTs were rinsed with Type I water, placed on a clean surface and opened with a screwdriver to expose the resin gel. The gel was picked with a plastic tweezers and dropped at the base of a 50mL propane tube. The elution of the gel was achieved by adding a mix of 0.5mL of Type I water and 0.5mL of 4M H_2SO_4 and left overnight. After the overnight elution a further 49mL of Type I water was added and the solution mixed well before analysis by Molybdate Blue Method (MBM) following the ISO standards (ISO 6878, 2004) for DIP and TDP by ICP-MS. Blank DGT samples were eluted in the same manner as the DGT samples after being immersed in Type I water for 2 days to obtain moisturation.

To identify the best method for the analysis TDP and DIP in the DGT, seven DGT samples representing each site were selected and analysed for orthophosphates according to ISO standards (ISO 6878:2004). However it was found out that the difference between TDP and DIP was negative for all samples, implying erroneous negative concentrations of DOP. Therefore repeat experiments and dummy samples were used to investigate the problem, but that unfortunately did not solve the problem. It was therefore decided that analysis of TDP would be by use of ICP-MS, but that the calibration of both the spectrophotometer and ICP-MS be done using the same calibration standards. This is because calibration by different standards resulted in inconsistency of the results. The interference of the iron content of the DGT in the MBM method was ruled out through measurement of the DGT iron concentration using ICP-OES. According the ISO standards (ISO 6878:2004) for MBM measurement, iron

concentration of more than 10mg/L results in 5% reduction in colour intensity. However all the measured samples had iron concentration of 9mg/L and below. More on the comparison of P measured by MBM and ICP-MS is being undertaken by Agaje Bedemo Beyene in his PhD study.

4.4.4.1 Determination of DIP by Molybdate Blue Method (MBM)

Determination of DIP (orthophosphates) in the DGTs was determined by molybdate blue method (MBM). This method is based on the principle that orthophosphate reacts with ammonium-molybdate to form a yellow-coloured phosphorous-molybdate acid, which is then reduced with ascorbic acid in the presence of antimony to form a strongly blue coloured complex. The blue colour correlates to the concentration of phosphates. The intensity of the blue colour can be determined spectrophotometrically at absorbance of 880nm. Analysis was done following ISO standards (ISO 6878:2004). Chemicals and reagents were prepared as per appendix B-1.

4.4.4.2 Determination of TDP by ICP-MS

This analysis of total P in the DGT samples was done using a Parkin Elmer Inductive Coupled Mass Spectrometer (ICP-MS), NexION^{TM}, using standards and kinetic energy discrimination mode. ICP-MS functions by ionizing the different analyte species in the high temperature plasma (6000-10000K). The analytes are separated from each other in the mass spectrometer based on their specific mass to charge ratio (m/z). Manual sample introduction method was used and the instrumentation parameters set as per Appendix B-2**.**

3.5 Quality control and quality assurance

Quality control (QC) and quality assurance (QA) were followed during the analytical procedures. These were achieved through the blank samples, replicate samples and use of internal standards. Calibration blanks and standards were run before, after every 10-15 samples and at the end of the analytical measurements. This was done in order to correct for the instrument drift and limit carry over from batch samples. Method blanks for blanks and filters were run after being treated in the exact way as regular samples. In addition, microwave acid blanks were included in each digestion session. Limit of detection (LOD) and limit of quantification (LOQ) was determined by use of blank method. Calibration blank of standard zero was used for phosphorous LOD determination for MBM and ICP-MS measurements while microwave acid blank was used for determination of LOD of the major cations and P as measured by ICP-OES. Specific details on the blank values used for the calculation of LOD and LOQ are presented in the appendix D for each instrument.

DGT parallel and sample replicates were analysed to measure the reproducibility of the sampling process. Relative percentage deviation (RPD) was calculated for all the replicates samples and the results are summarised in the appendix E. Calculations show decent reproducibility for samples above LOD and huge deviation for samples below LOD. In addition G-value test was performed on the DGT data, all the values were found to be valid with the maximum and lowest value of 1.154 and 0.101 respectively (appendix E). Other statistical tests were not performed due to lack of availability of 3 data sets for the DGT and due to time constrains.

For determination of TDP and DIP, internal standard was employed. Internal P standard was prepared by Senior Engineer, Anne-Marie Skramstad. P measured was all within the acceptable range of ±10% **(**appendix D**)**. Two Certified reference materials (CRM) were used for the analysis of major cations from the filter papers. Determined concentration was to be within the acceptable standard deviation values of the certified concentration. Detailed results are shown in appendix D.

3.6 Statistical Analysis

Calculation of means and standard deviations, G-test, and calculation of RPD were calculated in excel (Microsoft Office 2010) while charts plots were done in R 2.15.2. Details are explained in Appendix E. All the values below LOD were treated as LOD/2, such that all samples could be included in the statistical assessment of the results. Further statistical tests were not done due to the lack of 3 sets of data for the DGTs and also due to time constrains.

3.7 Uncertainty

Analytical uncertainties could be due to systematic and random errors. Possible errors could be due to sample storage and transport, loss of analyte, sample contamination, pipetting error, weighing of the samples, and dilution of stock solution/preparation of calibration standards. Uncertainty in of the DGT sampling and calculation could be attributed to temperature, DBL layer, DGT exposed area, sample window, membrane resistant and estimation of diffusion coefficient. Due to time constrains the author could not be able to do much in uncertainty calculation and therefore just pointed out the sources of uncertainty in the measurements. However due to time constrains the author was not able to calculate the uncertainties.

4.0 RESULTS AND DISCUSSION

There are multiple factors that govern the temporal and spatial distribution of P fractions in river water. Key among them is land use which can be used as a proxy for the distribution of different P fractions in the rivers. It is also stipulated that other explanatory variables such as runoff characteristics and physiochemical parameters of the soils are hugely influenced by land use. Therefore, in this study, land use was used as an explanatory parameter and hence the rivers are categorized based on their catchment land use. The land use as discussed earlier (chapter 3.3.1 and table 3) are categorized into five main groups namely forest, mixed 1, mixed 2, farmland and orchard.

- Forest represent the mountain catchment of Baxian,
- Mixed 1 represent the large mixed Lin river catchment,
- Mixed 2 represents the mountain catchment of Xiaojugenzhuang,
- Farmland represent the low land catchment of Yumaqiao/Mashen and
- Orchard represents the low land basin of Beixinzhuang.

4.1 Stream water chemistry

In order to understand the hydro-geochemical processes governing P mobility and transport in a watershed, it is important that water chemistry is characterized and understood. Water is both a transport medium and matrix for P chemistry. Fractionation, speciation and thus mobility are therefore influenced by the water chemistry. Water chemistry was assessed as discussed in chapter 3.4 and presented by figure 28. The data used in this section is from **227** samples collected and analyzed by TAES during 2012 and 2013 (Appendix C). Some of the river chemistry parameters are discussed in the subsequent chapters.

4.1.1 pH and alkalinity

pH is a measure of acidity and also determines the hydrolysis extent and ions speciation in water while alkalinity is the ability of water to neutralize acid inputs. Low pH and alkalinity is governed mainly by presence of organic acids in the dissolved organic matter while high pH and alkalinity is governed by the weathering of carbonates rocks or liming of the soils. There is no observed considerable significance different in pH values (Figure 30) but significant difference in bicarbonates from different land use could point out to the different hydro-geochemical processes governing the water chemistry of the sampled rivers as dictated by their and land use.

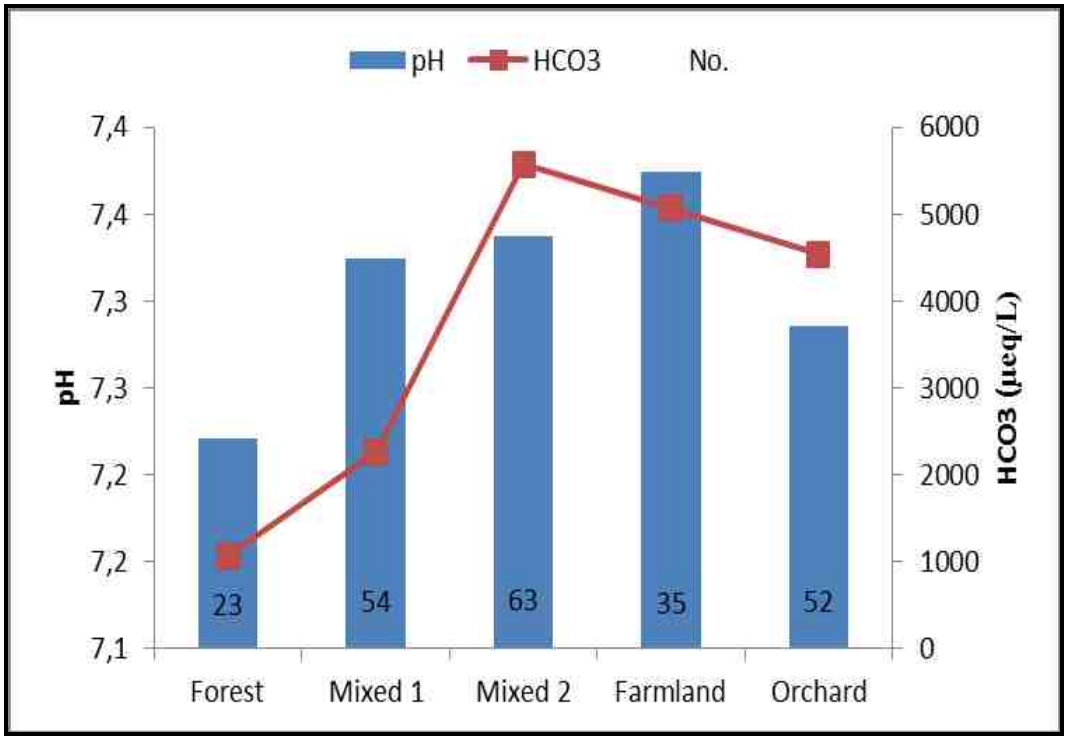

Figure 30: The stream pH and alkalinity (No of samples are given in each bar)

The results show that the river pH values are between 7 – 7.5, which is the pH range where P is dominated by the precipitation by Ca. These pH values are likely due to the buffering through weathering of carbonates rocks and liming of the agricultural soils.

The slightly lower pH in the runoff from the forest dominated watershed could be attributed to organic acids derived from the dissolved organic matter while high pH in farmlands is mainly through carbonates buffering and liming as these catchment are agriculture and human

influences. The expected precipitation of P by Ca at these pH could significantly increase the amount and concentration of river particulate matter and thereby the particulate P.

4.1.2 Major Cations and Anions in the rivers

In aquatic environment, the amount and composition of major cations and anions can be used as an indicator to the process governing weathering and leaching of elements from soil. The average composition of the major cations and anions of the sampled rivers are shown in the figure 31 below. There is large charge discrepancy in the runoff from the watershed dominated by farmland. The cause of this is unknown and will need to be further accessed. The ionic strength is lowest in the runoffs from forest and rather similar between other streams. The cation composition of the water chemistry is rather constant. The major cations are dominated by Ca^{2+} and Mg^{2+}. The amount of Ca^{2+} is commonly found to be 20% higher than Mg^{2+}, a ratio maintained through weathering of dolomite and ion exchange with the soil. The major anion is generally HCO_3^- though in the slightly more acid runoff from mountain forest the concentration of bicarbonate is relatively low, allowing SO_4^{2-} to be the dominant anion. The sulphate is likely derived from oxidation of pyrite.

The concentration of nutrients K^+ and NO_3^- are surprising low in the runoff from the farmland and orchard dominated watersheds relative to the runoff from mainly forest and the two mixed land use watersheds, considering that one would expect a large contribution from fertilizers added to the former.

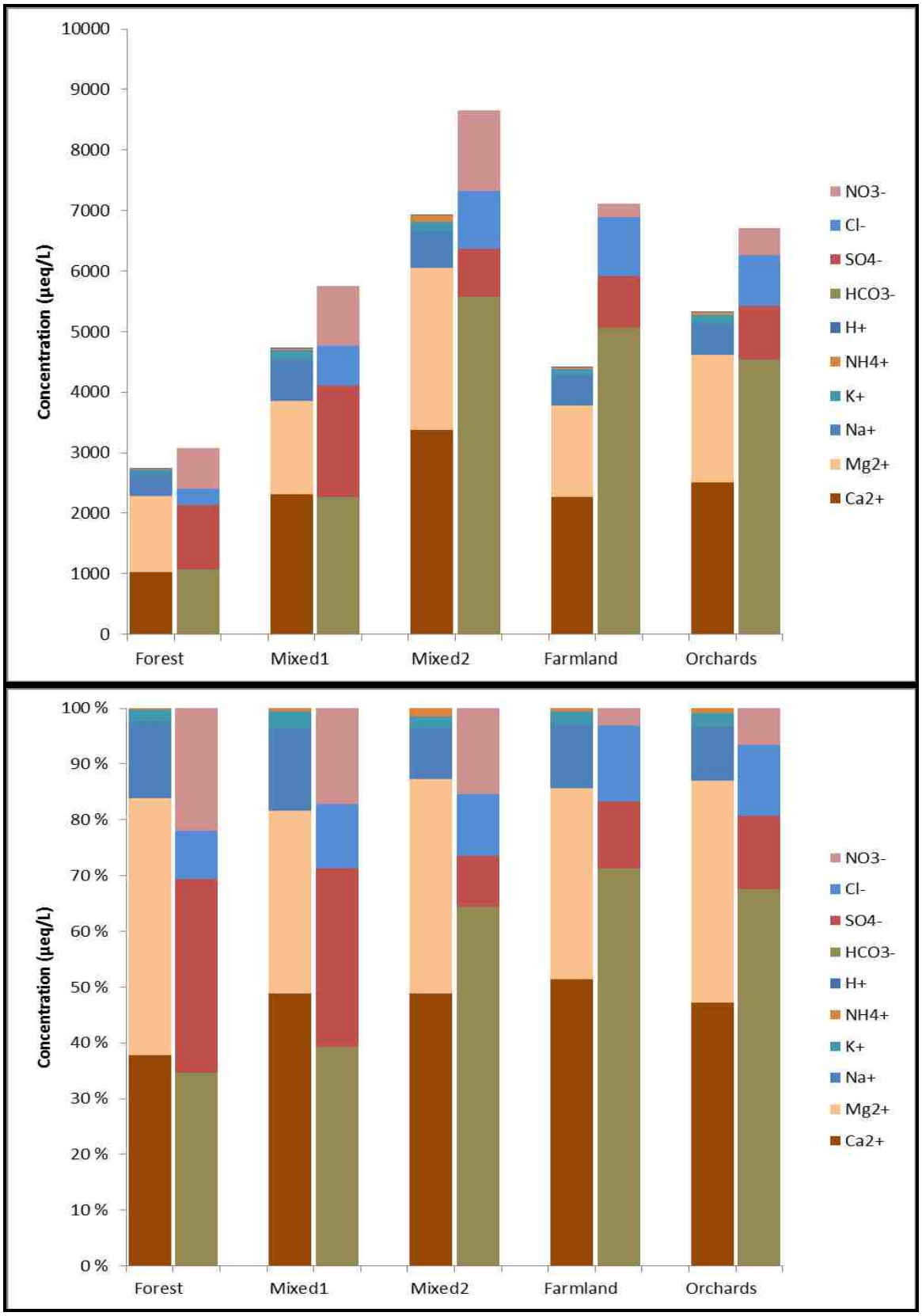

Figure 31: Concentrations (top plane) and relative charge contribution (lower plane) of average concentrations of major cations (left bar) and anions (right bar) in the river waters.

4.1.3 Major cations distribution with land use

The distribution of major cation with land use is given in the figure 32 below. The highest median concentration of Na^+ is observed in Mixed 1 and the lowest in forest. The median value concentration of 700 – 300µeq/L is observed in all the rivers except the forest that has value below 400µeq/L. The results indicate that there is no major significant difference in Na^+ from different land use except for forest. Na^+ is mainly derived from sea salt as the contribution by weathering of feldspars is assumed small in these soils. The low concentration in the forest is likely due to less evapotranspiration as the site is a mountain catchment with thin skeleton soil with limited water storage capacity. The soil in the area is also predominately by non-expanding 1:1 clay that is resistant to water adsorption.

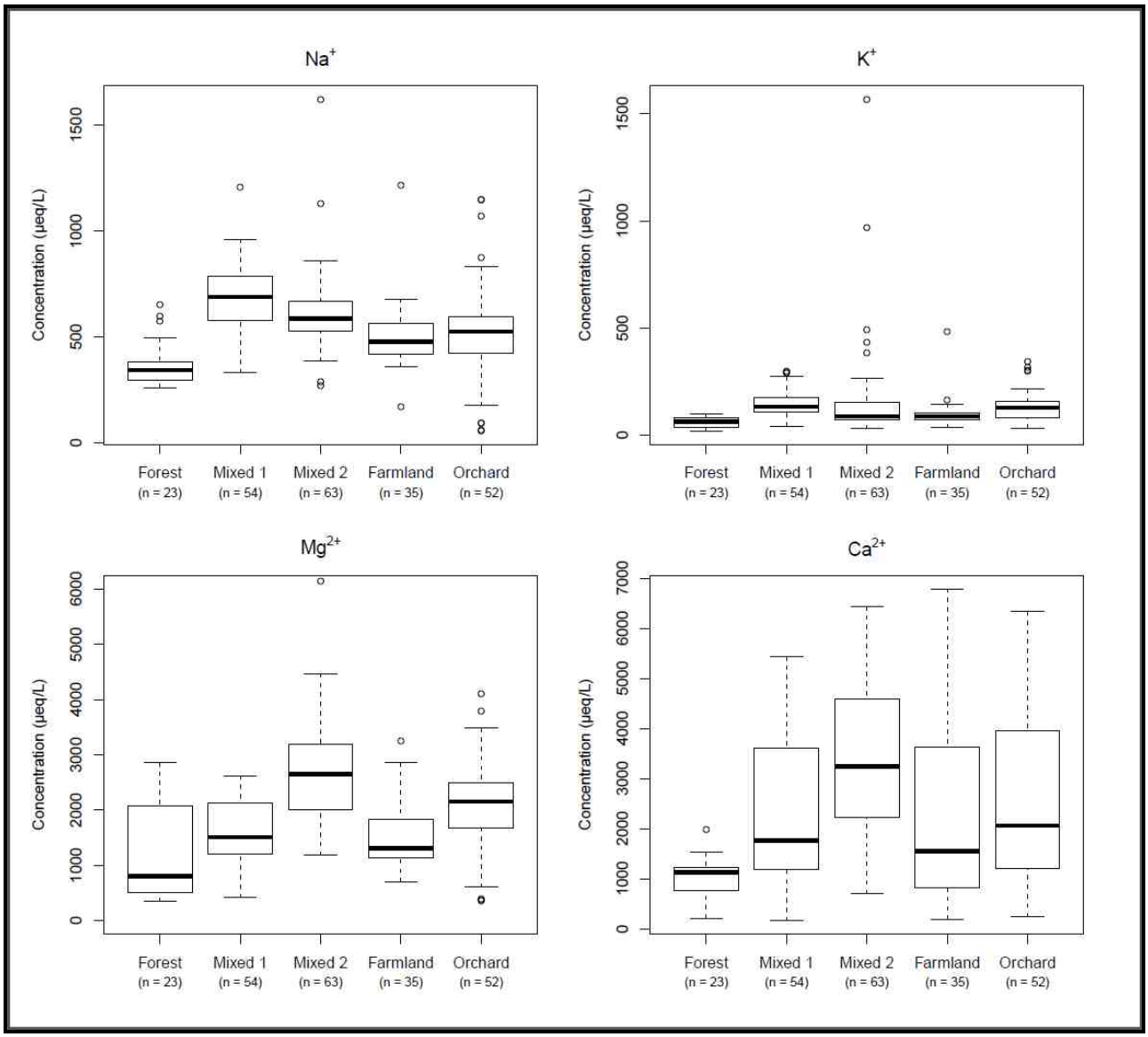

Figure 32: Variations in of the major cations by land use

Na^+ is mainly derived from sea salt or caused by lack of soil and soil water interaction. The latter is more likely the scenario in the forest as the site is a mountain catchment with thin soils depth that could limit soil and soil water interaction. The soil in the area is also predominately by non-expanding 1:1 clay that is resistant to water percolation.

The concentration of K^+ is basically the same for all the land use with the median concentration of about 100 µeq/L. K^+ is added to the soil through addition of fertilizers. Even though there is proven addition of fertilizers in the farmland and orchard, this does not translate to the elevated K^+ concentrations in the river water draining these catchments. Though the reason for the above may not be concretely stated the many outliers in sampling sites especially those observed in Mixed 2 which could be a factor to the observation made.

Concentration of Mg^{2+} shows significant variation and difference by land use with the highest median value of 2800µeq/L in Mixed 2 and lowest of 900µeq/L in the forest. Mixed 1 and farmland have close median value of about 1800µeq/L /L while orchard is slightly higher at 2800µeq/L. Farmland and orchards have similar concentration. The major source of the Mg is soil is through weathering processes and also liming of the soil.

Ca^2+ median concentration shows variations with land use, which could point to the effect of liming of the soils. The highest median value is found in Mixed 2 (3000 µeq/L) and lowest in the forest (1000 µeq/L). Ca^{2+} is the major component of the parent material in the study and its concentration is maintained through weathering of dolomite and ion exchange with the soil. The huge variation in the concentration of Ca^{2+} in Mixed 1, Mixed 2, farmland and orchard could point to the spatial variation in Ca^{2+} in these soils. The variation could be due to the liming of the soils, hydrological variation and management practices. The forest is composed of thin skeleton soil which could make natural weathering easier due to exposed parent material. The forest also being a mountain region, weathering could be enhanced through hydrological activities such soil erosion. The low Ca^{2+} in the forest is could therefore point to the fact that the natural weathering of parent material contributes less Ca^{2+} as compared to anthropogenic sources.

4.1. 4 River suspended particulate matter

The results of the averaged total suspended solids are given in figure 33. The highest loading of suspended particulate matter is in the large river draining Mixed 1 and the least is in the drainage water of the mountain forest, with particulate matter concentration of 477mg/L and 20mg/L, respectively. The concentration shows variation with land use, a factor that could be attributed to river volume and catchment size, soil and topography. The Mixed 1 stream is substantially different from the other streams. This is a large river draining a large watershed that has not been mapped in this study. It is apparent that major factors governing the high loading is the much greater flow and flow velocity of this river. The loading of suspended particles among the remaining rivers are in the sequence Forest < Orchard < Mixed1 < Farmland. This point to that the dominant land use is an explanatory factor. Farmland soils are more susceptible to soil erosion as a result of lack of perennial plants and tilling. These are factors that may significantly contribute to the observed elevated particulate matter in the runoff from predominantly farmland.

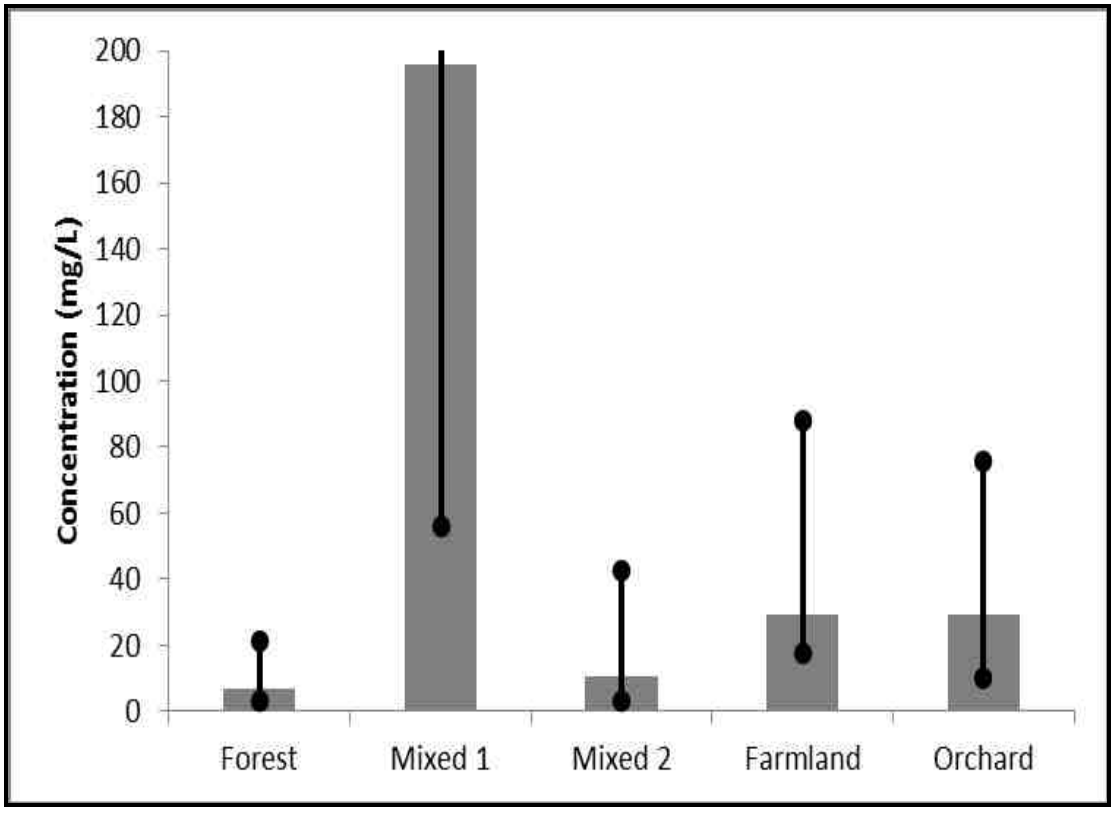

Figure 33: Concentration of suspended particles in the river water

The lowest concentration of suspended particle is found in the forest. This site is a mountain catchment with steep gradients that may be susceptible to soil erosion and thereby the increased eroded particle. The reason the erosion is low is due to the less amount of finer material in these soils (Pettersen, 2014) as well as the perennial vegetation cover and root system of the trees holding on to the soil

4.1.5 Phosphorous fractions in the rivers

The mean concentrations of P fractions are given in the figure 34**.** The sequence of total P (TP) concentration is from Forest<Farmland<Mixed2<Orchard<Mixed1. TP concentration for the forest, mixed 1, mixed 2, farmland and orchard are 64µg/L, 505µg/L, 295µg/L, 259µg/L and 393µg/L, respectively. Pettersen (2014), studying the soils in the local watershed, found the same sequence in the soil P concentration in Ap layer with 446mg P/Kg, 680mg P/Kg, 833 mg P/Kg for forest, farmland and orchards, respectively. Joshi (2014), also in a parallel study the soil in the watershed reported range of 150 – 3500 mg P/Kg with an average of 700 mg P/Kg for forest, farmland and orchards respectively.

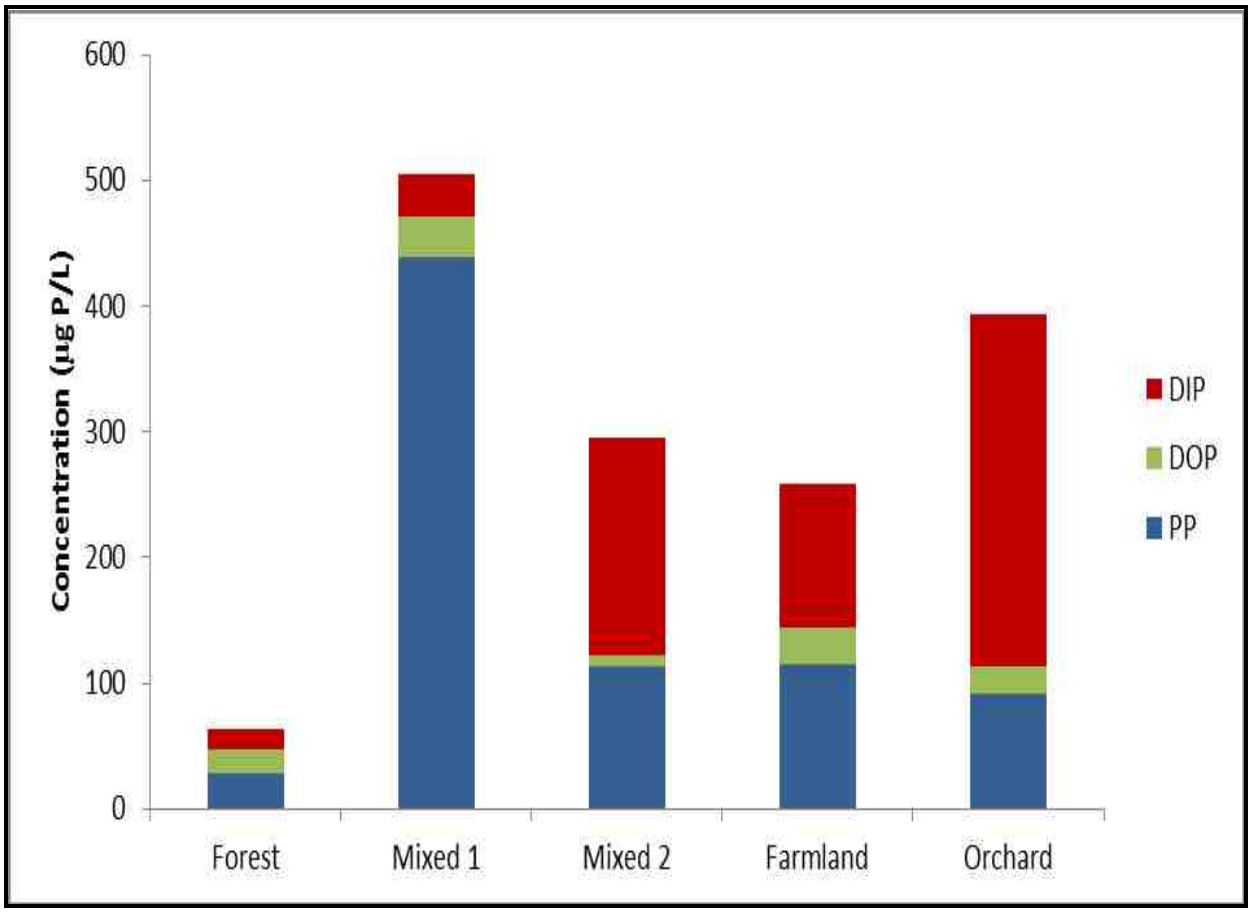

Figure 34: Phosphorous fractions in the rivers

The high concentration of Particulate P (PP) in the runoff from the Mixed1 is clearly linked to the high suspended particle loading of this river, despite that the mass fraction of P in the suspended particles is relatively low (figure 35).

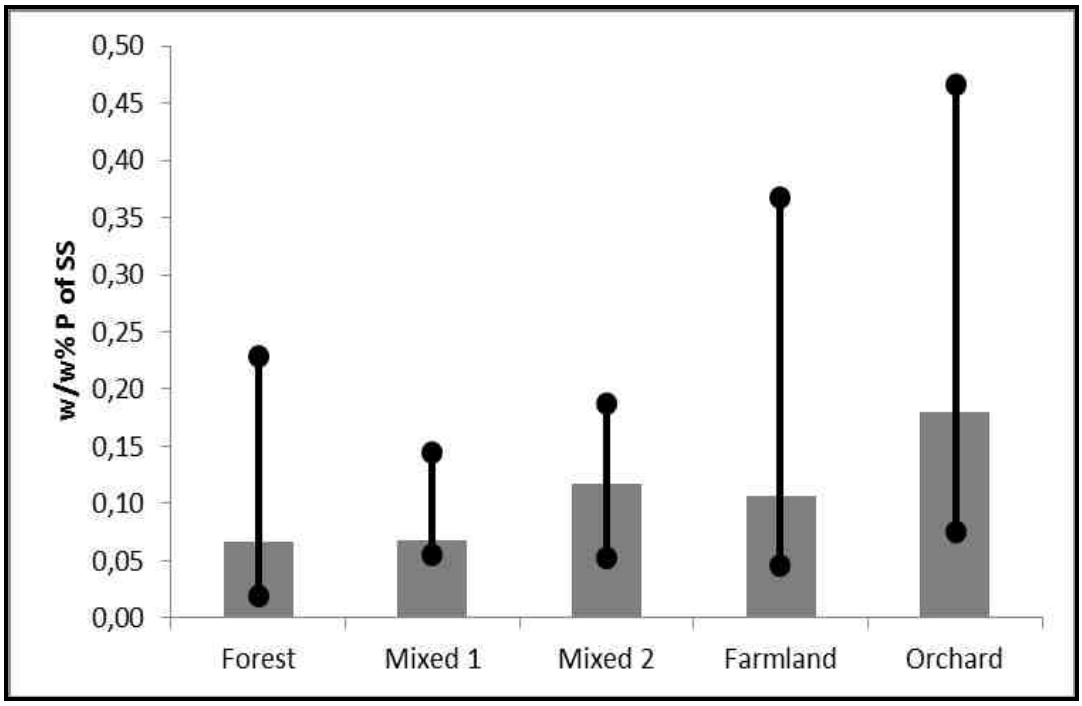

Figure 35: Median and quartiles of the weight percentage of PP in the suspended particles

The particles eroded from Farmland and Orchards had the highest PP content. The contributions of the different P fractions to the TP are given in figure 36. The fraction contribution in the forest is almost evenly distributed with 44%, 29% and 27% for PP, DOP and DIP fractions, respectively. The DOP fraction in the forest is the highest of all the sampled rivers. This is mainly due to the relatively high concentration of dissolved organic matter (4 mg C/L) in this runoff. The PP fraction is by far the most dominant P fraction in the large Mixed 1 catchment. This correlated well to the concentration of particulate matter as shown in figure 33 above. Mixed 2 are made up of 59% DIP, 38% PP and 3% DOP. The high fraction of DIP is contributed from the application of fertilizers. Farmland has almost equal contribution of DIP and PP i.e. 45% and 44%, respectively. The DIP is the contribution from the dissolved applied fertilizers while the PP is mainly through soil erosion as well as possibly some precipitation by Ca^{2+}. In the runoff from mainly orchards the DIP accounts for 71% of the TP, which is the highest DIP fraction of all the rivers. This reflects the large P pools found

in the soils in the orchards **(**Joshi, 2014; Pettersen, 2014**)** and the general poor ability of these soils to accumulate P in the soils.

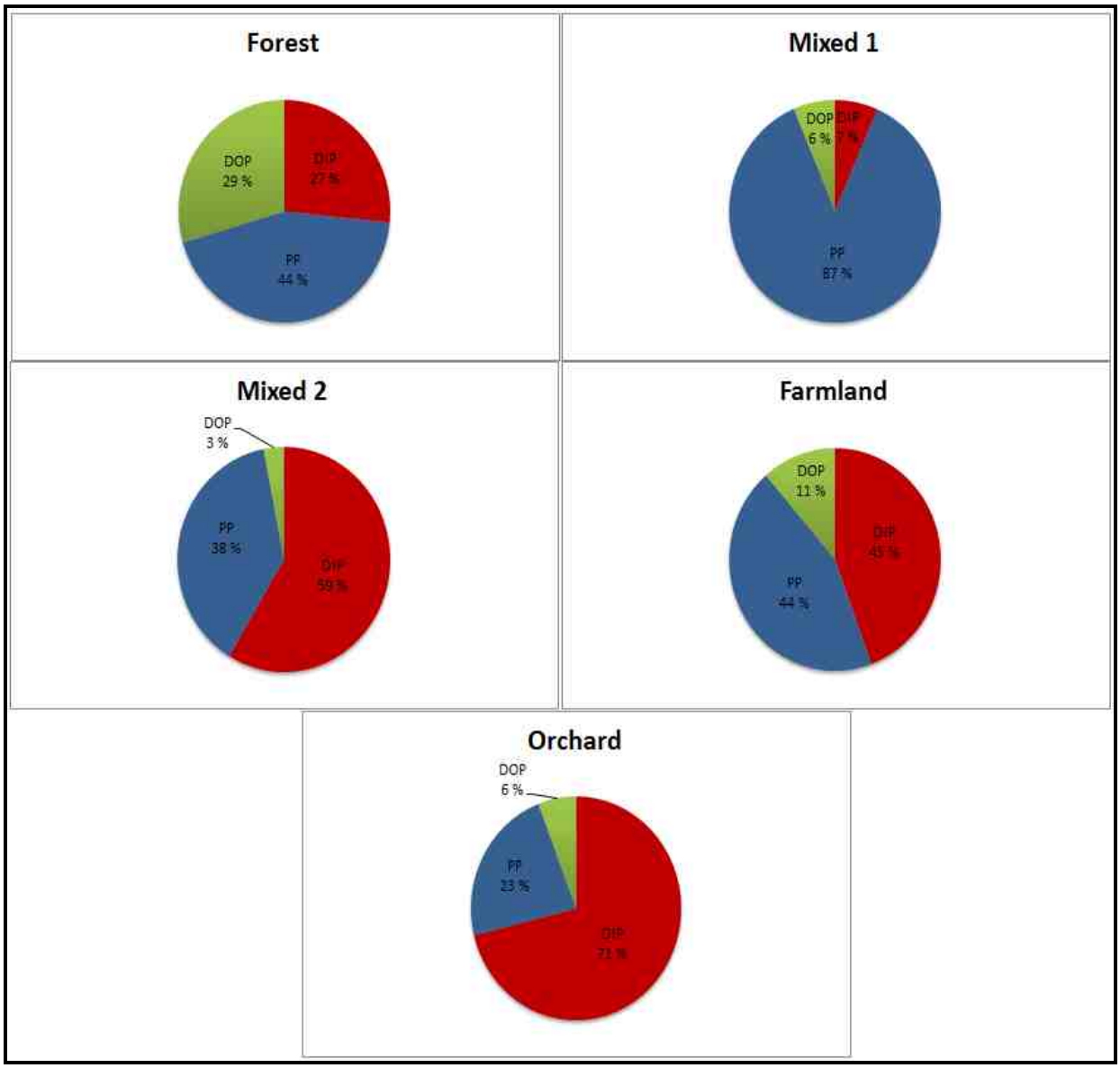

Figure 36: Percentage contribution of P fractions in the rivers

4.2 DGT phosphorous fractions

4.2.1 DGT-TDP

The DGT-TDP results are shown in figure 37 below and raw data is given in appendix C. There is observed increase in TDP concentration from the forest to the orchard. There is also quite significant difference between the fish ponds in use and the abandoned fish pond

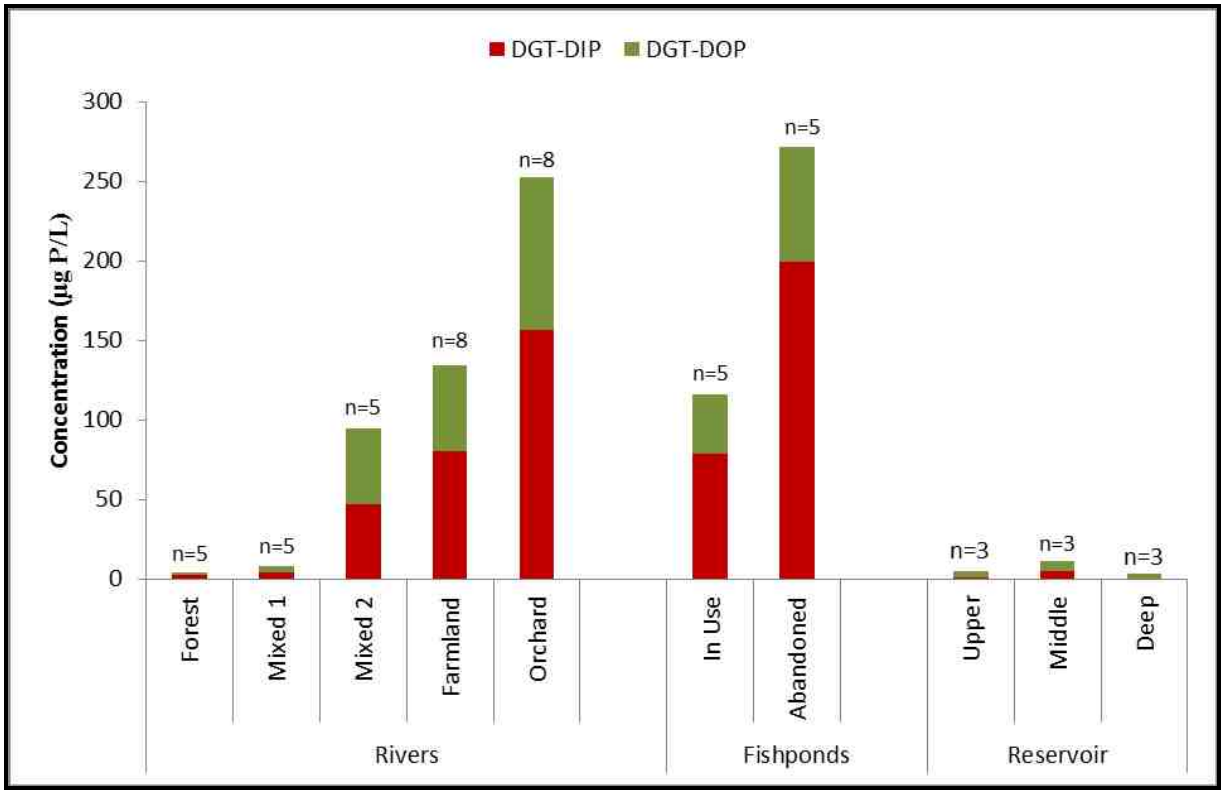

Figure 37: Phosphorous concentrations as sampled by DGTs

The relative differences in concentrations of dissolved P fractions measured with DGTs agree well with the relative differences measured in water grab samples shown in figure 34. Runoff from forests and the large mixed1 catchment has low concentrations while the runoff from orchards has high DTP concentrations.

There is also increased P associated with the relative land under settlement in each of the catchment from forest to orchards, this is mainly due to contribution of sewage and manure.

4.2.2 Relative contribution of DGT P fractions

The relative percentage composition of the DGT-TDP is shown in the **Figure 38** below. DIP contributes more than 50% of TDP in all the river and fish pond sites. However, in the reservoir, the dominant fraction is DOP. Sampling was done in the summer months of July – September when algae growth is high as a result of increased nutrients and sunlight hence high DOP as this is produced by the algae and the DIP is low due to that it is consumed by the algae.

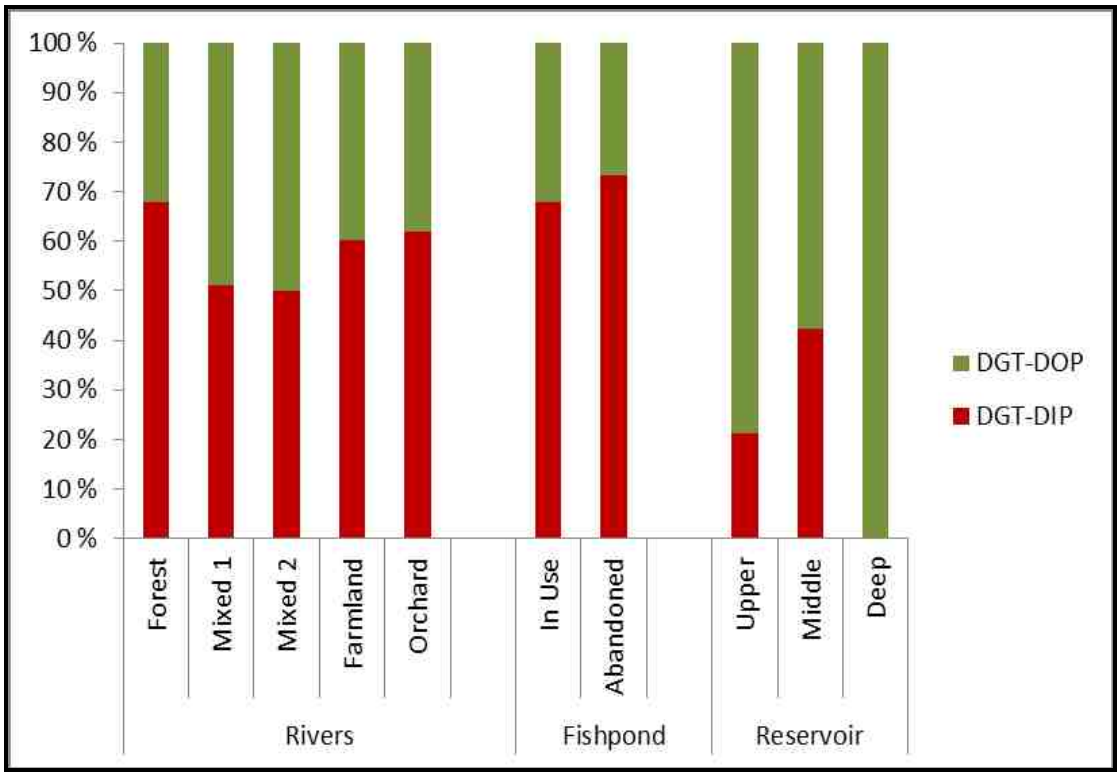

Figure 38: Relative DGT P fraction contribution

4.2.3 Dissolved P fractions as measured on water and by DGT

4.2.3.1 DIP fraction

The average Water-DIP and DGT-DIP collected during the same period is given in the **Figure 39**. The ideal situation for comparison of water and DGT values is to collect water samples at the start, during and at the end of the DGT deployment. However for practical reasons this was not possible, therefore data from water samples that fell in between the period of each DGT deployment period was used for comparison. This was done for all the sites and every DGT sampling frequency. Discrepancy between the Water-DIP and DGT-DIP may therefore be partly due to hydrological fluctuations causing fluctuations in DIP that were not captured by the grab samples comprising the water-DIP.

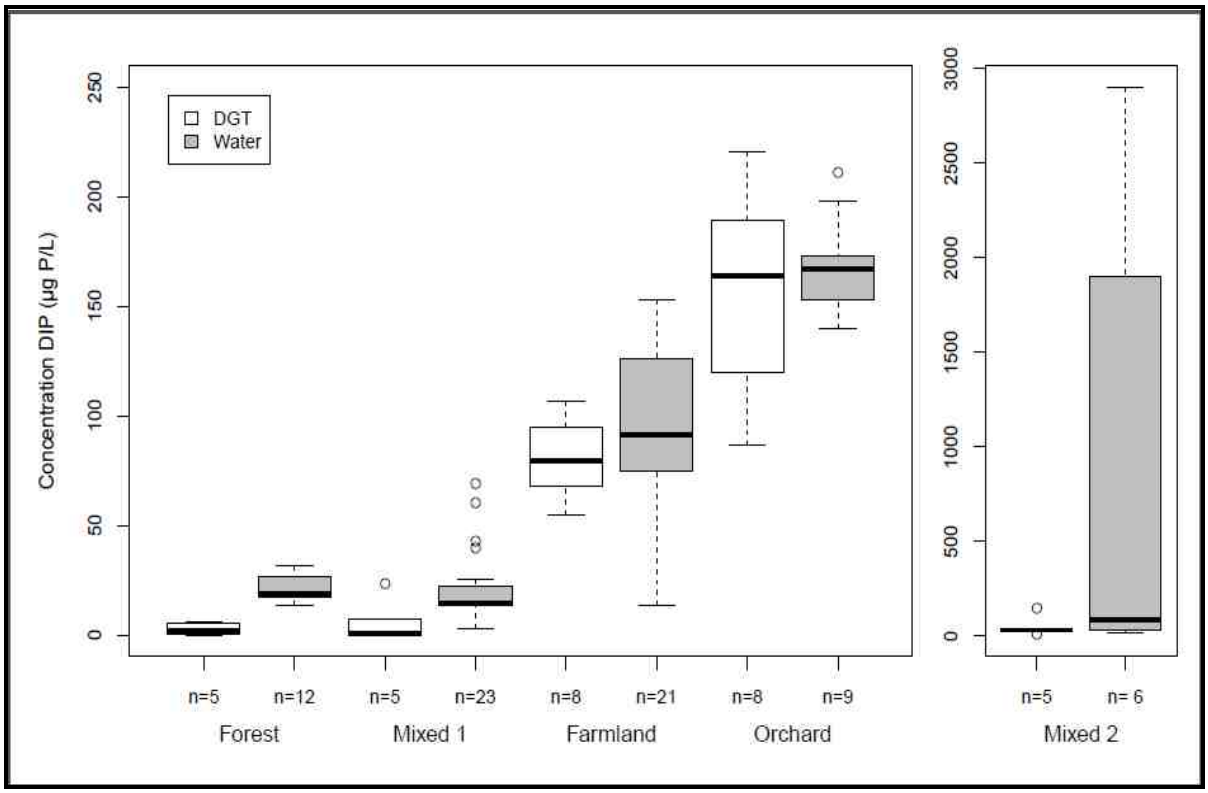

Figure 39: Comparisons of water-DIP and DGT DIP

The results show that the two approaches methods produce comparable DIP results with Water-DIP giving slightly higher values than the DGT-DIP. The difference could be attributed to the fact that grab water sample gives concentration at the given sampling time while DGT gives a time averaged concentration .The high concentration of DIP in the farmland and orchards represent the effect of fertilization that results in high concentration of

bioavailable P. There is huge variation in water-DIP in mixed 2. This is likely due to large fluctuations in the river flow captured by the grab samples collected intensively over runoff episodes.

4.2.3.2 DOP fraction

The DGT-DOP fraction results are given in **Figure 40**. The results show that the DGT-DOP concentrations are higher than water measurement. This is a paradox as the DGT only samples the low molecular weight DOP (LMWOP). The cause for this discrepancy is likely that the diffusion coefficient used for calculating the DGT-DOP is too high. Further work is thus needed in order to establish a sound diffusion coefficient value. The DGT-DOP value is potentially more interesting than the water-DGT as the DGT-DOP reflects better the bioavailable DOP. Furthermore, an inherent problem with determining the LMWOP has been that the concentrations are typically below detection limit. As the DGT accumulates the LMWOP over time the detection limit of LMWOP is not a problem using DGT. There is high variation in DGT measurement at farmland and orchard. This could be down to the large temporal variation captured during the episode studies comprising the sampling period.

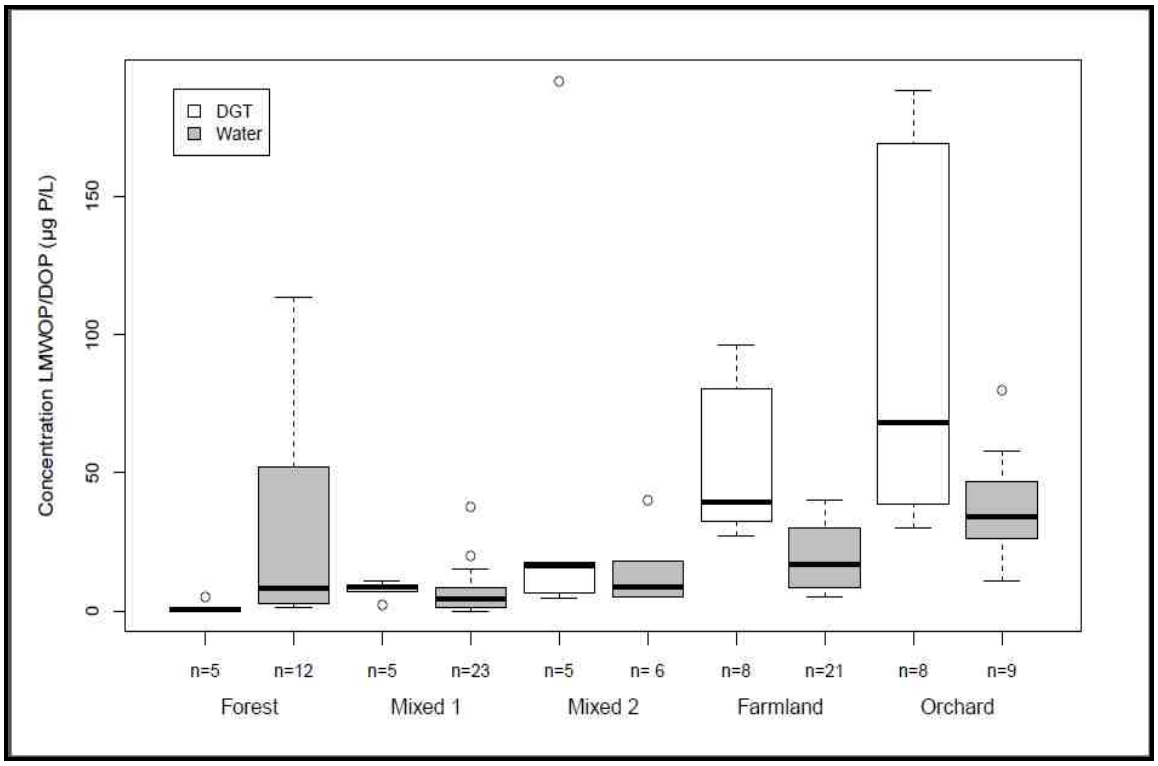

Figure 40: Comparison of Water-DOP and DGT-DOP

4.3 Particulate analyses

River suspended particles were collected as discussed in **chapter X** and LOI determined as shown in **appendix X.** The selection criteria was a discussed in **Chapter X,** with samples both drawn from low flow, high flow and from episodes studies.

4.3.1 Total rivers particulate matter

Particulate P is generally found to contribute significantly to P transport (Pacini and Gachter 1999). The result shown in figure 41 are the same as the results discussed in chapter 4.1.4, and will as such will not be discussed further in detail. The issue for this is try to relate the suspended solids concentration to elemental and mineral percentage composition of these particles.

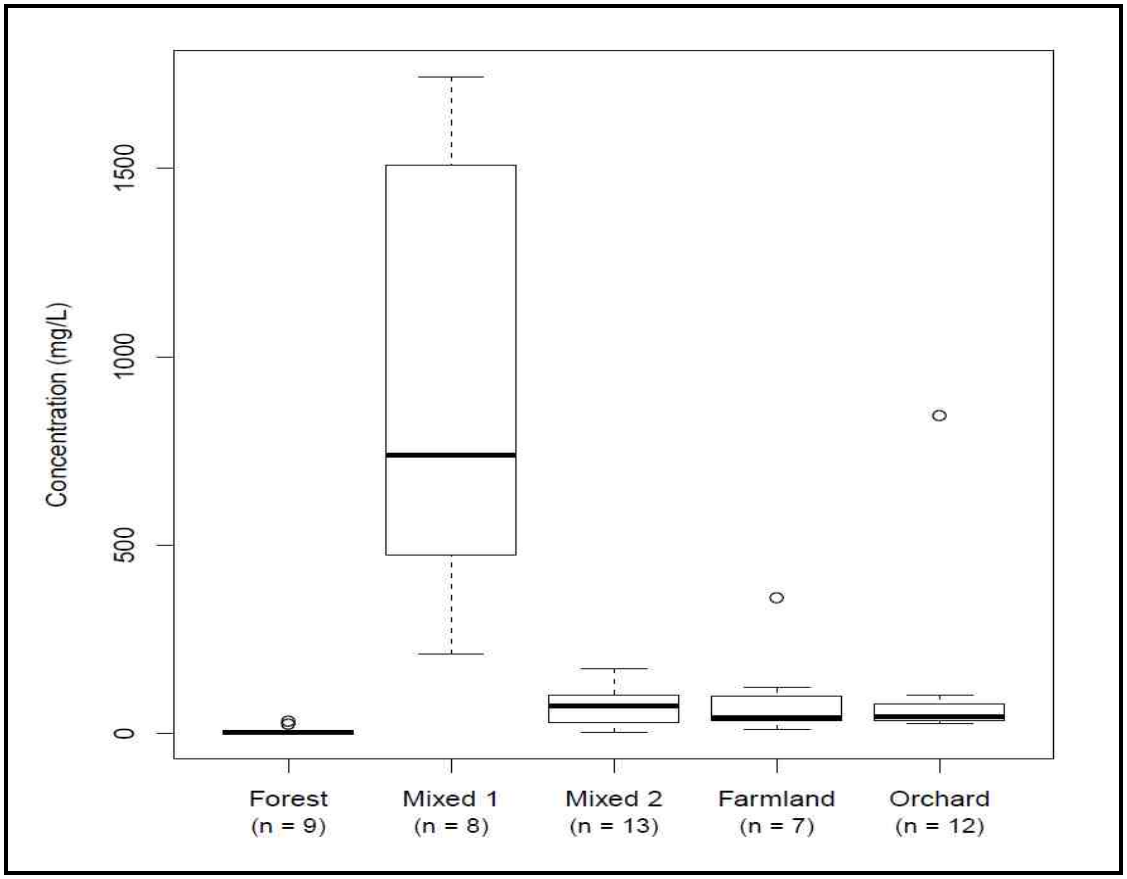

Figure 41: Concentration of particulate matter of the selected samples

Particulate P is associated with suspended particulates. Phosphorous is both absorbed to the particles while in the soil and may be adsorbed to the suspended particles in solution (Wærsted, 2014). The suspended particles can thereby increase the P mobility in the environment. Comparing the amount of P bound to the inorganic and organic constituents of the suspended particles shows that over 90% of the phosphorous bound to the suspended particles are in the inorganic pool (figure 42).

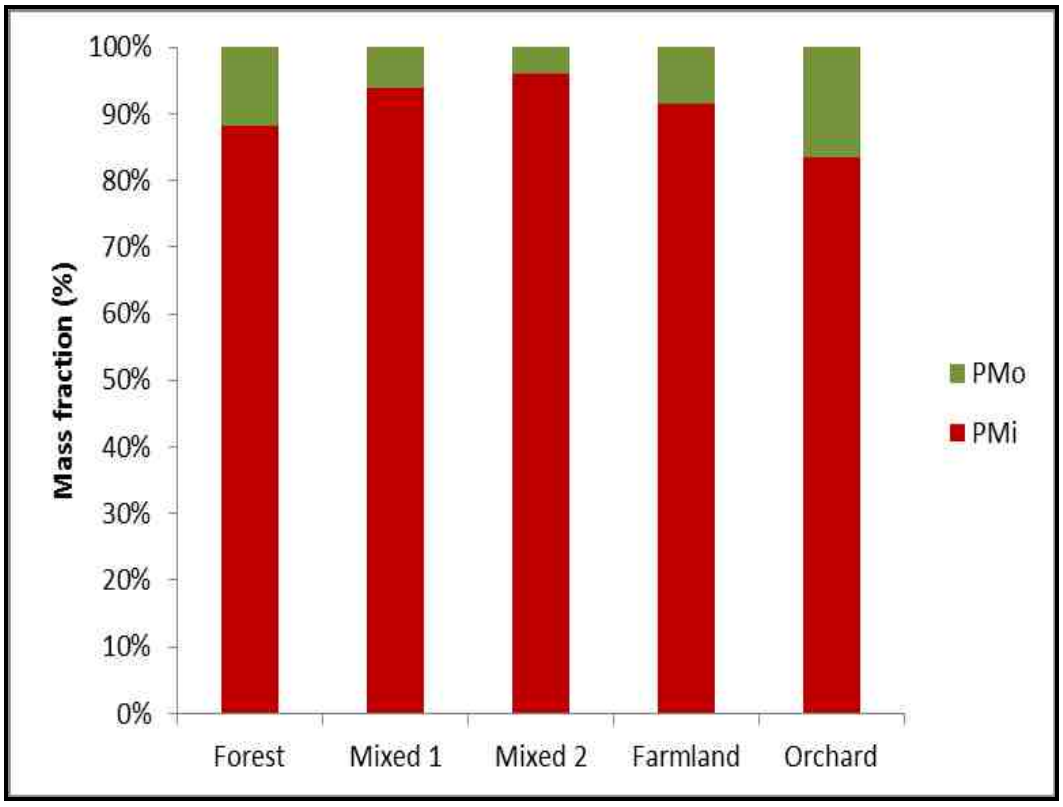

Figure 42: Mass fraction percentage fraction composition of the particulate matter

4.3.2 Cationic and PIP composition of the particles

The measurement of Fe, K and Na are not discussed as the values were below limit of detection. This was mainly due to the high concentration of these ions in the blank filters which resulted into negative values after blank correction.

Al is not significant difference between the streams, though the lower concentration in the mountain forests and orchard runoff is likely reflecting the lower clay content in these soils (Pettersen, 2014). The spatial differences in total P content in the suspended particles does not agree with the spatial differences depicted in figure 34 based on PP determined as the difference between TP in the digested unfiltered water samples and TDP in the digested filtered water sample. These differences must be due to the different methods used for detection of P (i.e. MBM and ICP-OES). Furthermore, the relative amounts of P determined using ICP-OES directly on the digested suspended particles is considerably higher than what was found using MBM on the digested water samples. The amount of P in the suspended solids was found to be the largest for forest runoff and the lowest in the runoff from the large mixed1 watershed and from orchards. This appears to be reflecting the differences in the phosphorous sorption index (PSI), which was the highest in forest soils and the lowest in orchard soils (Joshi, 2014). The amount of manganese in the suspended particles is especially high in the runoff from the mountain forests. This is likely due to that the amount of Mn and Fe in the weathering bedrock is considerably higher than in the very old unconsolidated fluvial deposits comprising the low-lands. This is also reflected in a higher sulphate content in the runoff as shown in figure 43 from the oxidation of the mineral pyrite. The digestion method was not strong enough to dissolve all of the particles. Silicates in crystalline quarts minerals were thus likely not detected. The silicates detected in the particles are therefore not straight forward to assess. The content of Ca and Mg in the particles generally gave the same picture with lowest values in the forest and orchards and highest in the mixed watersheds. This is reflecting that land left as forest or for growing fruit trees is the less fertile soils. These soils are generally found to have lower base saturation than the land used for farming (Joshi, 2014).

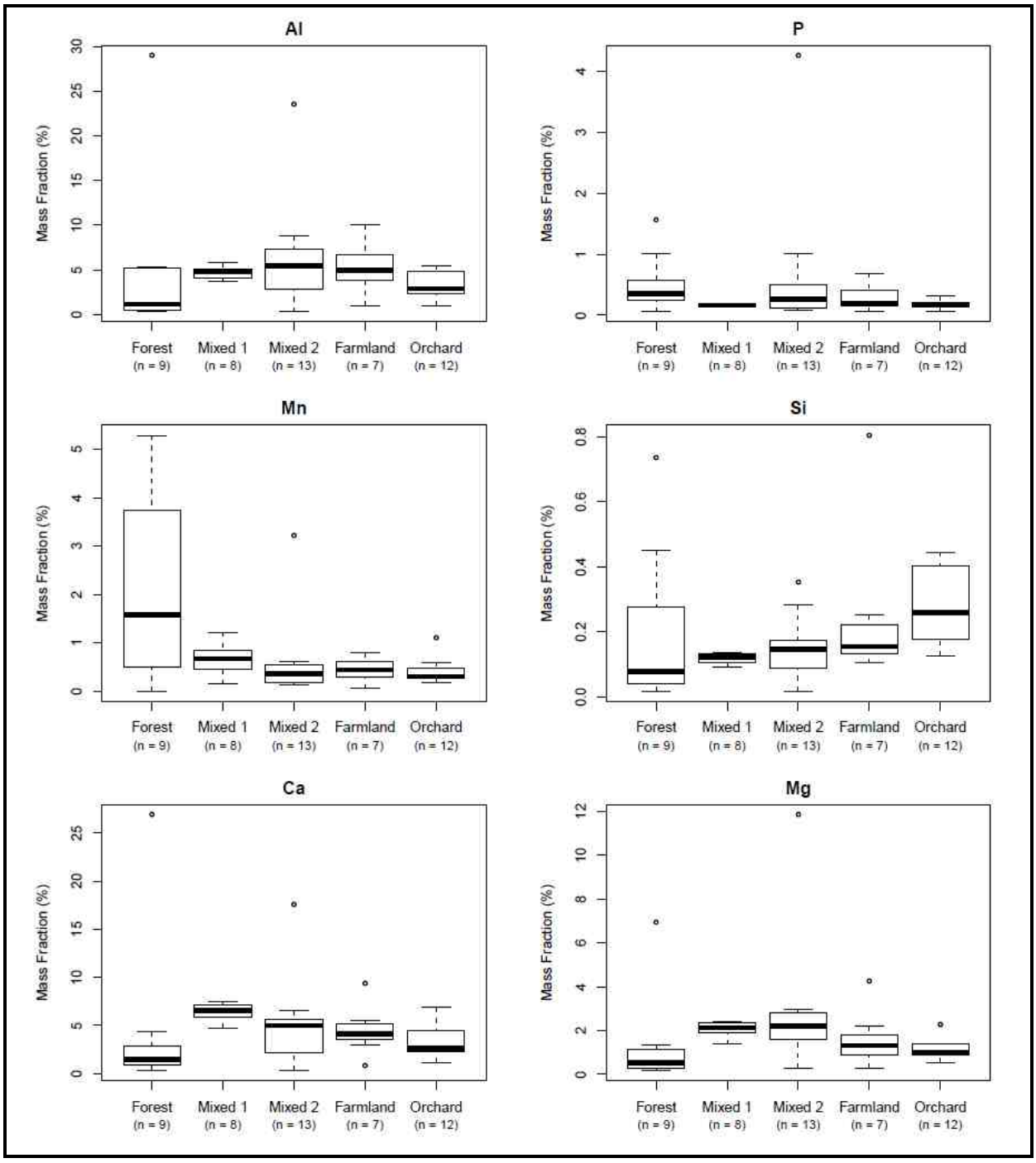

Figure 43: Variation of mass fraction cations and PIP with land use

4.3.3 Mineral composition of the particles

The data from the XRD analysis of crystalline minerals in the suspended particles are shown in figure 44. The mineralogy results show that there is no clear variation in the composition of the mineral with land use or fluctuation in the flow regime. This is in agreement with what was found by Pettersen (2014) in soil analysis. Pettersen (2014), found out that study site is made of silt loam soil with no clear spatial trend in soil texture. This study found out that the crystalline compound of the particulate matter is predominately 1:1 clay. These results are slight different from what was found in the soil. Pettersen (2014), found the main soil component was quartz (33-39%), halloysite (21-24%) and muscovite (20-27%). The variation could be due to the easy of clay erosion due to smaller particle size and loose soil especially in agricultural soils. One agreement though in the results is that in both cases, phosphorous containing minerals such as apatite and vivianite were not detected. This could mean that the P in the soil is mainly from anthropogenic sources. The erosion of mainly clay particle in could be interesting in relation to P mobility and transport in the watershed. Clay has a small surface area and therefore adsorbs more P than the large size grain particles like sand. Clay is also can also adsorb oxides and hydroxides of Al and Fe on its surface thereby increasing the P sorption to soils.

The analysis clearly shows that there is a dominance of 1:1 type clays. This is to be expected in such very old weathered soils. This is a non-expanding clay that when in the soils is compact and impermeable for water. Furthermore, it has a relatively low capacity to adsorb ions. The amount of 1:2 clays is higher in the mountain forest than in the farmland located in the low-lands. This is because the soils in the mountains are much younger than the soils in the low-land plains. The main crystalline mineral in most streams was quarts. The exception is forest and farmland. Forest was dominated by feldspar, due to the young soils, while the runoff from the older farmland was a mix of mainly quarts and dolomite. The presence of dolomite is likely due to the addition of dolomite as lime to the agricultural fields.

A large fraction of Berlinite ($AlPO_4$) in the large mixed 1 stream is interesting. As can be seen in the earlier discussion, mixed 1catchment has got high suspended particulate matter, high quartz and low 1:1 clay. Therefore it less likely that high particulate P is transported in association with clay but as crystalline Berlinite. There is a lot of industry in the watershed of mixed1 and it may be due to this that the content of Berlinite is high. The content of

Muscovite is low, as could be expected in the erosion products of weathered secondary minerals and old soil.

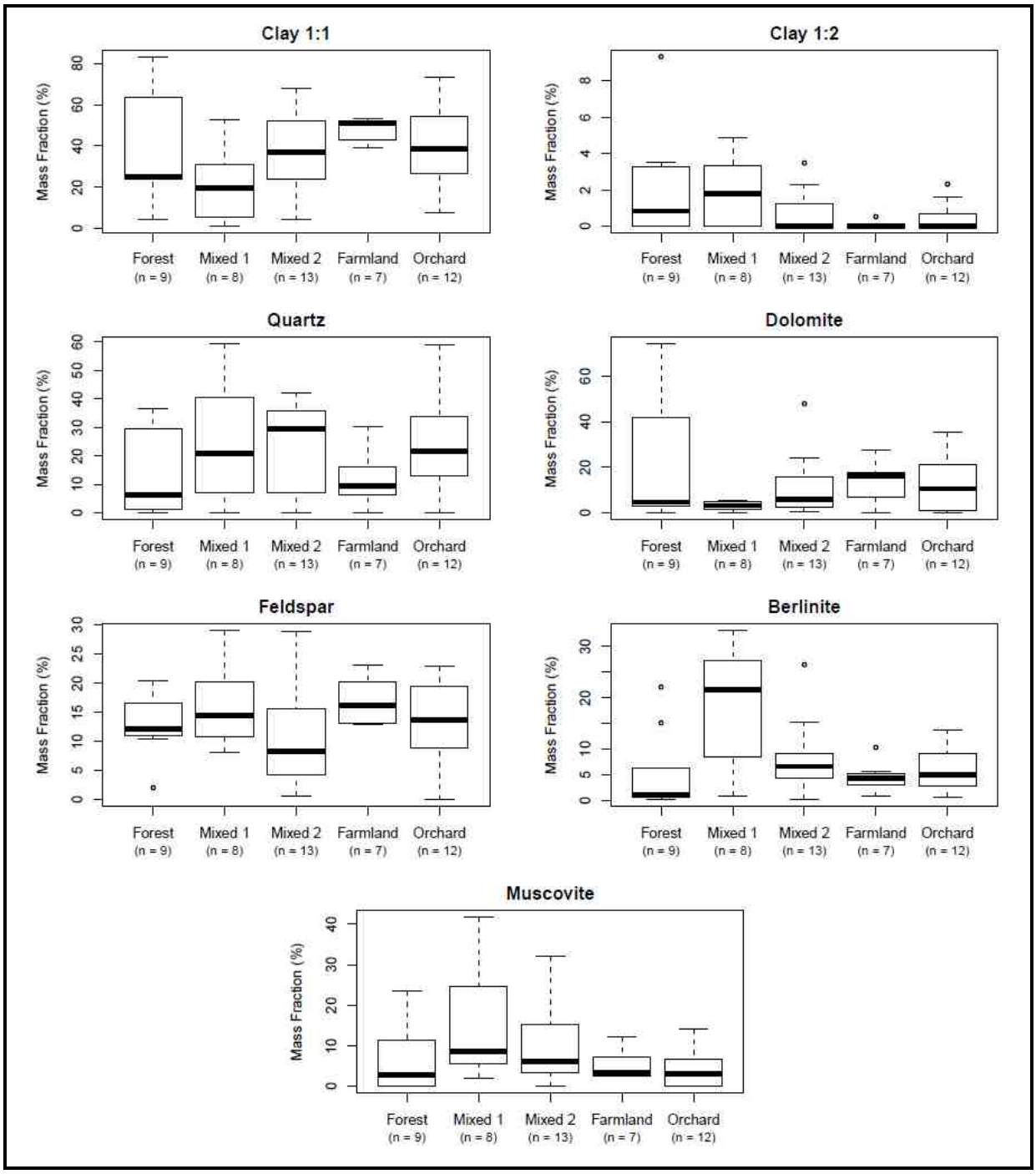

Figure 44: Variation of mineral mass percentage with land use

4.4 Conclusion

Water chemistry shows that that the river pH values are close between 7 – 7.5, which is the pH range where P is dominated by the precipitation by Ca, Therefore solubility of the orthophosphates is through calcium phosphate. The pH values also suggest that buffering is through weathering of carbonates rocks and liming of the agricultural soils. The cation composition of the water chemistry is rather constant being dominated by Ca^{2+} and Mg^{2+} which could also suggest P precipitation by Ca. The major anion is HCO_3^- though which is derived from the parent material.

River suspended solids seems to be related particulate phosphorous load and the soil type and texture. The proportion of the suspended solids in the rivers depends on the river volume, catchment size, soil and topography. Phosphorous fractions in the rivers show variations that are related to their physiochemical differences. The dominant fraction in the TP is DIP in the agricultural catchments. The relative differences in concentrations of dissolved P fractions measured with DGTs agree well with the relative differences measured in water grab samples for TDP and DIP but not DOP. It can therefore be concluded that the two methods are comparable and the difference in DOP is likely due to the uncertainty in DGT-DOP calculations. Therefore DGT can be used in the accessing the bioavailability of P.

The spatial differences in total P content in the suspended particles in water and particles is likely due to the difference in analysis methods. There is no clear variation in mineralogy from the stream under different flow regimes. The eroded particles is predominately 1:1 clay which is likely to adsorbed P due to its small surface area and formation of bridges with Al and Fe. The high particulate P in Mixed 1 is due to Berlinite which is likely originating from the industries in the watershed.

5.0 References

vanLoon, G. W. and S. J. Duffy (2011). Environmental Chemistry - A global perspective. New York, USA, Oxford University Press.

Anna, A. (2000). Evaluation of the P-AL method for fertilization of barley (Hordum vulgare L.), in relation to soil properties, especially P sorption. Department of soil sciences. Sweden, Swedish University of Agricultural Science (SLU), Uppsala. **PhD**.

Broberg, O. and G. Persson (1988). "Particulate and dissolved phosphorus forms in freshwater: composition and analysis." Hydrobiologia **170**(1): 61-90.

Carpenter, S. R., et al. (1998). "Nonpoint pollution of surface waters with phosphorous and nitrogen." Ecological Applications **8**(3): 559 - 568.

Chai, C., et al. (2006). "The Status and Characteristics of Eutrophication in the Yangtze River (Changjiang) Estuary and the Adjacent East China Sea, China." Hydrobiologia **563**(1): 313-328.

Chen, Y., et al. (2003). "Changes of nutrients and phytoplankton chlorophyll-a in a large shallow lake, Taihu, China: an 8-year investigation." Hydrobiologia **506-509**(1-3): 273-279.

Cordell, D., et al. (2009). "The story of phosphorus: Global food security and food for thought." Global Environmental Change **19**(2): 292-305.

Delgado, A. and R. Scalenghe (2008). "Aspects of phosphorus transfer from soils in Europe." Journal of plant nutrition and soil science **171**(4): 552-575.

Domagalski, J., et al. (2007). "Eutrophication study at the Panjiakou-Daheiting Reservoir system, northern Hebei Province, People's Republic of China: Chlorophyll-a model and sources of phosphorus and nitrogen." Agricultural Water Management **94**(1–3): 43-53.

EC, E. C. (2003). Common implementation stategry for the water framework directive (2000/60/EC) - Policy Summary. Guidance document no. 10. River and lakes - Typology, refence conditions and clasiffication system.

EPA, U. S. E. A., et al. (2003). Clean Water for Sustainable Cities in China.

EPA, U. S. E. A. and T. E. p. B. TEPB (2005). Annual Report of Sino-US Cooperative Project on Safe Drinking Water Research for 2005.

EU (2013). Water Framework Directive. Brussels, Belgium.

FAO (1978). Soil map of the world - Volume VIII North and Central Asia. Italy, UNESCO. **VIII:** 193.

FAO (2010). Current world fertilizer trends and outlook to 2014. Rome, Italy.

Gao, C. and T. Zhang (2010). "Eutrophication in a Chinese Context: Understanding Various Physical and Socio-Economic Aspects." Ambio **39**(5-6): 385-393.

Gburek, W. J., et al. (2005). "Phophorous mobility in the landscape." American Society of Agronomy **46**.

Gebreslasse, Y. K. (2012). Particle transport of phosphorus in streams draining catchments with different land uses. Department of Chemistry. Oslo, Norway, University of Oslo, UiO. **Masters**.

Haygarth, P. M., et al. (2005). "The phosphorus transfer continuum: Linking source to impact with an interdisciplinary and multi-scaled approach." Science of the total environment **344**(1-3): 5-14.

Haygarth, P. M. and S. C. Jarvis (1999). "Transfer of phosphorous from agricultural soils." Advances in agronomy **66**.

Heathwaite, A. L., et al. (2005). "Assessing the risk and magnitude of agricultural nonpoint source phosphorous polution." American Society of Agronomy **46**.

Holtan, H., et al. (1988). "Phosphorus in soil, water and sediment: an overview." Hydrobiologia **170**(1): 19-34.

House, W. (2003). "Geochemical cycling of phosphorus in rivers." Applied geochemistry **18**(5): 739-748.

Joshi, P. B. (2014). Assessment of phosphorous loss risk from soil - a case study from Yuqiao reservoir local watershed in north China. Department of Chemistry. Oslo, Norway, University of Oslo, UiO. **Masters:** 86.

Le, C., et al. (2010). "Eutrophication of Lake Waters in China: Cost, Causes, and Control." Environmental management **45**(4): 662-668.

Lin, P., et al. (2012). "Speciation and transformation of phosphorous and its mixing behaviour in te Bay of St. Louis estuary in the north Gulf of Mexico." Geochemica et Cosmochimica **87**(2012): 283-298.

Liu, W. and R. Qiu (2007). "Water eutrophication in China and the combating strategies." Journal of Chemical Technology & Biotechnology **82**(9): 781-786.

Maher, W. (1998). "Procedures for the storage and digestion of natural waters for the determination of filterable reactive phosphorus, total filterable phosphorus and total phosphorus." Analytica Chimica Acta **375**(1,2): 5.

Manning, A. C. D. (2008). "Phosphate Minerals, Environmental Pollution and Sustainable Agriculture." Elements **4**(2): 105-108.

Mohr, C. W. (2010). Monitoring of phosphorus fractions – Understanding geochemical and hydrological processes governing the mobilization of phosphorus from terrestrial to aquatic environment. Department of Chemistry. Oslo, Norway, University of Oslo, UiO. **Masters:** 104.

Mullins, G. (2009). Phosphorous, Agriculture & the Environment. Virginia, US, Virginia Polytechnic Institute and State University**:** 11.

Oddvar, R., et al. (2013). Sampling of dissolved inorganic and organic phosphorous compounds in natural water by Diffusion Gradient in Thin-films (DGT), Norwegian Institute of Water Research (NIVA)

Department of Chemistry, University of Oslo (UiO).

Orderud, G. I. and R. D. Vogt (2013). "Trans-disciplinarity required in understanding, predicting and dealing with water eutrophication." International Journal of Sustainable Development & World Ecology **20**(5): 404-415.

Pacini, N. and R. Gachter (1999). "Speciation of riverine particulate phosphorus during rain events." Biogeochemistry **47**(1): 87.

Pernet, C., Benoît, et al. (2012). "Sources and Pathways of Nutrients in the Semi-Arid Region of Beijing–Tianjin, China." Environmental science & technology **46**(10): 5294-5301.

Pettersen, E. (2014). Soil phosphorous pools and their relation to land-use and soil physiochemical properties - A case study of an agricultural watershed in north-easter China. Department of Chemistry. Oslo, Norway, University of Oslo, UiO. **Masters:** 113.

Pichette, C., et al. (2009). "Using diffusive gradients in thin-films for in situ monitoring of dissolved phosphate emissions from freshwater aquaculture." Aquaculture **286**(3-4): 198-202.

Pratt, A. (2006). "The curious case of phosphate solubility." Chemistry in New Zealand **70**(3): 78.

Qu, J. and M. Fan (2010). "The Current State of Water Quality and Technology Development for Water Pollution Control in China." Critical Reviews in Environmental Science and Technology **40**(6): 519-560.

Reynolds, C. S. and P. S. Davies (2001). "Sources and bioavailability of phosphorus fractions in freshwaters: a British perspective." Biological reviews **76**(1): 27-64.

Robards, K., et al. (1994). "Determination of carbon, phosphorus, nitrogen and silicon species in waters." Analytica Chimica Acta **287**(3): 147-190.

Schoumans, O. and W. Chardon (2003). "Risk assessment methodologies for predicting phosphorus losses." Journal of plant nutrition and soil science **166**(4): 403-408.

Sharpley, A., et al. (2001). "Phosphorus loss from land to water: integrating agricultural and environmental management." Plant and soil **237**(2): 287-307.

TAES, T. A. o. E. S. (2012). Comprehensive Village Management Plan in Yuqiao Reservoir Area - Final Report.

Uher, E., et al. (2012). "Impact of Biofouling on Diffusive Gradient in Thin Film Measurements in Water." Analytical chemistry **84**(7): 3111-3118.

Van Moorleghem, C., et al. (2011). "Effect of Organic P Forms and P Present in Inorganic Colloids on the Determination of Dissolved P in Environmental Samples by the Diffusive Gradient in Thin Films Technique, Ion Chromatography, and Colorimetry." Analytical chemistry **83**(13): 5317-5323.

WHO (2011). Millenium Development Goals (MDGs) - Technical information. Geneva, Switzerland.

WHO and E. C. EC (2002). Eutrophication and Health. Luxembourg.

Withers, P. J. A., et al. (2001). "Phosphorus cycling in UK agriculture and implications for phosphorus loss from soil." Soil Use and Management **17**(3): 139-149.

Withers, P. J. A. and P. Jarvie (2008). "Delivery and cycling of phosphorus in rivers: A review." Science of the total environment **400**(1-3): 379-395.

Worsfold, P., et al. (2005). "Sampling, sample treatment and quality assurance issues for the determination of phosphorus species in natural waters and soils." Talanta **66**(2): 273-293.

Yang, X.-e., et al. (2008). "Mechanisms and assessment of water eutrophication." Journal of Zhejiang University SCIENCE B **9**(3): 197-209.

Zhang, H. and W. Davison (1995). "Performance Characteristics of Diffusion Gradients in Thin Films for the in Situ Measurement of Trace Metals in Aqueous Solution." Analytical chemistry **67**(19): 3391-3400.

Zhang, H., et al. (1998). "In situ measurement of dissolved phosphorus in natural waters using DGT." Analytica Chimica Acta **370**(1): 29-38.

Zhang, H. and B. Shan (2008). "Historical Distribution and Partitioning of Phosphorus in Sediments in an Agricultural Watershed in the Yangtze-Huaihe Region, China." Environmental science & technology **42**(7): 2328-2333.

Zorica, S., et al. (2008). "Methods of management of eutrophictaion in fresh water ecosytems in Vojvodina." Geographica Pannonica **12**(1, 4-11).

6.0 Appendix

6.0 Appendix

List of appendix

Appendix A: Sampling

Appendix A-1: Mathematical equations used in DGT calculations

No	Equations	Formulas	Denotations
1	Flux by Ficks 1st law	$Flux = \frac{dm}{dt} = -D \cdot \frac{dC}{dz}$	Flux of molecules (dm/dt) over a given distance with a concentration gradient (dC/dz) and diffusion coefficient (D).
2	Time integrated uptake	$m(t) = Co \cdot t \cdot D \cdot \frac{A}{L}$	Mass (m) by time (t) uptake; diffusion coefficient (D), Length (L) and cross section area (A) of the diffusion membrane (by integration of Eqn. 1).
3	Time averaged concentration		Eqn. 2 solved for the time-averaged concentration (Co), forms the conventional passive sampler equation.

Apendix A-2: Calculations for deployment time reaching 50% of sorption capacity of the resin membrane in DGTs

A challenge is that the DGTs do not sample all of the DGT fractions. It is therefore not simply to base any calculations on TP values. Two scenarios of minimum and maximum uptakes were therefore calculated in order to determine the optimum deployment period for the DGTs.

Maximum uptake

We assume that the amount of P adsorbed by the DGT (DGT-TP) is governed by the sum of orthophosphate (PO_4-P) and Low-molecular-weight organic P (LMWOP) in solution. In this scenario both PO_4-P and LMWOP will be accumulated by the DGTs. The deployment time to reach 50% sorption capacity for the DGTs was calculated by the equation 3 (Table A-1) which is derived from Equation 1 in Table A-1 but but Δg is here exchanged with L and M is exchanged with m.

Determination of DOP was done using adenosine monophosphate (AMP) and Inisitol hexaphosphate (pytic acid, IP6) to represent the maximum and minimum low molecular weight organic phosphorous respectively **(**Mohr, 2012**)**. Diffusion coefficient of 3.2 (10^{-6} cm^2/sec) and 1.3 (10^{-6} cm^2/sec) were used for AMP and IP6 respectively while 6.0 (10^{-6} cm^2/sec) was used for orthophosphate ($H_2PO_4^-$) species. The calculations were as below.

m_{50} = 3350 ng P

A = 3.14 cm^2

L = 0.102 cm

D_{org} ≈ 2 · 10^{-6} cm^2 sec^{-1} @ ca. 20°C

D_{PO4} ≈ 6 · 10^{-6} cm^2 sec^{-1} @ ca. 20°C

Table A-1: Maximum uptake

Assuming maximum uptake : DGT-TP = PO_4 + LMWOP				
Basin	**River name site**	**LMWOP (µg P L^{-1})**	**PO_4^{3-} (µg P L^{-1})**	**t_{50} (days)**
Xiaojugezhuang Basin	Xiaojugezhuang bridge	18.2	27.4	6
Beixinzhuang Basin	Yumaqiao bridge	93	132	1
Beixinzhuang Basin	Beixinzhuang bridge	4.8	23.2	8
Lin River Basin	Baxianshan bridge	119	14.8	4
Lin River Basin	Lin river bridge	212	15.7	2
Yaquiao Reservoir	YQ01	32	10	7

Minimum Uptake

Assuming that only PO_4-P will be accumulated by the DGTs the deployment time to reach 50% sorption capacity for the DGTs is calculated by Eq XX which is also derived from Eq X

Table A-2: Minimum uptake

Assuming minimum uptake: DGT-TP = PO_4			
Sub-Basin	**River name site**	**PO_4^{3-} (mg P/L)**	**t (days)**
Xiaojugezhuang Basin	Xiaojugezhuang bridge	27.4	8
Beixinzhuang Basin	Yumaqiao Bridge	132	2
Beixinzhuang Basin	Beixinzhuang bridge	23.2	9
Lin River Basin	Baxianshan river bridge	14.8	14
Lin River Basin	Lin river bridge	15.7	13
Yaquiao Reservoir	YQ01	10	21

Field DGT deployment time

Table A-3: Recommended and actual deployment time

Sub-Basin	**River name site**	**Recommended Deployment time (**days)	**Actual deployement time (**days**)**
Xiaojugezhuang Basin	Xiaojugezhuang bridge	6 - 8	**7**
Beixinzhuang Basin	Yumaqiao bridge	1 - 2	**7**
Beixinzhuang Basin	Beixinzhuang bridge	8 -9	**7**
Lin River Basin	Baxianshan river bridge	4 -14	**7**
Lin River Basin	Lin river bridge	2 - 13	**7**
Yaquiao Reservoir	YQ01	7 - 21	**10**

Appendix A-2: Water filtration and Determination of LOI

Prior to filtration of water samples, filters were pre-burned at 450˚C. After heating and cooling, the filters were weighed (*W0*), and then used for filtrating 1000 - 2000 mL (V) of water samples. The filters were then dried at 105±5 ˚C and then re-weighed (*W1*). Particulate matter (PM_T) was calculated by the empirical equation A-1 below:

$PM_T = (W1-W0) /V$ Equation A-1

The inorganic particulate matter (PIM) was determined by igniting the filter paper at 450˚C for at least 4 hours, and weighing thereafter (W2). Inorganic particulate matter (PIM) was calculated by the equation A-2 below:

$PM_i = (W2 - W0)/V$ Equation A-2

The particulate organic matter (POM) was calculated by taking the difference between PM_T and PM_i:

$PMO = PM_T - PM_i$ Equation A-3

Filtration and drying at 105 ˚C was conducted according to ISO standard (ISO: 11923, 200)

These filter papers were then shipped to University of Oslo (UiO) for particle characterization

Appendix B: Instrumentation and calibration

Appendix B-1: MBM

Table B-1a: Preparation of reagents and solutions

Reagent	**Procedure**
H_2SO_4 (9 mol/L)	Add 500mL of water to a 2L beaker. Cautiously add, with continuous stirring and cooling, 500 ml of sulfuric acid, p = 1.84 g/ml. Mix well and allow the solution to cool to room temperature.
H_2SO_4 (4 mol/L)	Add 50ml of water into a beaker. Cautiously add, with continuous stirring and cooling, 21.7ml of sulfuric acid, p = 1.84 g/ml. Mix well and allow the solution to cool to room temperature.
Ascorbic Acid (100g/L)	Dissolve 10g of ascorbic acid ($C_6H_8O_6$) in 100mL water.
Acid molybdate Solution	Cautiously add 230 mL of sulfuric acid (H_2SO_4 = 9 mol/L) to 70mL of water and cool. Dissolve 13g of ammonium heptamolybdate tetrahydrate [$(NH_4)_6Mo_7O_{24}.4H_2O$] in 100mL of water. Add to the acid solution and mix well. Dissolve 0.35g antimony potassium tartrate hemihydrate [$K(SbO)C_4H_4O_6.1/2H_2O$] in 100 ml of water. Add to the molybdate-acid solution and mix well.
Orthophosphate stock standard solution, pp = 50 mg/L.	Orthophosphate stock solution was prepared from the spectral pure standards of P solution from a concentration of 10,000ppm. The formula $M_1V_1 = M_2V_2$ was used to get the desired concentration.
Orthophosphate stock standard solution, pp = 2 mg/L.	Pipette 20 ml of orthophosphate stock standard solution (Orthophosphate=50mg/L) into a 500 ml volumetric flask. Make up to the mark with water and mix well. Prepare and use this solution each day as required.

Calibration standards: Six calibration standards were prepared from single element P stock solution (Spectrascan from Teknolab AS, Kolbotn, Norway) as per Table 2 below.

Table B-1b: Preparation of MBM calibration solutions

Analyte	Std 0	Std 1	Std 2	Std 3	Std 4	Std 5
P (mg/L)	0	0.1	0.2	0.3	0.4	0.5

Analysis procedure: Exactly 10ml of calibration standards, control solutions, blank DGT sample and the eluted DGT test sample solution were used for analysis. Matrix matching was done through addition of 0.1mL of 4M H_2SO_4 to standards and controls and absorbance measured at 880 nm. The order of the analysis was calibration standards, control solution, DGT blank and then samples. After every 10-15 samples, standard 0 was measured to check the instrument drift (for samples $\leq$15) and if recalibration done (for samples $\geq$15). The instrument was calibrated again at the end of the measurement to check for drifts.

Appendix B-2: ICP-MS

Table B-2: Instrument settings

Parameter	**(Settings)**
RF power, kW	1.25kW
Plasma Ar flow, L min^{-1}	13.0L/min
Auxiliary Ar flow, L min^{-1}	1.2L/min
Nebulizer Ar flow, L min^{-1}	0.94L/min
Sample flow rate, mL min^{-1}	1mL/min
Reading time, s	5 seconds
Number of replicates	5
Reading per replicate	1 second
Pulse stage Voltage	1200V
Sweeps	20
Dwell time	50 (ms)
Scan rate	Peak hopping
Sample introduction	Manual

Preparation of ICP-MS calibration standards and procedure for analysis

All solutions for the experiment were prepared by Type I water (>1 MΩ cm) purified using Elix-5 water purification system (Millipore, Bedford, USA). The purge gas was argon of purity 99.99% from AGA (Oslo, Norway). Standards were prepared from single element P stock solution (Spectrascan from Teknolab AS, Kolbotn, Norway). From the stock solution, calibration standards preparation followed the same procedure as in Appendix B-1. The acid used was 98% (m/m) Sulphuric acid of p.a. quality from Merck (Darmstadt, Germany).

The instrument was rinsed with dilute Nitric acid and Type I water before reading the blank, Standard 0, 1, 2, 3 4, then rinsed again, blank, sample (1, 2,3…..n), rinse, LOD 1-10 in that sequence. After every 10-15 samples, standard 0 was measured to check the instrument drift (for samples ≤15) and if need be a recalibration done (for samples ≥15). Between sampling reading, the sampling tube was wiped with a clean soft tissue, rinsed with the 5% Nitric acid and Type I water to minimize contamination.

LOD was determined by running the standard 0, ten times at the end of sample analysis. The LOD was determined by through multiplying by three (3) the standard deviation of the ten standards 0 readings. Limit of quantification (LOQ) was determined through multiplication of LOD by 10.

Appendix B-3: Microwave oven

The experiment was carried out in a closed microwave system with controlled temperature. The micro wave system used was the Milestone Ethos 1600 microwave oven. About a third of filter paper were cut using a clean scarpel and weighed. 10mL of Nitric acid (Suerpure Nitric acid from Marck KgaA, Dramstadt, Germany) was added to the sample and program set as below.

Step 1: Time = 5 minutes, Temperature = 210^{o}C, Power = 100 Watts and Pressure = 50 bar

Step 2: Time = 30 minutes, Temperature = 210^{o}C, Power = 100 Watts and Pressure = 50 bar

Step 3: Time = 5 minutes, Temperature = 0^{o}C, Power = 0 Watts and Pressure = 0 bar.

Ventilation time: 15 minutes

Some samples were crushed using a clean glass rod to increase their surface area and achieve complete digestion. Microwave acid blanks, Filter paper blanks and CRM were also digested.

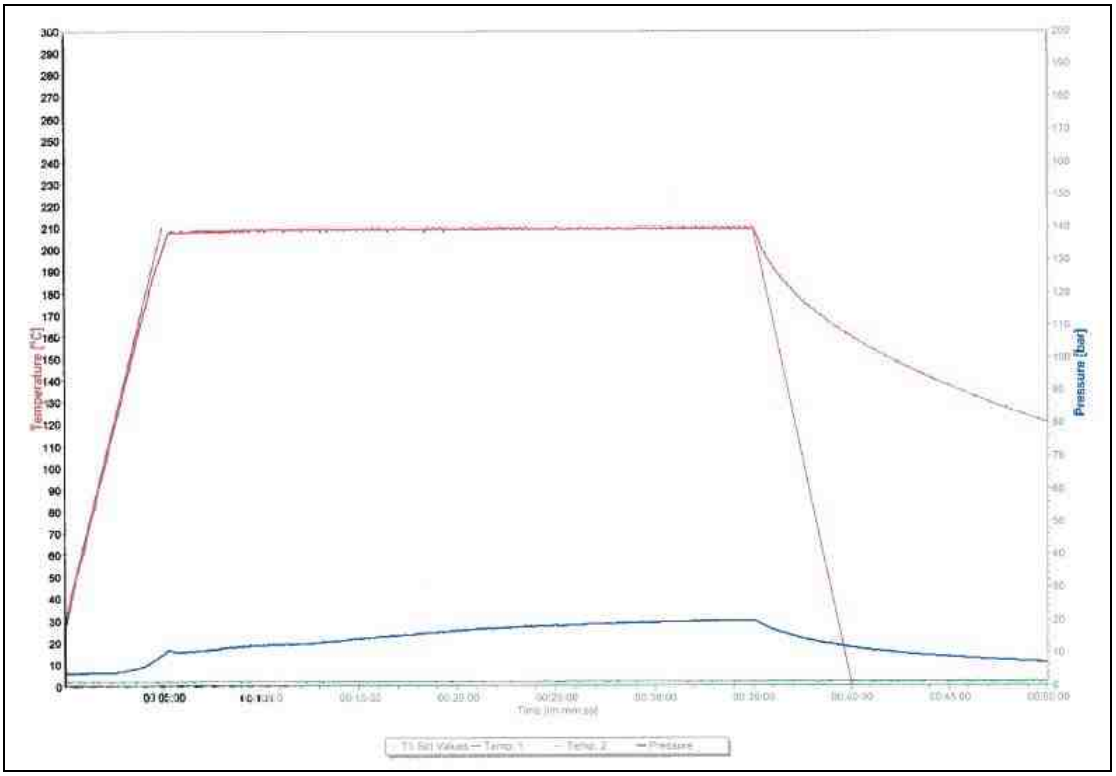

Figure B-1: Microwave oven program print out

Appendix B-4: ICP-OES

Standard solutions were prepared from prepared from single element stock solutions. To each standard, 1% of Cesium was added to minimize ionization.

Table B-4: Calibration standards prepared from single element stock solution

Analyte (mg/L)	Std 0	Std 1	Std 2	Std 3	Std 4	Std 5	Std 6	Std 7
Ca	0	1	3	5	10	20	40	60
Mg	0	1	3	5	10	20	40	60
Al	0	1	3	5	10	20	40	60
Fe	0	1	3	5	10	20	40	60
Mn	0	1	3	5	10	20	40	60
Na	0	1	3	5	10	20	40	60
K	0	1	3	5	10	20	40	60
P	0	1	3	5	10	20	40	60
Si	0	1	3	5	10	20	40	60

The instrument was rinsed after every sample reading using Std 0 solution and recalibrated after every 15 samples. At the end of the experiment, microwave oven blanks, filter blanks, CRM and calibration standards were run in the given order. LOD was determined as discussed in Appendix B-2 though in this case, measurements of microwave acid blanks were used instead.

Table B-5: Instrument settings

Parameter	(Settings)
RF power, kW	1.0kW
Plasma Ar flow, L min^{-1}	15.0L/min
Auxiliary Ar flow, L min^{-1}	1.5L/min

Nebulizer Ar flow, L min^{-1}	0.75L/min
Sample flow rate, mL min^{-1}	1mL/min
Reading time, s	3 seconds
Number of replicates	3
Reading per replicate	1 second
Rinse time	30s
Sample update delay	60s
Rump rate	20rpm
Sample introduction	Autosampler

The wavelength for each element was chosen by ensuring that it was accessible by the instrument, is appropriate for the sample concentrations, selected by the origin of the emission lines (atomic or ionic) and also being free from spectral interferences. At least two (2) wavelengths were chosen for each element (See Table B-6)

Table B-6: Wavelength selection

Analyte (mg/L)	Wavelength 1	Wavelength 2	Wavelength 3	Wavelength 4
Ca	Ca 393.366	Ca 317.933	Ca 396.847	Ca 422.673
Mg	Mg 279.553	Mg 280.270	Mg 285.213	
Al	Al 237.312	Al 396.152		
Fe	Fe 238.204	Fe 259.940		
Mn	Mn 259.372	Mn 257.610		
Na	Na 588.995	Na 589.592		
K	K 766.491	K 769.897		

P	P 213.618	P 177.434		
Si	Si 288.158	Si 251.611		

Appendix C: Raw Data

Table C-1: Measured DGT concentrations, Ortho P (MBM) and TDP (ICP-MS)

				Ortho P (PO4-)- MBM (mg/L)				**TDP ($PO4^-$+DNOM)-ICP-MS (µg/L)**	
				Measurements				**Measurements**	
Sampling point	**Sampling No**	**Parellel No**	**Label**	**1st**	**2nd**	**3rd**	**4th**	**1st**	**2nd**
Xiao	Sampling 1	Parallel 1b	1-1-b	68,15	66,12			70,51	61,65
		Parallel 1c	1-1-c	81,46	79,94			92,35	77,93
	Sampling 2	Paralel 2a	2-1-a	340,22	364,08			**497,96**	**418,18**
		Paralel 2b	2-1-b	15,69	16,03			17,75	16,05
		Paralel 2c	2-1-c	74,39	81,01			88,7	75,59
				0,00	0,00				
Baxian	Sampling 1	Parallel 1b	1-2-b	19,03	20,10			21,76	13,38
		Parallel 1c	1-2-c	18,68	18,78			17,77	18,3
	Sampling 2	Parallel 2a	2-2-a	2,39	5,78			2,66	0,61
		Parallel 2b	2-2-b	4,46	6,95			3,81	3,13
		Parallel 2c	2-2-c	6,53	**11,93**			6,6	6,98
				0,00	**0,00**				
Beix	Sampling 1	Parallel 1b	1-3-b	306,70	315,94			351,32	317,61
		Parallel 1c	1-3-c	541,03	532,46			598,36	532,53
	Sampling 2	Parallel 2a	2-3-a	276,09	0,00			309,15	265,76
		Parallel 2b	2-3-b	213,69	0,00			237,12	204,24
		Parallel 2c	2-3-c	416,94	0,00			438,54	389,35
	Sampling 3	Parallel 3a	3-3-a	382,78	382,26			**517,72**	389,39
		Parallel 3b	3-3-b	459,63	465,53			584,08	472,23
		Parallel 3c	3-3-c	457,26	463,48			603,72	478,79
				0,00	**0,00**				
Mashen (Yuma)	Sampling 1	Parallel 1b	1-4-b	165,78	156,90			182,5	164,9
		Parallel 1c	1-4-c	139,06	135,54			162,74	141,93
	Sampling 2	Paralel 2a	2-4-a	254,77	0,00			280,91	235,87
		Paralel 2b	2-4-b	262,49	0,00			293,93	244,59

		Parallel 2c	2-4-c	176,01	0,00			195,36	168,07
	Sampling 3	Parallel 3a	3-4-a	212,54	210,44			278,08	217,99
		Parallel 3b	3-4-b	187,12	190,50			242,48	202,64
		Parallel 3c	3-4-c	194,51	217,18			278,11	234,75
				0,00	0,00				
Lin	Sampling 1	Parallel 1b	1-5-b	22,10	23,23			22,58	24,19
		Parallel 1c	1-5-c	62,67	59,25			67,67	67,51
	Sampling 2	Paralel 2a	2-5-a	5,05	8,71			**1,83**	**10,66**
		Parallel 2b	2-5-b	-1,15	2,84			**-4,37**	**5,87**
		Parallel 2c	2-5-c	1,21	4,60			**-2,29**	**8,06**
				0,00	0,00				
Fish Pond	Sampling 1	Parallel 1b	C-1-7-b	243,45	254,89			262,45	251,64
		Parallel 1c	C-1-7-c	141,56	140,17			164,86	163,32
	Sampling 2	Parallel 2a	C-2-7-a	228,20	223,63			277,38	264,71
		Parallel 2b	C-2-7-b	192,14	203,69			234,64	229,57
		Parallel 2c	C-2-7-c	151,36	170,56			169,72	170,13
				0,00	0,00				
Abandoned Fish Pond	Sampling 1	Parallel 1b	1-7-b	595,89	595,81			621	600,75
		Parallel 1c	1-7-c	538,83	528,14			575,56	528,15
	Sampling 2	Parallel 2a	2-7-a	315,39	313,65			356,94	350,22
		Parallel 2b	2-7-b	540,91	596,01			663,89	644,23
		Parallel 2c	2-7-c	406,72	423,31			480,57	467,86
				0,00	0,00				
Yuqiao Reservoir	Upper Depth	Parallel 1a	D-1-a	0,61	4,45			**2,44**	**8,15**
		Parallel 1b	D-1-b	4,13	8,59			**2,13**	**8,27**
		Parallel 1c	D-1-c	18,06	12,52			**7,89**	**15,82**
	Middle Depth	Parallel 2a	D-2-a	11,67	11,96			**11,86**	**17,55**
		Parallel 2b	D-2-b	20,41	24,03			**21,18**	**25,90**
		Parallel 2c	D-2-c	29,88	0,00			29,94	36,38
	Deeper Depth	Parallel 3a	D-3-a	3,38	1,63			**-0,48**	**4,96**
		Parallel 3b	D-3-b	1,63	5,81			**-0,84**	**4,72**
		Parallel 3c	D-3-c	-2,63	1,96			-3,14	5,12
				0,00	0,00				
DGT Blanks	Blank 1		Blank 1	-0,61	-0,88	0,005		-2,48	5,61
			Blank 1-2nd	0,00	0,00				5,84
	Blank 2		Blank 2	-1,23	-0,88	0,005		-2,56	2,91
			Blank 2-2nd	0,00	0,00				2,87
	Blank 3		Blank 3	-0,61	-0,25	0,005		-2,8	2,81

			Blank 3-2nd	0,00	0,00				2,74
	Blank 4		Blank 4	-2,63	-0,09			-8,33	3,31
			Blank 4-2nd	0,00	0,00			-6,21	3,04
Calibration Standards			Std 0 - R1						2,89
			Std 0 - R2						3,16
			Std 0 - R3						5,15
			Std 0 - R4						3,60
			Std 0 - R5						2,99
			Std 0 - R6						3,37
			Std 0 - R7						3,10
			Std 0 - R8						3,24
			Std 0 - R9						3,40
			Std 0 - R10						3,33
			Std 0 - R11						3,51
			Std 0 - R12						3,65
Control Samples	X1		Conrol X1	91,49	96,71	88,65			92,3
	Y1		Conrol Y1	45,13	46,97	43,58	43,89		44,9
	Xp		Control Xp	62,95	62,95	61,21	62,66		62,6
	Yp		Control Yp	92,61	92,61	92,83	94.61		93,5

Table C-2: XRD results

	Ye No.	Site	Minerals (%)						
	Number	Sampling site	Clay 1:1	Clay 1:2	Quarts	Dolomite	Fieldspar	Berlinite	Muscovite
1	TS130715-03	Baxian Mountain	23,04	9,32	29,56	3,76	12,18	22,14	0
2	TS130906-01	Baxian Mountain	23,79	3,51	35,66	1,46	11,08	0,97	23,53
3	TS130906-02	Baxian Mountain	25,18	3,25	36,63	2,94	10,96	0,79	20,26
4	TS130906-03	Baxian Mountain	4,31	1,14	6,39	74,09	1,99	0,57	11,5
5	TS130906-04	Baxian Mountain	63,38	0,27	14,14	0,07	19,25	0,06	2,84
6	TS130906-05	Baxian Mountain	26,38	0	1,76	43,71	20,3	6,17	1,67
7	TS130807-01	Baxian mountain	70,8	0	1,24	10,52	16,6	0,84	0
8	TS130807-02	Baxian mountain	83,13	0	0	4,85	10,44	1,59	0
9	TS130807-03	Baxian mountain	25	0,84	0,46	41,98	12,99	15,15	3,57
10	TS120727-05	Beixinzhuang bridge	2,41	0,57	47,18	34,28	2,26	9,59	3,7
11	TS120727-06	Beixinzhuang bridge	2,93	0,76	51,97	25,83	5,76	9,4	3,35
12	TS120727-08	Beixinzhuang bridge	28,39	0,28	15,18	14,24	1,39	30,55	9,97
13	TS120801-05	Beixinzhuang bridge	36,3	1,26	47,43	0,95	4,41	4,7	4,95
14	TS120801-06	Beixinzhuang bridge	32,28	0,48	31,86	13,41	9,5	8,42	4,05
15	TS120801-08	Beixinzhuang bridge	64,36	1,99	8,89	3,44	5,7	5,88	9,74
16	TS120801-12	Beixinzhuang bridge	42,9	0,92	11,6	23,42	7,91	12,73	0,52
17	TS120801-13	Beixinzhuang bridge	63,8	0,56	8,05	0,08	3,6	4,08	19,83
18	TS120801-14	Beixinzhuang bridge	68,84	1,06	6,93	3,07	4,27	4,68	11,14
19	TS120807-03	Beixinzhuang bridge	67,41	0,87	7,57	2,78	4,09	2,71	14,57
20	TS120807-04	Beixinzhuang bridge	11,77	1,04	6,84	55,1	2,84	1,48	20,92
21	TS130906-13	Baixian bridge	13,48	2,33	45,86	0,68	22,85	0,63	14,18
22	TS130906-14	Baixian bridge	42,72	0,9	18,1	19,34	12,99	3,29	2,66
23	TS130906-15	Baixian bridge	7,44	1,6	58,97	3,28	16,35	2,67	9,69
24	TS130906-16	Baixian bridge	22,8	0	39,82	2,67	18,68	9,09	6,93

25	TS130906-17	Baixian bridge	65,98	0	0	23,56	0	10,46	0
26	TS130906-18	Baixian bridge	30	0	24,71	35,26	7,77	1,51	0,76
27	TS130906-19	Baixian bridge	38,08	0	22,77	22,77	11,32	5,06	0
28	TS130906-20	Baixian bridge	47,36	0	3,2	20	20,19	9,25	0
29	TS130906-21	Baixian bridge	38,88	0	27,75	0,76	14,47	13,77	4,37
30	TS130906-22	Baixian bridge	61,71	0	20,68	1,03	10	2,93	3,64
31	TS130906-23	Baixian bridge	73,55	0	12,76	0,24	6,14	7,32	0
32	TS130715-02	Baixian bridge	37	0,41	13,09	18,19	20,21	4,65	6,44
33	TS130307-03	Lin bridge	4,26	0,73	26,34	0	13	25,19	30,49
34	TS130410-03	Lin bridge	13,44	0,24	10,62	1,21	7,24	15,88	51,36
35	TS130715-04	Lin bridge	15,4	4,85	17,46	4,26	8,17	33,09	16,77
36	TS130906-06	Lin bridge	52,81	0,07	8,55	5,64	10,57	20,25	2,13
37	TS130906-07	Lin bridge	1,02	0	59,36	1,59	22,72	7,68	7,62
38	TS130906-08	Lin bridge	5,01	4,73	39,56	0,21	17,24	0,78	32,47
39	TS130906-09	Lin bridge	23,92	1,94	24,15	1,24	17,5	25,08	6,18
40	TS130906-10	Lin bridge	35,93	1,99	0	5,19	29	22,79	5,1
41	TS130906-11	Lin bridge	5,51	1,66	5,4	4,51	11,71	29,48	41,72
42	TS130906-12	Lin bridge	26,29	0	41,64	2,29	10,93	9,1	9,74
43	TS130819-05	Mashen Bridge	46,57	0	0	17,68	22,93	10,19	2,62
44	TS130819-06	Mashen Bridge	38,96	0,53	30,43	0,16	16,12	1,58	12,23
45	TS130819-07	Mashen Bridge	51,36	0	19,81	1,11	13,35	4,23	10,14
46	TS130819-08	Mashen Bridge	52,48	0	9,37	12,49	17,41	5,52	2,73
47	TS130819-09	Mashen Bridge	51,09	0	6,31	16,18	23,08	0,71	2,62
48	TS130819-11	Mashen Bridge							
49	TS130812-12	Mashen Bridge	53,25	0	6,48	18,25	12,81	4,56	4,65
50	TS130812-13	Mashen Bridge	39,33	0	12,5	27,68	12,86	4,3	3,32

51	TS120727-01	Xiaojugezhuang bridge	23,74	3,51	35,7	1,47	11,08	0,97	23,53
52	TS120727-02	Xiaojugezhuang bridge	17,81	0	42,28	23,94	0,61	0,15	15,21
53	TS120727-03	Xiaojugezhuang bridge	20,33	0	34,14	1,24	4,34	7,91	32,04
54	TS120727-04	Xiaojugezhuang bridge	4,14	0,7	37,42	47,64	1,88	4,74	3,48
55	TS120801-01	Xiaojugezhuang bridge	43,14	0,94	34,39	4,9	6,32	6,57	3,74
56	TS120801-02	Xiaojugezhuang bridge	37,27	1,22	36,56	2,76	8,27	10,13	3,79
57	TS120801-07	Xiaojugezhuang bridge	51,96	1,78	21,18	2,74	6,98	9,13	6,23
58	TS120912-01	Xiaojugezhuang bridge	23,46	0,55	42,34	7,06	1,35	1,89	23,36
59	TS121103-03	Xiaojugezhuang bridge	28,68	0,03	41,23	1,97	0,34	0,52	27,24
60	TS130307-01	Xiaojugezhuang bridge	18,71	0,57	46,72	8,42	0,68	1,14	23,76
61	TS130819-01	Xiaojugezhuang bridge	26,06	2,3	14,95	16,04	14,19	26,45	0
62	TS130819-02	Xiaojugezhuang bridge	36,83	0	29,47	6,17	15,58	3,26	8,69
63	TS130819-03	Xiaojugezhuang bridge	55,44	0	0,12	16,74	17,9	7,63	2,16
64	TS130819-04	Xiaojugezhuang bridge							
65	TS130715-05	Xiaojugezhuang bridge	35,48	0	6,73	8,25	28,86	4,34	16,34
66	TS130723-04	Xiaojugezhuang bridge	57,53	0	0	10,18	4,09	15,26	12,94
67	TS130723-07	Xiaojugezhuang	67,66	0	7,15	0,81	18,76	5,63	0

		bridge							

ICP-OES recalibration

Due to the high range of the calibration standards and less concentration of the analyte, a recalibration was done for all the elements measured. Calibration was chosen that fell in between the range of the concentration of the element to be determined.

Table C-3: ICP: OES results

		Concentration mg/L									
Sample		**Al**	**P**	**Mn**	**Si**	**Ca**	**Fe**	**K**	**Mg**	**Na**	**Sample Point**
1	Low flow	14,01	0,83	1,94	0,61	10,77	1,46	5,37	2,55	8,09	Baxian Mountain
2	Episode 1a	1,39	0,33	1,76	0,20	0,56	1,54	5,51	0,53	16,58	Baxian Mountain
3	Episode 1b	2,58	**0,33**	2,33	0,18	0,99	2,40	7,39	0,78	21,33	Baxian Mountain
4	Episode 1c	1,24	0,34	1,26	0,16	0,56	1,11	4,27	0,44	13,21	Baxian Mountain
5	Episode 1d	2,55	**0,28**	2,05	0,17	1,14	1,65	5,70	0,64	17,06	Baxian Mountain
6	Episode 1e	1,39	**0,30**	1,36	0,14	0,63	1,16	4,61	0,46	14,47	Baxian Mountain
61	Low flow	1,46	0,36	2,14	0,14	0,53	1,24	4,55	0,45	15,21	Baxian Mountain
62	Low flow	1,18	0,20	1,67	0,13	0,35	1,35	4,68	0,41	15,15	Baxian Mountain
63	Low flow	5,64	0,42	0,93	0,24	4,34	1,12	2,31	1,41	5,64	Baxian Mountain
7	Episode 1-a	9,57	0,65	1,71	0,42	9,03	5,77	3,92	4,29	8,83	Beixinzhuang bridge
8	Episode 1-b	8,90	0,65	2,18	0,45	8,26	6,80	3,82	4,17	9,16	Beixinzhuang bridge

9	Episode 1-c	15,26	0,53	1,35	0,37	11,06	1,27	5,07	3,15	9,55	Beixinzhuang bridge
10	Episode 2-a	12,81	0,64	1,07	0,30	10,10	1,21	3,46	2,83	5,70	Beixinzhuang bridge
11	Episode 2-b	15,92	0,52	1,41	0,32	11,23	1,27	5,10	3,25	8,71	Beixinzhuang bridge
12	Episode 2-c	24,16	0,75	1,47	0,40	16,78	2,15	6,98	4,98	9,72	Beixinzhuang bridge
13	Episode 3-a	11,09	0,64	2,98	1,43	8,42	2,97	4,48	3,05	9,78	Beixinzhuang bridge
14	Episode 3-b	13,89	0,62	1,12	0,31	9,27	1,27	4,96	2,69	9,88	Beixinzhuang bridge
15	Episode 4-a	17,25	0,57	1,55	0,35	13,35	1,52	4,06	3,53	5,13	Beixinzhuang bridge
16	Episode 4-b	12,30	0,69	3,30	0,74	15,88	3,05	5,46	5,21	11,78	Beixinzhuang bridge
17	Episode 4-c	10,90	0,57	1,53	0,33	7,75	2,18	4,93	2,53	11,62	Beixinzhuang bridge
18	Episode 5-a	9,31	0,38	1,25	0,76	7,55	4,13	4,22	2,60	8,92	Beixinzhuang bridge
19	Episode 5-b	10,43	0,29	1,95	0,57	7,81	4,06	5,87	2,69	12,94	Beixinzhuang bridge
20	Episode 5-c	13,63	0,63	1,76	1,02	11,28	10,31	6,41	4,21	13,52	Beixinzhuang bridge
21	Episode 5-d	31,52	1,37	8,14	0,94	44,49	7,27	7,64	14,86	3,83	Beixinzhuang bridge
22	Episode 6-a	4,90	0,77	2,08	0,63	4,16	19,59	4,18	1,91	13,47	Beixinzhuang bridge
23	Episode 6-b	4,45	0,56	1,67	0,54	3,56	27,60	4,52	1,97	15,35	Beixinzhuang bridge
24	Episode 6-c	10,86	0,87	1,58	0,87	9,14	38,30	4,91	4,02	11,21	Beixinzhuang bridge
25	Episode 6-d	22,66	1,27	3,06	1,20	18,21	70,63	7,68	7,26	11,76	Beixinzhuang bridge
26	Episode 6-e	16,12	0,93	2,75	2,49	13,84	73,56	5,54	5,65	9,88	Beixinzhuang bridge
27	Episode 6-f	7,14	0,72	1,60	1,06	6,20	15,72	3,87	2,41	10,79	Beixinzhuang bridge
28	Episode 6-g	4,11	0,70	1,91	0,72	3,43	29,85	3,59	1,94	12,31	Beixinzhuang bridge
64	Low flow	10,74	0,62	1,44	0,98	8,60	3,39	4,12	2,97	8,23	Beixinzhuang bridge
29	Low flow	15,88	0,91	4,17	0,67	37,43	8,23	2,83	11,87	2,38	Lin bridge
30	Low flow	23,11	1,42	7,82	1,94	81,35	9,39	3,36	16,81	2,83	Lin bridge
31	Low flow	33,62	1,50	5,86	1,25	47,48	8,94	7,75	16,11	2,99	Lin bridge
32	Episode 1a	23,08	0,89	5,37	0,74	31,60	4,82	5,89	10,36	5,05	Lin bridge

33	Episode 1b	24,43	1,07	3,95	0,68	34,79	5,41	6,21	11,44	5,18	Lin bridge
34	Episode 1c	15,61	0,64	4,33	0,50	20,60	3,20	4,42	6,97	5,07	Lin bridge
35	Episode 1d	21,80	0,81	3,81	0,61	29,28	4,81	5,58	9,93	4,39	Lin bridge
36	Episode 1e	21,94	1,01	4,66	0,60	32,08	5,14	5,34	10,73	2,91	Lin bridge
37	Episode 1f	19,86	0,92	2,57	0,59	29,83	4,79	4,62	9,89	2,62	Lin bridge
38	Episode 1g	17,71	0,67	1,35	0,49	13,69	3,22	6,41	4,25	9,98	Lin bridge
39	Episode 1-a	24,36	1,02	4,80	0,73	19,73	8,80	6,60	10,93	5,46	Mashen bridge
40	Episode 1-b	15,71	0,41	2,20	0,41	11,33	2,05	5,11	3,24	7,65	Mashen bridge
41	Episode 1-c	10,33	0,46	1,59	0,41	7,31	2,38	5,46	2,26	11,97	Mashen bridge
42	Episode 1-d	8,09	0,67	1,56	0,48	5,97	2,68	5,05	1,98	13,01	Mashen bridge
43	Episode 1-e	2,75	0,44	0,96	0,22	1,86	0,95	4,45	0,69	14,80	Mashen bridge
44	Episode 1-f	9,44	0,74	1,44	0,80	7,89	8,40	8,28	3,83	20,01	Mashen bridge
59	Low flow	7,19	0,54	1,77	0,79	5,59	3,41	3,46	2,05	8,12	Mashen bridge
60	Low flow	7,62	0,52	2,23	0,77	5,93	7,84	4,83	3,09	11,64	Mashen bridge
45	Episode 1-a	14,28	0,51	1,44	0,41	8,97	3,82	8,52	5,41	17,42	Xiaojugezhuang bridge
46	Episode 1-b	17,03	0,76	2,20	0,75	11,94	3,36	5,76	6,83	8,01	Xiaojugezhuang bridge
47	Episode 1-c	15,18	1,17	2,01	0,43	12,79	3,25	3,44	5,75	6,66	Xiaojugezhuang bridge
48	Episode 1-d	25,32	0,45	1,49	0,59	21,12	4,19	4,11	8,29	4,14	Xiaojugezhuang bridge
49	Episode 2-a	12,03	1,16	1,28	0,31	8,86	6,31	4,37	5,22	6,51	Xiaojugezhuang bridge
50	Episode 2-b	14,70	1,21	1,33	0,63	13,30	7,59	6,93	6,17	13,51	Xiaojugezhuang bridge
51	Episode 2-c	17,57	0,68	1,18	0,46	12,40	3,20	5,60	5,26	7,03	Xiaojugezhuang bridge
52	Low flow	0,86	0,21	0,99	0,13	0,12	1,03	2,68	0,45	9,04	Xiaojugezhuang bridge
53	Low flow	0,94	0,22	1,35	0,13	0,05	1,58	4,87	0,43	14,76	Xiaojugezhuang bridge
54	Low flow	0,86	0,22	1,11	0,14	0,25	1,08	2,51	0,45	8,55	Xiaojugezhuang bridge
55	Episode 3-a	10,46	0,55	1,78	0,41	8,04	4,50	4,04	4,44	7,77	Xiaojugezhuang bridge

56	Episode 3-b	11,23	2,00	2,32	0,28	7,68	9,94	4,88	5,41	8,25	Xiaojugezhuang bridge
57	Episode 3-c	7,09	2,32	2,07	0,27	4,68	10,57	4,38	3,66	10,74	Xiaojugezhuang bridge
58	Episode 3-d	2,33	0,31	1,89	0,16	0,78	2,91	11,23	0,78	28,52	Xiaojugezhuang bridge
65	Low flow	1,76	0,40	1,69	0,18	0,76	3,32	6,44	0,89	21,13	Xiaojugezhuang bridge
66	Low flow	14,22	0,54	1,45	0,51	10,43	4,31	5,07	5,37	9,20	Xiaojugezhuang bridge
67	Low flow	3,56	0,34	1,57	0,27	2,60	1,99	3,03	1,70	10,50	Xiaojugezhuang bridge
1	Acid Blank 1	0,280	0,229	0,325	0,174	0,120	-0,151	0,072	0,128	-0,142	
2	Acid Blank 2	0,244	0,163	0,196	0,133	0,074	-0,199	0,034	0,089	-0,194	
3	Acid Blank 3	0,238	0,088	0,198	0,125	0,063	-0,205	0,023	0,080	-0,197	
4	Acid Blank 4	0,241	0,220	0,185	0,124	0,067	-0,197	0,027	0,081	-0,206	
5	Acid Blank 5	0,233	0,075	0,151	0,124	0,065	-0,208	0,021	0,081	-0,194	
6	Acid Blank 6	0,247	0,036	0,228	0,124	0,063	-0,182	0,049	0,080	-0,136	
7	Acid Blank 7	0,224	0,089	0,161	0,124	0,067	-0,209	0,026	0,078	-0,171	
8	Acid Blank 8	0,242	0,231	0,167	0,124	0,063	-0,179	0,022	0,083	-0,120	
9	Acid Blank 9	0,235	0,174	0,167	0,124	0,060	-0,213	0,020	0,080	-0,179	
10	Acid Blank 10	0,222	0,178	0,142	0,124	0,059	-0,215	0,018	0,079	-0,208	
11	Acid Blank 11	0,236	1,317	0,147	0,124	2,654	-0,168	0,024	0,080	-0,184	
1	Blank filter 1	0,817	0,251	1,009	0,125	0,113	1,154	4,035	0,238	13,623	
2	Blank filter 2	0,973	0,183	0,699	0,127	0,113	1,500	4,717	0,305	14,618	
3	Blank filter 3	0,820	0,141	0,916	0,126	0,098	1,064	3,792	0,234	12,775	
4	Blank filter 4	1,043	0,189	1,065	0,130	0,142	1,941	4,680	0,331	14,442	
5	Blank filter 5	0,885	0,225	0,758	0,129	0,108	1,247	3,883	0,276	12,240	
6	Blank filter 6	1,105	0,164	0,680	0,126	0,102	1,716	5,327	0,339	16,456	
7	Blank filter 7	1,789	0,143	1,309	0,127	0,128	2,486	7,931	0,445	22,858	
8	Blank filter 8	1,232	0,087	1,028	0,127	0,102	2,159	6,806	0,384	20,647	

1	CRM 1a	49,148	11,688	8,695	1,123	38,804	848,191	15,157	54,548	46,388	
2	CRM 1b	22,578	1,067	3,318	0,550	20,129	23,502	7,281	9,884	6,673	
3	CRM 1c	26,736	1,239	2,959	0,604	23,388	25,963	8,661	11,331	7,715	
4	CRM 1d	22,620	1,230	2,981	0,473	19,892	18,002	7,295	9,117	5,216	
6	CRM 2a	8,667	1,886	2,578	0,280	6,525	154,215	2,505	8,614	6,282	
7	CRM 2b	7,349	1,758	3,127	0,251	6,475	122,452	2,148	6,917	5,061	
8	CRM 2c	8,339	1,864	1,688	0,270	6,514	144,334	2,398	8,217	5,797	

Table C-4: Water Chemistry data

Number						Alkalinity	SS	Ca2+	Mg2+	Na+	K+	NH4+-N	SO42-	NO3- -N	Cl-	Tot-N	Tot-P	DOM-P+PO4	Free PO4	Particualte P	Org-P
Ye No.	Site	Land Use	Type	Date	pH	mmol/L	mg/L	mg L-1	mg L-1	mg L-1	mg L-1	mg N L-1	mg SO4 L-1	mg N L-1	mg L-1	mg N L-1	mg P L-1	mg P L-1	mg P L-1	mg P L-1	mg P L-1
TS120703-005	Baxianshanriver bridge	Forest	R	3.7.2012	7,54	2,18	3,00	23,10	9,75	11,40	1,47	0,03	36,30	5,02	12,20	5,07	0,13	0,07	0,01	0,07	0,05
TS120716-02	Baxianshan spring	Forest	Re	16.7.2012	7,24	0,49	2,00	30,70	4,56	6,08	0,74	0,04	61,50	13,90	9,95	14,80	0,02	0,02	0,02	0,00	0,00
TS130715-03	Baxian Mountain (after rain)	Forest	R	9.7.2013	7,42	0,72	3,00	7,71	8,21	6,67	0,76	0,14	57,00	12,00	8,99	12,20	0,34	0,02	0,02	0,32	0,00
TS130723-12	Baxian Mountain (before rain 5:00)	Forest	Re	15.7.2013	7,34	0,98	3,00	39,70	34,80	8,59	2,12	0,02	58,00	11,80	9,91	12,00	0,03	0,03	0,01	0,00	0,01
TS130723-09	Baxiang Mountain (after rain 8:00)	Forest	Re	15.7.2013	6,81	0,71	29,00	4,27	6,68	5,95	2,24	0,56	43,80	8,58	7,90	8,23	0,12	0,04	0,03	0,07	0,02
TS130807-01	Baxian mountain	Forest	Re	23.7.2013	7,20	0,98	7,00	12,90	4,41	8,74	2,14	0,02	60,00	11,30	10,40	12,30	0,01	0,01	0,01	0,00	0,00
TS130807-02	Baxian mountain	Forest	Re	26.7.2013	7,24	1,14	4,00	14,00	4,48	7,48	3,12	0,04	61,40	11,10	10,30	12,30	0,02	0,01	0,01	0,00	0,00
TS130807-03	Baxian mountain	Forest	Re	31.7.2013	7,04	0,83	28,00	12,00	4,19	6,69	2,62	1,08	51,40	8,63	8,19	10,90	0,03	0,02	0,02	0,01	0,00
TS130807-04	Baxian mountain	Forest	Re	1.8.2013	7,19	0,85	10,00	14,00	6,54	7,16	2,98	0,14	102,00	9,34	9,24	11,20	0,03	0,02	0,02	0,01	0,00
TS130826-04	Baxian Mountain	Forest	R	7.8.2013	7,76	1,15	12,00	22,70	24,90	8,94	3,04	0,05	45,00	9,13	9,17	9,44	0,02	0,02	0,02	0,00	0,00
TS130826-05	Baxian Mountain	Forest	R	7.8.2013	7,78	1,10	7,00	27,30	27,30	8,51	2,64	0,06	44,40	9,01	8,48	9,53	0,02	0,02	0,02	0,00	0,00
TS130826-06	Baxian Mountain	Forest	R	7.8.2013	7,56	1,18	10,00	26,70	28,10	8,75	2,45	0,03	46,00	9,12	8,61	9,61	0,02	0,02	0,02	0,00	0,00
TS130826-07	Baxian Mountain	Forest	R	7.8.2013	7,55	1,13	6,00	24,70	23,90	8,43	2,45	0,04	45,80	7,69	8,67	9,16	0,02	0,02	0,01	0,00	0,00
TS130826-08	Baxian Mountain	Forest	R	7.8.2013	7,50	1,15	23,00	24,70	20,80	8,13	2,10	0,06	46,40	9,32	8,77	9,99	0,02	0,03	0,01	-0,01	0,01
TS130906-01	Baxian Mountain	Forest	R	11.8.2013	7,13	1,28	19,00	24,50	17,20	13,20	3,57	0,04	49,10	8,87	10,50	9,45	0,09	0,08	0,03	0,01	0,05
TS130906-02	Baxian Mountain	Forest	R	11.8.2013	7,38	1,26	109,00	24,50	25,40	15,00	3,57	0,09	48,70	10,00	9,27	10,70	0,07	0,05	0,03	0,02	0,02
TS130906-03	Baxian Mountain	Forest	R	11.8.2013	7,18	1,31	42,00	24,10	27,20	13,80	3,93	0,11	48,80	10,00	9,22	10,20	0,10	0,09	0,03	0,01	0,06
TS130906-04	Baxian Mountain	Forest	R	11.8.2013	7,18	1,31	3,00	24,00	20,40	7,91	3,79	0,10	49,00	9,41	9,28	9,61	0,19	0,14	0,03	0,05	0,11
TS130906-05	Baxian Mountain	Forest	R	11.8.2013	7,46	1,28	117,00	22,80	27,10	7,79	3,86	0,07	49,10	10,20	9,30	10,70	0,10	0,08	0,03	0,02	0,05
TS131010-04	Baxian Mountain	Forest	NA	28.8.2013	6,92	1,05	4,00	17,00	6,66	6,89	1,45	0,01	41,30	4,96	16,00	1,06	0,01	0,00	0,00	0,01	0,00
TS131010-05	Baxian Mountain	Forest	NA	28.8.2013	6,99	1,09	5,00	16,90	6,04	6,77	0,99	0,03	44,50	9,25	8,50	1,37	0,02	0,00	0,00	0,01	0,00
TS131010-06	Baxian Mountain	Forest	NA	28.8.201	7,09	1,04	3,00	18,00	6,26	6,96	0,90	0,02	44,50	9,19	8,31	1,21	0,02	0,00	0,00	0,01	0,00

				3																	
TS131010-07	Baxian Mountain	Forest	NA	28.8.2013	7,14	1,02	3,00	19,10	6,14	6,32	1,17	0,02	43,90	9,05	8,46	3,98	0,02	0,02	0,02	0,00	0,00
TS120409-02	Lin river bridge	Mix1	R	9.4.2012	7,88	NA	157,00	61,70	22,80	21,20	7,83	0,23	87,00	9,66	29,00	NA	0,24	0,03	0,03	0,21	0,00
TS120710-02	Lin river bridge 2012/7/9 1:30 pm	Mix1	Re	9.7.2012	8,04	2,31	224,00	30,10	15,00	17,50	5,19	0,62	88,10	9,13	25,20	9,83	0,17	0,02	0,02	0,15	0,00
TS120710-01	Lin river bridge 2012/7/9 12:30 pm	Mix1	Re	9.7.2012	7,99	2,92	95,00	53,50	14,80	18,20	5,18	0,63	89,20	11,40	31,10	12,10	0,08	0,02	0,02	0,07	0,00
TS120710-03	Lin river bridge 2012/7/9 3:00 pm	Mix1	Re	9.7.2012	8,12	2,25	109,00	34,60	16,70	18,10	5,34	0,66	87,60	10,20	25,30	11,20	0,09	0,02	0,01	0,07	0,00
TS120710-04	Lin river bridge 2012/7/9 4:00 pm	Mix1	Re	9.7.2012	8,09	2,51	505,00	36,30	14,80	19,00	5,87	0,91	89,90	6,93	28,60	7,90	0,55	0,02	0,02	0,53	0,00
TS120716-04	Lin river bridge	Mix1	Re	16.7.2012	7,78	2,23	2,00	47,60	18,40	17,30	2,99	0,04	92,00	15,20	27,20	16,20	0,02	0,02	0,02	0,00	0,00
TS120912-03	Lin river bridge	Mix1	R	12.9.2012	7,17	2,36	49,00	62,90	25,80	14,60	6,49	0,14	104,00	17,40	72,60	18,00	0,04	0,01	0,01	0,03	0,00
TS120925-01	Lin river bridge	Mix1	R	25.9.2012	7,34	2,18	56,00	73,00	18,40	16,80	5,90	0,16	105,00	18,90	28,80	20,00	0,37	0,01	0,01	0,36	0,00
TS121009-01	Lin river bridge	Mix1	R	9.10.2012	7,58	2,41	7,00	72,30	18,20	16,00	5,90	0,04	99,80	22,20	32,20	24,30	0,01	0,01	0,01	0,00	0,00
TS121020-03	Lin river bridge	Mix1	R	20.10.2012	7,53	2,46	720,00	85,10	23,00	19,70	6,10	0,10	99,90	23,03	32,70	23,80	0,73	0,01	0,01	0,71	0,00
TS121103-02	Lin river bridge	Mix1	R	3.11.2012	7,52	2,25	245,00	77,50	20,20	18,90	4,29	0,12	105,00	26,19	35,70	28,10	0,17	0,01	0,01	0,16	0,00
TS121114-02	Lin river bridge	Mix1	R	14.11.2012	7,59	2,10	1300,00	102,00	27,30	21,40	10,60	0,09	123,00	22,58	32,60	24,60	0,85	0,02	0,02	0,83	0,00
TS121201-02	Lin river bridge	Mix1	R	1.12.2012	7,38	2,20	65,00	65,40	31,90	27,70	5,31	0,05	128,00	29,81	39,90	31,70	0,15	0,02	0,02	0,13	0,00
TS121216-01	Lin river bridge	Mix1	R	16.12.2012	7,48	2,24	27,00	80,00	25,80	16,70	3,36	0,04	105,00	28,67	36,30	29,80	0,02	0,01	0,01	0,01	0,00
TS130125-03	Lin river bridge	Mix1	R	25.1.2013	7,43	2,18	26,00	81,60	22,10	14,70	3,68	0,03	104,00	19,00	35,20	20,64	0,03	0,02	0,01	0,01	0,01
TS130222-03	Lin river bridge	Mix1	R	22.2.2013	7,44	2,00	3,00	75,30	16,20	17,40	3,47	0,03	91,70	20,90	NA	25,10	0,03	0,02	0,01	0,00	0,01
TS130307-03	Lin river bridge	Mix1	R	7.3.2013	7,54	2,18	NA	57,70	16,70	18,90	1,60	0,16	94,20	20,50	29,50	21,18	2,35	0,02	0,02	2,33	0,01
TS130326-03	Lin river bridge	Mix1	R	26.3.2013	7,54	2,11	42,00	109,00	15,50	18,10	4,64	0,14	94,20	18,10	28,90	20,21	0,43	0,02	0,02	0,41	0,00
TS130410-03	Lin river bridge	Mix1	R	10.4.2013	7,60	2,10	196,00	34,50	26,20	16,90	3,12	0,25	109,00	16,60	30,20	16,88	3,31	0,03	0,03	3,28	0,00
TS130501-03	Lin river bridge	Mix1	R	1.5.2013	7,38	2,51	32,00	22,10	27,00	19,80	4,17	0,12	103,00	19,90	37,60	20,72	0,16	0,02	0,02	0,14	0,00
TS130508-03	Lin river bridge	Mix1	R	8.5.2013	7,46	2,07	25,00	3,31	15,40	22,10	5,42	0,10	117,00	15,00	34,10	16,75	0,46	0,01	0,01	0,44	0,01
TS130715-04	Lin river bridge(after rain)	Mix1	R	9.7.2013	7,62	1,79	52,00	14,50	10,80	12,40	7,29	0,27	97,80	8,98	12,30	13,10	1,42	0,02	0,02	1,40	0,00
TS130723-05	Lin river bridge	Mix1	Re	16.7.2013	7,45	1,39	40,00	5,43	10,90	9,90	2,66	0,26	71,10	10,60	12,30	13,25	0,16	0,02	0,01	0,14	0,01
TS130807-05	Lin River	Mix1	R	31.7.201	7,35	3,89	109,00	14,90	5,04	17,30	5,13	0,28	98,00	17,60	26,90	18,10	0,08	0,02	0,01	0,06	0,01

				3																	
TS130807-06	Lin River	Mix1	R	31.7.2013	7,47	3,95	86,00	14,30	7,24	17,60	5,02	0,06	98,20	17,50	27,10	17,90	0,36	0,02	0,02	0,34	0,00
TS130807-07	Lin River	Mix1	R	31.7.2013	7,51	3,99	325,00	14,80	7,61	18,20	5,22	0,21	97,10	17,80	26,70	20,20	0,25	0,02	0,01	0,23	0,01
TS130807-08	Lin River	Mix1	R	31.7.2013	7,52	3,74	1290,00	14,70	10,70	17,10	5,64	0,17	94,70	15,10	24,20	17,30	0,86	0,02	0,01	0,83	0,01
TS130807-09	Lin River	Mix1	R	31.7.2013	7,26	3,61	2180,00	14,20	7,79	14,40	6,90	0,27	94,80	11,70	21,40	14,40	1,52	0,05	0,04	1,47	0,01
TS130807-10	Lin River	Mix1	R	31.7.2013	7,06	3,50	1400,00	15,40	6,73	14,20	7,74	0,30	91,60	10,80	20,40	12,70	1,30	0,08	0,07	1,22	0,01
TS130819-13	Lin River	Mix1	R	4.8.2013	7,10	2,19	312,00	70,00	10,20	13,20	4,13	0,02	78,60	10,90	24,40	13,30	0,14	0,02	0,01	0,12	0,00
TS130819-14	Lin River	Mix1	R	4.8.2013	7,16	2,00	462,00	90,50	12,00	13,60	4,89	0,35	85,90	11,90	22,50	13,10	0,12	0,03	0,03	0,08	0,01
TS130819-15	Lin River	Mix1	R	4.8.2013	7,12	2,08	178,00	55,00	15,10	12,80	4,23	0,05	3,06	0,08	1,90	13,90	0,12	0,02	0,01	0,10	0,00
TS130819-16	Lin River	Mix1	R	4.8.2013	6,94	1,82	505,00	80,00	17,00	12,10	5,09	0,20	65,90	11,00	13,60	12,70	0,32	0,02	0,01	0,31	0,00
TS130819-17	Lin River	Mix1	R	4.8.2013	6,88	1,84	107,00	91,70	14,20	11,40	4,28	0,15	95,90	13,70	23,30	14,40	0,31	0,02	0,01	0,30	0,00
TS130819-18	Lin River	Mix1	R	4.8.2013	6,84	1,86	310,00	63,10	15,80	13,10	4,97	0,05	94,90	14,40	23,20	15,30	0,14	0,04	0,06	0,10	-0,02
TS130819-19	Lin River	Mix1	R	4.8.2013	6,76	1,87	113,00	95,70	14,70	12,80	4,49	0,03	95,10	14,50	23,60	15,20	0,05	0,02	0,01	0,04	0,00
TS130812-03	Lin River 1:30	Mix1	R	4.8.2013	7,40	2,02	331,00	50,80	27,90	15,80	6,30	0,16	86,70	13,00	22,00	13,50	0,52	0,04	0,02	0,48	0,02
TS130812-04	Lin River 2:10	Mix1	R	4.8.2013	7,44	2,13	578,00	42,80	23,70	15,20	4,78	0,18	56,70	5,94	23,60	16,60	0,34	0,02	0,01	0,32	0,01
TS130812-05	Lin River 21:50	Mix1	R	4.8.2013	7,53	1,84	154,00	47,30	18,70	18,30	5,10	0,18	82,50	13,40	21,20	16,50	0,05	0,02	0,00	0,03	0,02
TS130812-06	Lin River 22:30	Mix1	R	4.8.2013	7,27	5,05	456,00	32,80	22,20	18,80	6,37	0,15	64,70	8,69	24,40	9,13	0,14	0,06	0,03	0,08	0,04
TS130819-20	Lin River after rain	Mix1	R	5.8.2013	7,20	2,18	52,00	78,40	12,40	11,70	3,86	0,02	87,10	15,30	21,50	15,70	0,03	0,02	0,02	0,02	0,00
TS130826-10	Lin River	Mix1	R	11.8.2013	7,51	1,92	106,00	26,40	25,20	15,10	9,66	0,03	94,90	11,20	15,90	11,40	0,11	0,02	0,01	0,09	0,00
TS130826-11	Lin River	Mix1	R	11.8.2013	7,76	1,82	950,00	27,50	20,90	13,30	7,44	0,09	99,50	11,10	22,40	12,10	0,69	0,02	0,02	0,67	0,00
TS130826-12	Lin River	Mix1	R	11.8.2013	7,50	1,73	524,00	22,70	20,30	14,30	10,40	0,19	97,20	10,60	16,30	11,60	0,37	0,05	0,04	0,31	0,01
TS130826-13	Lin River	Mix1	R	11.8.2013	7,56	1,86	210,00	25,30	26,10	15,20	10,70	0,40	98,90	11,30	17,00	11,80	0,18	0,02	0,02	0,16	0,00
TS130826-09	Lin River before rain	Mix1	R	11.8.2013	7,77	1,88	271,00	23,60	21,90	15,90	11,60	0,11	95,80	11,60	16,10	11,90	0,45	0,02	0,01	0,43	0,00
TS130906-06	Lin River	Mix1	R	16.8.2013	6,96	1,40	834,00	24,40	27,60	7,58	3,68	1,65	64,40	6,27	10,20	9,72	1,54	0,61	0,13	0,93	0,48
TS130906-07	Lin River	Mix1	R	16.8.2013	7,22	1,51	869,00	23,80	27,50	7,95	3,76	0,53	82,10	10,70	12,60	12,10	0,68	0,21	0,02	0,47	0,18
TS130906-08	Lin River	Mix1	R	16.8.2013	7,53	1,55	648,00	24,00	27,50	8,50	3,13	0,73	85,80	10,70	13,10	12,40	0,46	0,06	0,03	0,40	0,03

TS130906-09	Lin River	Mix1	R	16.8.2013	7,24	1,44	624,00	24,50	26,60	16,40	11,50	0,42	79,40	10,50	12,70	11,20	0,81	0,19	0,14	0,62	0,06
TS130906-10	Lin River	Mix1	R	16.8.2013	7,08	1,50	1360,00	24,10	23,90	15,30	9,61	2,07	40,10	5,44	6,79	8,93	1,26	0,63	0,03	0,63	0,60
TS130906-11	Lin River	Mix1	R	16.8.2013	7,03	1,33	5810,00	24,80	26,90	14,70	11,30	2,33	41,70	5,51	6,85	8,48	1,53	0,22	0,05	1,31	0,16
TS130906-12	Lin River	Mix1	R	16.8.2013	7,84	3,37	130,00	24,10	27,60	15,80	10,70	3,61	42,20	4,76	22,90	8,62	0,58	0,55	0,54	0,03	0,01
TS131010-08	Lin River	Mix1	NA	24.9.2013	7,45	1,96	5,00	30,10	11,40	12,10	4,83	0,12	94,50	11,70	15,00	4,02	0,12	0,02	0,00	0,10	0,02
S120702-013	Xiaojugezhuang bridge(09：00)	Mix2	Re	29.6.2012	7,70	5,79	8,00	84,40	26,50	14,60	2,42	0,11	29,00	78,00	35,20	NA	0,05	0,03	0,03	0,01	0,01
S120702-012	Xiaojugezhuang bridge(10：00)	Mix2	Re	29.6.2012	7,71	5,74	9,00	84,50	27,50	15,40	2,96	0,07	27,40	74,40	33,60	NA	0,05	0,05	0,04	0,00	0,01
TS120710-09	Xiaojugezhuang bridge 2012/7/9 11:40	Mix2	Re	9.7.2012	7,19	5,79	3,00	57,60	32,20	13,60	3,09	0,06	34,80	17,60	38,20	18,20	0,04	0,03	0,03	0,01	0,00
TS120710-10	Xiaojugezhuang bridge 2012/7/9 12:40	Mix2	Re	9.7.2012	7,14	5,99	3,00	58,60	30,70	13,80	3,22	0,12	34,80	18,40	40,50	18,70	0,03	0,03	0,02	0,01	0,00
TS120710-11	Xiaojugezhuang bridge 2012/7/9 13:40	Mix2	Re	9.7.2012	7,14	5,76	3,00	41,40	34,70	14,20	3,11	0,37	35,70	17,60	38,00	18,60	0,10	0,03	0,02	0,07	0,00
TS120710-12	Xiaojugezhuang bridge 2012/7/9 14:40	Mix2	Re	9.7.2012	7,10	6,02	3,00	43,10	34,20	13,00	3,42	0,12	33,30	17,70	37,00	18,30	0,03	0,03	0,03	0,01	0,00
TS120710-13	Xiaojugezhuang bridge 2012/7/9 15:40	Mix2	Re	9.7.2012	7,08	5,71	3,00	47,00	29,40	13,40	3,16	0,17	34,60	18,30	39,50	18,70	0,03	0,03	0,02	0,00	0,00
TS120710-14	Xiaojugezhuang bridge 2012/7/9 16:40	Mix2	Re	9.7.2012	7,15	5,97	75,00	45,80	34,90	13,30	3,36	0,46	35,40	17,30	39,10	18,20	0,05	0,04	0,03	0,01	0,00
TS120710-15	Xiaojugezhuang bridge 2012/7/9 17:40	Mix2	Re	9.7.2012	7,16	5,84	4,00	48,50	27,10	13,20	3,57	0,09	36,30	17,80	39,40	18,20	0,04	0,04	0,03	0,00	0,00
TS120713-001	Xiaojugezhuang bridge（05：30）	Mix2	Re	10.7.2012	7,46	6,15	3,00	86,40	38,80	11,70	1,73	12,50	32,80	NA	34,80	NA	0,03	0,02	0,02	0,01	0,00
TS120713-002	Xiaojugezhuang bridge（06：30）	Mix2	Re	10.7.2012	7,44	6,46	5,00	94,10	38,70	11,70	1,46	11,60	33,60	NA	35,30	NA	0,03	0,02	0,02	0,01	0,00
TS120713-003	Xiaojugezhuang bridge（07：30）	Mix2	Re	10.7.2012	7,64	6,61	3,00	58,90	38,00	11,00	1,36	11,40	30,20	NA	33,80	NA	0,03	0,02	0,02	0,01	0,00
TS120713-004	Xiaojugezhuang bridge（08：30）	Mix2	Re	10.7.2012	7,60	6,76	4,00	59,90	37,10	10,60	1,16	11,20	28,70	NA	33,20	NA	0,03	0,03	0,02	0,00	0,00
TS120727-01	Xiaojugezhuang bridge（05：30）	Mix2	Re	21.7.2012	7,10	3,18	829,00	58,20	17,40	6,24	10,20	0,22	48,70	9,42	16,40	9,92	0,76	0,38	0,35	0,38	0,03
TS120727-02	Xiaojugezhuang bridge（05：31）	Mix2	Re	21.7.2012	7,04	2,92	300,00	48,50	18,40	6,68	10,40	0,23	49,30	10,80	16,60	13,30	0,89	0,38	0,36	0,51	0,02
TS120727-03	Xiaojugezhuang bridge（05：32）	Mix2	Re	22.7.2012	7,12	3,23	486,00	52,40	19,60	8,84	15,00	0,15	54,80	14,30	21,10	16,20	0,89	0,48	0,46	0,41	0,03
TS120727-04	Xiaojugezhuang bridge（05：33）	Mix2	Re	22.7.2012	7,06	3,79	786,00	65,10	22,80	10,50	17,00	0,14	56,70	16,80	23,00	18,00	0,93	0,44	0,43	0,49	0,02
TS120801-01	Xiaojugezhuang bridge2012/7/28 05：00	Mix2	Re	28.7.2012	7,38	7,33	14,00	97,80	38,90	19,40	8,74	0,08	52,00	15,30	47,50	15,80	0,88	0,64	0,60	0,24	0,05
TS120801-02	Xiaojugezhuang bridge2012/7/28 06：00	Mix2	Re	28.7.2012	7,28	7,27	7,00	107,00	40,10	19,80	7,86	1,10	52,80	21,60	49,60	24,30	0,66	0,53	0,48	0,13	0,05

TS120801-03	Xiaojugezhuang bridge2012/7/28 21：00	Mix2	Re	28.7.2012	7,46	4,12	419,00	73,90	24,00	15,40	7,38	0,22	44,60	18,20	36,30	19,50	1,26	0,47	0,45	0,79	0,02
TS120801-07	Xiaojugezhuang bridge2012/7/29 05：00	Mix2	Re	29.7.2012	7,35	4,56	120,00	80,50	26,40	13,40	6,67	0,17	42,90	19,60	29,00	21,70	0,60	0,46	0,46	0,14	0,00
TS120801-09	Xiaojugezhuang bridge2012/7/31 05：00	Mix2	Re	31.7.2012	7,42	6,02	3,00	107,00	74,60	19,60	6,21	0,05	67,70	30,70	45,80	32,30	0,16	0,15	0,14	0,01	0,01
TS120801-10	Xiaojugezhuang bridge2012/7/31 11：30	Mix2	Re	31.7.2012	7,18	5,53	39,00	95,80	32,20	15,90	6,13	0,08	59,50	27,00	39,70	28,00	0,35	0,30	0,29	0,06	0,01
TS120801-11	Xiaojugezhuang bridge2012/7/31 12：30	Mix2	Re	31.7.2012	7,14	5,28	43,00	90,10	31,60	15,80	6,46	0,14	62,90	25,10	37,00	27,90	0,30	0,25	0,23	0,05	0,02
TS120807-01	Xiaojugezhuang bridge2012/8/1 19：00	Mix2	Re	1.8.2012	7,36	5,79	17,00	101,00	38,00	17,50	8,57	0,05	68,20	28,70	43,30	29,30	0,34	0,32	0,29	0,02	0,03
TS120807-02	Xiaojugezhuang bridge2012/8/1 20：00	Mix2	Re	1.8.2012	7,62	5,35	32,00	90,60	35,80	16,00	6,46	0,08	63,20	25,10	39,10	25,90	0,30	0,27	0,24	0,04	0,03
TS120912-01	Xiaojugezhuang bridge	Mix2	R	12.9.2012	7,30	5,89	4,00	78,80	33,20	14,60	2,51	0,03	36,70	14,00	27,40	14,10	0,04	0,04	0,04	0,00	0,00
TS120925-03	Xiaojugezhuang bridge	Mix2	R	25.9.2012	7,32	6,10	3,00	94,30	38,60	15,00	4,09	0,02	49,50	24,80	38,90	26,80	0,01	0,01	0,00	0,00	0,01
TS121009-03	Xiaojugezhuang bridge	Mix2	R	9.10.2012	7,41	6,15	10,00	92,70	31,60	13,20	4,46	0,03	43,50	23,30	39,80	24,70	0,02	0,01	0,01	0,01	0,00
TS121020-02	Xiaojugezhuang bridge	Mix2	R	20.10.2012	7,31	5,76	11,00	91,60	36,30	13,80	2,90	0,02	41,70	23,26	34,60	24,10	0,03	0,02	0,01	0,01	0,00
TS121103-03	Xiaojugezhuang bridge	Mix2	R	3.11.2012	7,33	5,58	3,00	83,50	28,20	14,40	1,94	0,02	33,00	14,81	35,40	15,00	0,25	0,02	0,02	0,23	0,00
TS121114-03	Xiaojugezhuang bridge	Mix2	R	14.11.2012	7,46	5,79	325,00	129,00	51,90	15,80	2,91	0,02	42,90	24,16	35,80	28,60	0,02	0,02	0,02	0,00	0,00
TS121201-01	Xiaojugezhuang bridge	Mix2	R	1.12.2012	7,34	3,97	16,00	95,70	54,30	18,60	3,44	0,02	44,70	25,74	37,50	26,60	0,03	0,02	0,02	0,00	0,00
TS121216-03	Xiaojugezhuang bridge	Mix2	R	16.12.2012	7,56	5,53	3,00	86,20	42,80	10,30	1,95	0,02	33,20	9,64	37,80	4,47	0,04	0,03	0,02	0,01	0,01
TS130125-02	Xiaojugezhuang bridge	Mix2	R	25.1.2013	7,47	5,75	3,00	96,60	39,40	10,70	1,43	0,03	31,60	17,80	38,90	19,97	0,03	0,02	0,02	0,01	0,01
TS130222-02	Xiaojugezhuang bridge	Mix2	R	22.2.2013	7,44	6,06	13,00	101,00	37,00	14,40	2,53	0,05	32,80	20,80	NA	23,70	0,03	0,02	0,01	0,00	0,01
TS130307-01	Xiaojugezhuang bridge	Mix2	R	7.3.2013	7,20	5,43	NA	92,40	30,40	37,30	1,77	0,03	29,80	17,38	28,40	18,17	0,48	0,02	0,02	0,46	0,01
TS130326-01	Xiaojugezhuang bridge	Mix2	R	26.3.2013	7,52	5,75	5,00	116,00	33,40	11,10	2,66	0,56	29,50	18,44	31,00	29,20	0,02	0,02	0,02	0,00	0,00
TS130410-02	Xiaojugezhuang bridge	Mix2	R	10.4.2013	7,22	5,58	8,00	44,00	38,00	12,20	1,94	0,08	29,10	16,90	39,30	18,50	0,03	0,03	0,02	0,00	0,00
TS130501-02	Xiaojugezhuang bridge	Mix2	R	1.5.2013	7,60	6,05	6,00	23,90	48,80	10,70	2,80	0,02	31,20	18,02	35,50	20,00	0,02	0,02	0,02	0,00	0,00
TS130508-02	Xiaojugezhuang bridge	Mix2	R	8.5.2013	7,34	6,10	8,00	44,60	43,20	12,00	2,28	0,03	31,20	18,20	34,70	20,05	0,02	0,01	0,01	0,00	0,01
TS139616-02	Xiaojugezhuang bridge	Mix2	R	8.5.2013	7,14	6,22	5,00	27,40	23,80	16,10	3,99	0,02	31,10	17,20	36,50	18,85	0,03	0,03	0,02	0,01	0,00
TS130628-01	Xiaojugezhuang bridge 22:50	Mix2	R	28.6.2013	7,99	5,92	6,00	40,60	38,90	13,20	3,80	0,12	29,00	17,50	28,60	17,80	0,03	0,01	0,01	0,02	0,00
TS130628-02	Xiaojugezhuang bridge 23:10	Mix2	R	28.6.2013	7,38	5,85	18,00	43,90	39,00	13,50	3,65	0,14	28,80	17,14	28,50	17,30	0,03	0,02	0,01	0,01	0,01

TS130628-03	Xiaojugezhuang bridge 23:30	Mix2	R	28.6.2013	7,40	5,64	54,00	44,70	38,80	12,80	3,39	0,31	28,40	16,57	27,30	17,00	0,06	0,02	0,01	0,05	0,01
TS130628-04	Xiaojugezhuang bridge 23:50	Mix2	R	28.6.2013	7,42	5,74	22,00	53,20	39,10	12,70	3,46	0,26	28,10	16,82	27,70	17,20	0,04	0,01	0,01	0,03	0,00
TS130701-01	Xiaojugezhuang bridge 13:55	Mix2	R	1.7.2013	8,02	5,89	38,00	54,50	29,90	13,50	3,84	0,46	30,30	17,50	29,70	18,10	0,13	0,08	0,08	0,05	0,00
TS130701-02	Xiaojugezhuang bridge 14:20	Mix2	R	1.7.2013	7,36	5,75	42,00	52,70	37,70	13,20	3,81	0,57	31,00	17,03	29,70	17,80	0,09	0,04	0,04	0,06	0,00
TS130701-03	Xiaojugezhuang bridge 14:40	Mix2	R	1.7.2013	7,70	5,98	32,00	87,50	40,50	13,70	3,79	0,34	30,70	17,57	30,80	18,20	0,07	0,02	0,02	0,05	0,00
TS130701-04	Xiaojugezhuang bridge 15:00	Mix2	R	1.7.2013	7,43	5,99	15,00	82,90	40,00	14,10	3,53	0,16	30,70	17,91	31,20	18,14	0,04	0,03	0,03	0,01	0,00
TS130715-05	Xiaojuge Village Bridge (after rain)	Mix2	Re	9.7.2013	7,68	6,05	3,00	37,40	24,30	13,50	2,64	0,19	31,40	18,20	30,80	21,10	0,02	0,02	0,02	0,00	0,00
TS130723-04	Xiaojuge Village Bridge (8:15)	Mix2	R	15.7.2013	7,22	5,17	20,00	14,10	22,50	12,20	2,96	0,19	30,80	15,50	28,40	16,10	0,08	0,06	0,05	0,02	0,01
TS130723-07	Xiaojuge Village Bridge	Mix2	R	16.7.2013	7,17	6,35	3,00	27,00	24,50	15,20	3,18	0,90	36,00	18,90	53,00	20,00	0,14	0,14	0,12	0,00	0,02
TS130819-01	Xiaoju Village Bridge	Mix2	R	4.8.2013	7,34	5,34	110,00	69,50	14,40	11,40	3,35	0,02	37,80	15,20	29,60	15,70	0,12	0,05	0,04	0,06	0,02
TS130819-02	Xiaoju Village Bridge	Mix2	R	4.8.2013	7,08	5,54	377,00	114,00	16,30	19,70	37,80	15,50	38,80	0,88	40,80	26,70	2,76	1,91	1,90	0,85	0,01
TS130819-03	Xiaoju Village Bridge	Mix2	R	4.8.2013	7,37	6,88	242,00	71,40	16,30	26,00	61,30	19,60	28,80	0,89	47,90	36,50	4,41	2,94	2,90	1,47	0,04
TS130812-01	XiaoJuGe Village Bridge 8:40	Mix2	R	4.8.2013	7,38	3,82	55,00	49,30	20,00	11,80	5,90	0,13	36,30	13,20	23,40	15,10	0,38	0,13	0,13	0,25	0,01
TS130819-04	Xiaoju Village Bridge after rain 7:00	Mix2	R	5.8.2013	7,36	6,05	68,00	99,80	19,10	12,50	3,44	0,03	36,90	16,40	32,40	17,00	0,03	0,03	0,03	0,00	0,00
TS130812-02	XiaoJuGe Village Bridge 7:00	Mix2	R	5.8.2013	7,50	6,23	3,00	35,70	20,50	13,50	3,07	0,14	36,90	20,20	33,20	21,40	0,05	0,02	0,01	0,03	0,01
TS130826-01	Xiaoju Bridge	Mix2	R	11.8.2013	8,24	6,17	8,00	24,10	27,20	15,90	4,45	0,03	37,30	20,70	33,90	21,80	0,02	0,02	0,02	0,00	0,00
TS130826-02	Xiaoju Bridge	Mix2	R	11.8.2013	7,46	5,99	6,00	24,20	24,20	14,60	4,29	0,12	37,90	19,30	32,70	19,90	0,05	0,03	0,03	0,02	0,00
TS130826-03	Xiaoju Bridge	Mix2	R	11.8.2013	7,72	6,08	69,00	23,60	26,80	15,60	3,85	0,20	35,60	18,70	30,80	20,10	0,02	0,02	0,02	0,00	0,00
TS131010-10	Xiaoju Bridge	Mix2	NA	24.9.2013	7,48	2,02	22,00	39,10	22,80	10,70	19,20	0,16	35,10	18,20	26,30	4,56	0,04	0,02	0,01	0,01	0,02
TS120416-02	Mashenqiao river	Farmland	R	16.4.2012	7,88	NA	20,00	114,00	29,80	3,88	2,87	0,25	9,00	2,05	5,00	NA	0,15	0,05	0,02	0,09	0,04
TS120416-05	Yuma river north	Farmland	R	16.4.2012	7,96	NA	34,00	131,00	34,80	15,00	6,40	0,35	20,00	0,79	29,00	NA	0,43	0,14	0,09	0,29	0,05
TS120416-06	Yuma river south	Farmland	R	16.4.2012	7,64	NA	108,00	136,00	39,60	27,90	18,80	0,68	40,00	0,09	54,00	NA	1,23	0,27	0,02	0,96	0,25
TS120423-03	Mashenqiao river	Farmland	R	23.4.2012	7,04	NA	5,00	81,30	24,00	9,61	1,58	0,02	101,00	41,40	230,00	NA	0,61	0,02	0,01	0,59	0,01
TS120710-24	Yuma bridge	Farmland	R	10.7.2012	7,34	3,13	8,00	49,60	26,80	9,35	5,69	1,51	31,90	0,17	22,10	1,68	0,23	0,15	0,13	0,07	0,02
TS130715-01	Yuma bridge (after rain)	Farmland	R	9.7.2013	7,75	4,87	18,00	13,10	19,70	12,70	3,03	1,11	55,60	3,36	27,60	5,48	0,21	0,18	0,15	0,04	0,03

TS130723-02	Yuma Bridge 8:30	Farmland	R	15.7.2013	7,38	2,82	58,00	3,80	10,40	8,28	3,61	0,99	25,80	2,60	12,50	4,17	0,55	0,20	0,18	0,35	0,02
TS130807-11	Mashen Bridge river	Farmland	R	31.7.2013	7,72	3,59	52,00	15,70	8,53	9,57	3,22	0,43	76,10	2,69	24,10	4,72	0,14	0,08	0,07	0,06	0,01
TS130807-12	Mashen Bridge river	Farmland	R	31.7.2013	7,56	5,55	26,00	15,40	13,70	9,98	3,39	0,11	37,10	2,57	37,90	4,92	0,16	0,09	0,08	0,06	0,01
TS130807-13	Mashen Bridge river	Farmland	R	31.7.2013	7,36	5,47	876,00	17,60	9,56	10,30	3,44	0,19	37,40	3,50	32,80	4,76	0,18	0,10	0,09	0,08	0,01
TS130807-14	Mashen Bridge river	Farmland	R	31.7.2013	7,66	5,35	55,00	10,10	9,30	15,10	3,88	0,37	37,10	2,98	29,30	4,98	0,18	0,12	0,11	0,06	0,01
TS130807-15	Mashen Bridge river	Farmland	R	31.7.2013	7,52	5,41	19,00	14,50	9,07	9,69	3,45	0,22	35,80	2,78	27,00	4,98	0,17	0,10	0,10	0,06	0,01
TS130819-05	Mashen Bridge river sluice gate	Farmland	R	4.8.2013	7,24	4,99	340,00	90,40	13,00	9,09	2,90	0,03	35,40	2,53	24,90	3,08	0,27	0,11	0,09	0,17	0,02
TS130819-06	Mashen Bridge river sluice gate	Farmland	R	4.8.2013	6,86	5,25	320,00	75,40	14,60	8,76	2,84	0,04	35,90	0,97	25,30	2,30	0,23	0,09	0,07	0,13	0,02
TS130819-07	Mashen Bridge river sluice gate	Farmland	R	4.8.2013	7,21	5,40	82,00	72,60	15,50	8,52	3,04	0,04	35,40	2,18	25,20	3,39	0,21	0,15	0,14	0,06	0,02
TS130819-08	Mashen Bridge river sluice gate	Farmland	R	4.8.2013	7,14	5,33	80,00	81,90	16,50	8,99	2,86	0,03	33,90	1,49	25,00	3,60	0,21	0,17	0,14	0,04	0,03
TS130819-09	Mashen Bridge river sluice gate	Farmland	R	4.8.2013	7,41	5,72	39,00	72,50	11,50	9,27	2,61	0,08	33,70	1,73	25,00	2,46	0,20	0,18	0,15	0,02	0,03
TS130812-07	Mashen Bridge river sluice gate 21:10	Farmland	R	4.8.2013	7,29	4,98	1180,00	29,60	15,20	10,60	3,43	0,37	35,40	0,54	24,90	4,26	0,23	0,10	0,06	0,13	0,04
TS130812-08	Mashen Bridge river sluice gate 21:50	Farmland	R	4.8.2013	7,42	5,19	141,00	24,30	15,00	11,30	3,67	0,12	36,80	1,00	26,10	6,30	0,21	0,15	0,11	0,06	0,04
TS130812-09	Mashen Bridge river sluice gate 22:50	Farmland	R	4.8.2013	7,26	5,63	324,00	31,10	19,00	11,00	3,66	0,09	33,70	2,57	36,60	5,16	0,14	0,12	0,09	0,02	0,04
TS130812-10	Mashen Bridge river sluice gate	Farmland	R	5.8.2013	7,72	7,04	20,00	33,00	14,50	14,60	5,32	1,79	41,60	0,40	49,10	12,40	0,25	0,12	0,09	0,13	0,03
TS130819-10	Mashen Bridge river sluice gate	Farmland	R	5.8.2013	7,20	3,83	132,00	82,30	16,40	13,30	4,31	0,10	42,50	1,42	34,40	3,18	0,30	0,16	0,13	0,14	0,03
TS130819-11	Mashen Bridge	Farmland	R	7.8.2013	7,17	5,20	94,00	67,10	10,60	11,50	3,28	1,20	42,50	0,94	34,80	3,14	0,18	0,15	0,12	0,03	0,02
TS130819-12	Mashen Bridge after rain	Farmland	R	7.8.2013	7,26	5,28	25,00	50,10	15,50	12,00	3,66	0,08	51,50	3,50	31,80	3,90	0,20	0,18	0,15	0,02	0,02
TS130812-12	Mashen Brigde	Farmland	R	7.8.2013	7,69	5,31	35,00	36,80	14,00	14,60	4,38	0,07	46,50	3,30	32,40	4,68	0,20	0,06	0,03	0,13	0,03
TS130812-13	Mashen Brigde	Farmland	R	7.8.2013	7,66	5,18	17,00	24,60	21,30	14,70	4,74	0,08	51,90	3,30	33,10	5,60	0,22	0,21	0,17	0,02	0,04
TS130812-14	Mashen Brigde after rain	Farmland	R	7.8.2013	7,67	5,32	23,00	42,50	20,10	15,60	4,76	0,28	51,20	3,61	32,20	10,90	0,21	0,21	0,17	0,00	0,04
TS130826-15	Mashen Bridge	Farmland	R	11.8.2013	7,89	5,56	24,00	24,20	21,90	12,30	3,93	0,09	41,70	2,46	27,80	3,11	0,22	0,21	0,18	0,01	0,03
TS130826-16	Mashen Bridge	Farmland	R	11.8.2013	7,84	5,66	15,00	26,30	26,80	12,90	4,11	0,45	38,50	1,76	27,60	3,41	0,28	0,27	0,22	0,01	0,05
TS130826-17	Mashen Bridge	Farmland	R	11.8.2013	7,66	5,76	11,00	24,40	26,10	12,20	3,36	0,11	38,10	2,61	26,80	2,89	0,23	0,23	0,21	0,01	0,02
TS130826-14	Mashen Bridge before rain	Farmla	R	11.8.201	7,76	5,61	9,00	24,70	26,00	13,00	3,29	0,04	39,80	1,38	26,80	3,13	0,21	0,20	0,18	0,00	0,03

		nd		3																	
TS131010-01	Mashen Bridge river sluice gate	Farmland	R	28.8.2013	7,16	6,12	6,00	12,70	15,80	10,10	1,88	0,07	36,00	0,23	23,80	3,42	0,18	0,15	0,15	0,02	0,00
TS131010-02	Mashen Bridge river sluice gate	Farmland	R	28.8.2013	7,23	5,85	8,00	11,80	20,70	9,81	1,68	0,05	35,60	0,20	23,20	2,78	0,19	0,16	0,16	0,03	0,01
TS131010-03	Mashen Bridge river sluice gate	Farmland	R	28.8.2013	7,22	5,94	13,00	13,30	15,90	9,76	1,96	0,06	36,90	0,23	24,20	3,05	0,17	0,15	0,14	0,02	0,01
TS131010-09	Mashen Bridge river sluice gate	Farmland	NA	24.9.2013	7,25	1,75	29,00	34,00	22,70	11,20	1,34	0,10	44,40	5,35	33,70	4,15	0,12	0,04	0,03	0,09	0,01
TS120423-04	Beixinzhuang river	Orchard	R	23.4.2012	7,74	NA	3,00	79,00	24,30	4,05	1,28	0,02	9,00	2,56	7,00	NA	0,03	0,02	0,02	0,00	0,00
TS120710-05	Beixinzhuang bridge 2012/7/9 1:40 pm	Orchard	Re	9.7.2012	7,38	5,05	3,00	41,70	20,40	10,10	4,07	1,77	31,00	0,85	20,50	2,65	0,21	0,18	0,16	0,03	0,02
TS120710-07	Beixinzhuang bridge 2012/7/9 3:40 pm	Orchard	Re	9.7.2012	7,37	4,76	4,00	43,00	19,80	11,00	4,17	1,78	32,80	0,60	19,60	2,47	0,20	0,18	0,16	0,02	0,02
TS120710-08	Beixinzhuang bridge 2012/7/9 4:40 pm	Orchard	Re	9.7.2012	7,35	5,02	5,00	40,90	21,80	8,96	4,05	1,90	36,50	0,64	19,90	2,87	0,21	0,18	0,16	0,03	0,02
TS120710-06	Beixinzhuang bridge2012/7/9 2:40 pm	Orchard	Re	9.7.2012	7,35	4,74	3,00	42,60	21,40	10,50	3,90	1,81	31,20	0,97	21,60	2,83	0,21	0,18	0,16	0,03	0,02
TS120710-17	Beixinzhuang bridge	Orchard	Re	10.7.2012	7,58	5,94	137,00	38,40	21,20	9,96	3,66	1,41	27,00	0,06	22,20	1,75	0,24	0,14	0,12	0,09	0,02
TS120713-005	Beixinzhuang bridge 2012/7/10 05：30	Orchard	Re	10.7.2012	7,58	6,20	3,00	50,20	27,20	12,30	2,65	1,02	36,80	NA	23,60	NA	0,19	0,17	0,16	0,02	0,01
TS120713-006	Beixinzhuang bridge 2012/7/10 06：30	Orchard	Re	10.7.2012	7,59	5,23	3,00	45,50	27,40	12,30	2,28	1,04	41,70	NA	22,60	NA	0,19	0,17	0,16	0,01	0,01
TS120713-007	Beixinzhuang bridge 2012/7/10 07：30	Orchard	Re	10.7.2012	7,58	5,43	3,00	49,90	25,90	12,60	3,33	0,94	38,20	NA	22,80	NA	0,19	0,17	0,16	0,02	0,01
TS120713-008	Beixinzhuang bridge 2012/7/10 08：30	Orchard	Re	10.7.2012	7,60	4,97	3,00	52,30	27,50	12,80	3,41	1,05	36,70	NA	21,40	NA	0,19	0,18	0,17	0,01	0,00
TS120710-22	Beixinzhuang river	Orchard	R	10.7.2012	7,32	6,07	3,00	87,70	40,70	20,10	2,16	0,10	48,10	19,40	74,10	21,10	0,02	0,02	0,02	0,00	0,01
TS120727-05	Beixinzhuang bridge 2012/7/21 20：30	Orchard	Re	21.7.2012	7,22	7,48	41,00	112,00	39,50	26,40	4,18	0,08	75,60	20,10	71,80	22,20	0,13	0,11	0,10	0,03	0,01
TS120727-06	Beixinzhuang bridge 2012/7/21 21：30	Orchard	Re	21.7.2012	7,31	7,22	42,00	113,00	40,10	26,40	4,37	0,07	76,20	20,40	71,00	23,30	0,13	0,11	0,10	0,03	0,01
TS120727-07	Beixinzhuang bridge 2012/7/22 05：00	Orchard	Re	22.7.2012	6,51	0,51	197,00	8,21	4,64	1,37	5,88	0,42	19,10	4,61	8,64	5,97	0,76	0,51	0,49	0,25	0,01
TS120727-08	Beixinzhuang bridge 2012/7/22 06：00	Orchard	Re	22.7.2012	6,52	0,56	281,00	5,18	4,48	1,28	5,02	0,51	14,40	5,08	5,86	6,01	1,37	1,02	1,01	0,35	0,01
TS120801-04	Beixinzhuang bridge 2012/7/28 05：00	Orchard	Re	28.7.2012	6,66	0,64	69,00	4,98	7,38	2,18	5,91	0,58	19,70	6,07	5,49	7,12	0,92	0,79	0,74	0,14	0,05
TS120801-05	Beixinzhuang bridge 2012/7/28 06：00	Orchard	Re	28.7.2012	6,80	0,95	64,00	4,88	4,91	2,18	5,54	0,72	19,00	5,62	8,47	6,88	0,90	0,75	0,72	0,14	0,03
TS120801-06	Beixinzhuang bridge 2012/7/28 21：00	Orchard	Re	28.7.2012	6,86	1,38	202,00	39,20	10,20	4,45	8,36	1,09	36,30	9,46	25,00	12,10	1,01	0,80	0,74	0,21	0,06
TS120801-08	Beixinzhuang bridge 2012/7/29 05：00	Orchard	Re	29.7.2012	6,94	1,69	273,00	48,40	11,20	4,14	8,03	0,89	35,40	9,62	18,40	11,90	1,24	0,83	0,81	0,41	0,02

TS120801-12	Beixinzhuang bridge 2012/7/31 05：00	Orchard	Re	31.7.2012	7,16	5,79	29,00	127,00	42,00	13,70	13,50	0,20	120,00	35,70	102,00	37,50	0,61	0,57	0,54	0,04	0,03
TS120801-13	Beixinzhuang bridge 2012/7/31 11：30	Orchard	Re	31.7.2012	7,12	1,54	85,00	31,70	10,60	4,12	4,60	0,38	46,80	11,70	16,80	13,40	1,21	1,05	1,04	0,16	0,01
TS120801-14	Beixinzhuang bridge 2012/7/31 12：30	Orchard	Re	31.7.2012	7,30	2,10	106,00	31,70	11,30	4,28	5,93	0,42	41,00	12,20	15,90	13,90	1,97	1,78	1,76	0,19	0,02
TS120807-03	Beixinzhuang bridge2012/8/1 19：00	Orchard	Re	1.8.2012	7,46	3,13	21,00	83,10	29,20	9,49	6,64	0,12	77,70	27,10	48,00	29,20	0,67	0,66	0,61	0,01	0,05
TS120807-04	Beixinzhuang bridge2012/8/1 20：00	Orchard	Re	1.8.2012	7,04	3,00	13,00	88,60	25,20	10,30	6,00	0,12	82,00	29,10	51,20	31,50	0,91	0,91	0,88	0,00	0,04
TS120912-02	Beixinzhuang bridge	Orchard	R	12.9.2012	7,30	5,38	3,00	89,20	36,40	15,10	2,75	0,07	73,10	11,60	46,00	11,90	0,09	0,08	0,06	0,01	0,02
TS120925-02	Beixinzhuang bridge	Orchard	R	25.9.2012	7,40	2,46	16,00	39,40	19,00	18,80	6,16	0,07	78,60	3,09	30,40	3,53	0,19	0,14	0,13	0,05	0,01
TS121009-02	Beixinzhuang bridge	Orchard	R	9.10.2012	7,51	3,16	14,00	45,70	20,20	17,00	5,59	1,85	77,20	2,46	30,40	4,51	0,34	0,15	0,13	0,19	0,02
TS121020-01	Beixinzhuang bridge	Orchard	R	20.10.2012	7,61	5,49	18,00	76,40	29,20	10,40	2,48	0,03	33,60	6,12	31,20	7,03	0,09	0,07	0,06	0,02	0,01
TS121103-01	Beixinzhuang bridge	Orchard	R	3.11.2012	7,78	5,74	23,00	74,60	41,70	10,60	2,34	0,10	35,30	4,61	32,40	5,14	0,11	0,08	0,07	0,04	0,01
TS121114-01	Beixinzhuang bridge	Orchard	R	14.11.2012	7,09	6,15	35,00	124,00	46,10	19,10	5,06	0,73	60,70	0,03	44,10	1,57	0,12	0,08	0,07	0,03	0,01
TS121201-03	Beixinzhuang bridge	Orchard	R	1.12.2012	7,61	4,41	61,00	101,00	49,90	17,70	2,89	0,21	49,80	7,77	43,70	9,77	0,14	0,08	0,07	0,07	0,01
TS121216-02	Beixinzhuang bridge	Orchard	R	16.12.2012	8,07	2,69	3,00	57,00	26,00	24,60	6,05	0,28	125,00	4,85	36,50	5,00	0,06	0,02	0,01	0,03	0,02
TS130125-01	Beixinzhuang bridge	Orchard	R	25.1.2013	7,59	5,28	18,00	84,10	31,50	8,03	1,41	0,42	35,70	6,32	31,10	6,99	0,08	0,05	0,03	0,03	0,01
TS130222-01	Beixinzhuang bridge	Orchard	R	22.2.2013	7,83	5,47	7,00	79,30	24,40	9,08	2,11	0,35	28,30	4,43	NA	4,89	0,18	0,03	0,02	0,15	0,01
TS130307-02	Beixinzhuang bridge	Orchard	R	7.3.2013	7,66	5,48	NA	80,10	22,60	11,60	1,53	0,59	30,10	4,58	27,10	4,86	0,22	0,04	0,02	0,18	0,01
TS130326-02	Beixinzhuang bridge	Orchard	R	26.3.2013	7,76	5,70	35,00	115,00	31,60	12,10	3,59	0,04	39,10	3,55	36,20	4,19	0,22	0,06	0,05	0,16	0,01
TS130410-01	Beixinzhuang bridge	Orchard	R	10.4.2013	7,62	5,69	47,00	35,00	34,80	10,10	2,61	0,12	31,60	3,34	31,40	3,83	0,12	0,05	0,04	0,07	0,01
TS130501-01	Beixinzhuang bridge	Orchard	R	1.5.2013	7,62	5,53	29,00	19,10	36,40	11,30	8,00	0,73	35,00	0,84	26,50	3,02	0,36	0,12	0,09	0,24	0,03
TS130508-01	Beixinzhuang bridge	Orchard	R	8.5.2013	7,65	5,64	37,00	18,00	42,30	12,10	3,10	0,12	18,90	0,54	25,90	1,37	0,31	0,14	0,12	0,17	0,02
TS139616-01	Beixinzhuang bridge	Orchard	R	8.5.2013	7,38	5,70	86,00	12,70	19,50	17,00	11,90	0,54	36,40	1,88	35,30	3,32	0,42	0,15	0,13	0,27	0,02
TS130715-02	Beixinzhuang water-gate	Orchard	R	9.7.2013	7,64	4,82	15,00	20,50	19,70	13,60	3,19	0,18	53,80	3,41	28,90	5,74	0,33	0,24	0,20	0,10	0,04
TS130906-18	Beixin Village river sluice gate	Orchard	R	11.8.2013	8,08	5,56	82,00	25,50	28,00	12,20	6,39	0,14	36,50	1,94	30,30	3,81	0,19	0,18	0,17	0,01	0,01
TS130906-19	Beixin Village river sluice gate	Orchard	R	11.8.2013	7,84	5,76	16,00	24,80	27,70	13,40	6,29	0,09	37,40	3,64	30,00	3,85	0,29	0,23	0,15	0,06	0,08

TS130906-20	Beixin Village river sluice gate	Orchard	R	11.8.2013	7,78	4,87	110,00	24,40	25,60	12,20	5,73	0,18	0,36	3,27	28,60	4,43	0,22	0,20	0,14	0,02	0,06
TS130906-21	Beixin Village river sluice gate	Orchard	R	11.8.2013	8,06	5,66	100,00	24,00	22,70	11,70	5,74	0,12	0,47	3,64	28,60	4,82	0,20	0,18	0,15	0,02	0,03
TS130906-22	Beixin Village river sluice gate	Orchard	R	11.8.2013	7,99	6,01	56,00	24,30	26,60	12,10	5,66	0,80	33,70	3,86	28,30	5,12	0,26	0,26	0,21	0,01	0,05
TS130906-23	Beixin Village river sluice gate	Orchard	R	11.8.2013	8,20	5,44	82,00	24,10	27,70	12,10	5,68	0,90	34,60	2,35	28,10	3,75	0,23	0,20	0,17	0,03	0,03
TS130906-17	Beixin Village river sluice gate	Orchard	R	12.8.2013	7,84	5,44	27,00	25,10	27,60	11,90	6,29	0,19	35,00	1,65	28,70	3,33	0,33	0,22	0,17	0,11	0,05
TS130906-13	Beixin Village river sluice gate	Orchard	R	15.8.2013	7,86	5,64	37,00	24,70	27,80	15,10	12,30	0,14	34,00	2,64	25,80	3,43	0,23	0,22	0,20	0,01	0,02
TS130906-14	Beixin Village river sluice gate	Orchard	R	15.8.2013	7,86	5,56	47,00	25,50	27,60	15,70	5,80	0,08	34,20	2,39	25,30	3,67	0,23	0,20	0,17	0,03	0,03
TS130906-15	Beixin Village river sluice gate	Orchard	R	15.8.2013	7,74	5,69	23,00	24,10	21,10	13,70	6,39	0,12	34,10	2,21	25,70	3,89	0,51	0,25	0,23	0,26	0,02
TS130906-16	Beixin Village river sluice gate	Orchard	R	16.8.2013	7,40	3,25	138,00	24,20	26,40	13,30	11,60	3,84	41,90	5,42	23,00	10,10	0,68	0,56	0,51	0,11	0,05

Appendix D: Quality control

Table D-1: Internal standards recovery (MBM)

Standard	**True Value**		**Replicates measurements (µg/L)**				
			1	**2**	**3**	**4**	**Average**
Cotrol X1	92	Measuremnet	91,49	96,71	88,65		
		Recovery (%)	99,4	105,1	96,4		**100,3**
Control Y1	46	Measuremnet	45,13	46,97	43,58	43,89	
		Recovery (%)	98,1	102,1	94,7	95,4	**97,6**
Control Xp	64	Measuremnet	62,95	62,95	61,21	62,66	
		Recovery (%)	98,4	98,4	95,6	97,9	**97,6**
Control Yp	96	Measuremnet	92,61	92,61	92,83	94.61	
		Recovery (%)	96,5	96,5	96,7	98,6	**97,0**

Table D-2: Internal standards recovery (ICP-MS)

Standard	**True Conc.**	**Measured Conc (µg/L)**	**Recovery (%)**
Control X1	92	92.3	100.3
Control Y1	46	44.9	97.0
Control Xp	64	62.6	97.8
Control Yp	96	93.5	97.4

Table D-3: Limit of Detection (LOD) for MBM method

MBM	**Concentration (µg P/L)**
Std 0 - R1	-1,54
Std 0 - R2	0,31
Std 0 - R3	0,38
Std 0 - R4	1,31
Std 0 - R5	0,06
Std 0 - R6	5,81
Std 0 - R7	4,88
Std 0 - R8	-3,22
Std 0 - R9	-2,93
Std 0 - R10	-2,63
Std 0 - R11	0,21
Std 0 - R12	-0,38
Std 0 - R13	-0,09
STDEV	2,70
LOD	8,10
LOQ	81,04

Table D-4: Limit of Detection (LOD) for ICP-MS)

LOD	**Concentration (µg P/L)**
Std 0 - R1	2,9
Std 0 - R2	3,2
Std 0 - R3	5,2
Std 0 - R4	3,6
Std 0 - R5	3,0
Std 0 - R6	3,4
Std 0 - R7	3,1
Std 0 - R8	3,2
Std 0 - R9	3,4
Std 0 - R10	3,3
Std 0 - R11	3,5
Std 0 - R12	3,6
STDEV	0,6
LOD	1,8
LOQ	17,5

Table D-5: Limit of Detection for ICP-OES

	Concentration mg/L								
Sample	**Al**	**P**	**Mn**	**Si**	**Ca**	**Fe**	**K**	**Mg**	**Na**
AB1	0,08	0,15	-0,58	-0,42	-0,40	-0,15	-0,36	0,32	-0,43
AB2	0,04	0,12	-0,62	-0,57	-0,45	-0,20	-0,40	0,28	-0,49
AB3	0,02	0,12	-0,63	-0,57	-0,46	-0,20	-0,41	0,27	-0,49
AB4	0,04	0,10	-0,63	-0,59	-0,46	-0,20	-0,41	0,28	-0,50
AB5	0,03	0,11	-0,63	-0,62	-0,46	-0,21	-0,41	0,28	-0,49
AB6	0,04	0,10	-0,63	-0,53	-0,46	-0,18	-0,38	0,27	-0,43
AB7	0,02	0,09	-0,63	-0,61	-0,46	-0,21	-0,41	0,27	-0,46
AB8	0,03	0,12	-0,63	-0,60	-0,46	-0,18	-0,41	0,28	-0,41
AB9	0,02	0,12	-0,63	-0,60	-0,47	-0,21	-0,41	0,27	-0,47
AB10	0,01	0,10	-0,63	-0,63	-0,47	-0,22	-0,42	0,27	-0,50
AB11	0,06	1,16	-0,63	-0,63	2,33	-0,17	-0,41	0,27	-0,48
Stdv	0,02	0,32	0,02	0,06	0,84	0,02	0,02	0,01	0,03
LOD	0,06	0,95	0,05	0,19	2,52	0,06	0,05	0,04	0,09
LOQ	0,60	9,48	0,51	1,85	25,16	0,62	0,51	0,40	0,93

Appendix E: Statistics

Table E-1: G-test and RPD test

			Ortho P (PO4-)- MBM (mg/L)								TDP-ICP-MS (µg/L)						
				Measurements					Statistics		Measurements					Statistics	
Sampling point	**Sampling No**	**Parellel No**	**Label**	**1st**	**2nd**	**Average**	**Mean sample**	**Mean site**	**G-value**	**RPD (%)**	**1st**	**2nd**	**Average**	**Mean Sample**	**Mean Site**	**G-Value**	**RPD (%)**
Baxian	Sampling 1	Parallel 1b	1-2-b	0,019	0,020	0,020				**5,439**	21,8	13,4	17,6				**47,7**
		Parallel 1c	1-2-c	0,019	0,019	0,019	0,019			**0,549**	17,8	18,3	18,0	17,803			**2,9**
	Sampling 2	Parallel 2a	2-2-a	0,002	0,006	0,004			**0,857**	**82,793**	2,7	0,6	1,6			**0,892**	**125,4**
		Parallel 2b	2-2-b	0,004	0,007	0,006			**0,241**	**43,571**	3,8	3,1	3,5			**0,189**	**19,6**
		Parallel 2c	2-2-c	0,007	0,012	0,009	0,006	0,013	**1,099**	**58,507**	6,6	7,0	6,8	3,965	10,884	**1,081**	**5,6**
Beix	Sampling 1	Parallel 1b	1-3-b	0,307	0,316	0,311				**2,969**	351,3	317,6	334,5				**10,1**
		Parallel 1c	1-3-c	0,541	0,532	0,537	0,406			**1,595**	598,4	532,5	565,4	449,955			**11,6**
	Sampling 2	Parallel 2a	2-3-a	0,276		0,276			**0,251**		309,2	265,8	287,5			**0,203**	**15,1**
		Parallel 2b	2-3-b	0,214		0,214			**0,850**		237,1	204,2	220,7			**0,883**	**14,9**
		Parallel 2c	2-3-c	0,417		0,417	0,302		**1,102**		438,5	389,4	413,9	307,360		**1,086**	**11,9**
	Sampling 3	Parallel 3a	3-3-a	0,383	0,382	0,383			**1,154**	**0,136**	517,7	389,4	453,6			**1,144**	**28,3**
		Parallel 3b	3-3-b	0,460	0,466	0,463			**0,601**	**1,277**	584,1	472,2	528,2			**0,433**	**21,2**
		Parallel 3c	3-3-c	0,457	0,463	0,460	0,435	0,381	**0,553**	**1,351**	603,7	478,8	541,3	507,655	421,657	**0,710**	**23,1**
Lin	Sampling 1	Parallel 1b	1-5-b	0,022	0,023	0,023				**4,962**	22,6	24,2	23,4				**6,9**
		Parallel 1c	1-5-c	0,063	0,059	0,061	0,042			**5,625**	67,7	67,5	67,6	45,488			**0,2**
	Sampling 2	Paralel 2a	2-5-a	0,005	0,009	0,007			**1,088**	**53,105**	1,8	10,7	6,2			**1,066**	**141,4**
		Parallel 2b	2-5-b	-0,001	0,003	0,001			**0,880**	**472,588**	-4,4	5,9	0,8			**0,918**	**1365,3**

		Parallel 2c	2-5-c	0,001	0,005	0,003	0,004	0,023	**0,208**	**116,647**	-2,3	8,1	2,9	3,293	24,390	**0,147**	**358,8**
Mashen (Yuma)	Sampling 1	Parallel 1b	1-4-b	0,166	0,157	0,161				**5,502**	182,5	164,9	173,7				**10,1**
		Parallel 1c	1-4-c	0,139	0,136	0,137	0,149			**2,563**	162,7	141,9	152,3	163,018			**13,7**
	Sampling 2	Paralel 2a	2-4-a	0,255		0,255			**0,495**		280,9	235,9	258,4			**0,460**	**17,4**
		Paralel 2b	2-4-b	0,262		0,262			**0,656**		293,9	244,6	269,3			**0,687**	**18,3**
		Parallel 2c	2-4-c	0,176		0,176	0,231		**1,151**		195,4	168,1	181,7	236,455		**1,147**	**15,0**
	Sampling 3	Parallel 3a	3-4-a	0,213	0,210	0,211			**0,800**	**0,993**	278,1	218,0	248,0			**0,323**	**24,2**
		Parallel 3b	3-4-b	0,187	0,190	0,189			**1,121**	**1,790**	242,5	202,6	222,6			**1,122**	**17,9**
		Parallel 3c	3-4-c	0,195	0,217	0,206	0,202	0,194	**0,322**	**11,015**	278,1	234,8	256,4	242,342	213,938	**0,799**	**16,9**
Xiao	Sampling 1	Parallel 1b	1-1-b	0,068	0,066	0,067				**3,034**	70,5	61,7	66,1				**13,4**
		Parallel 1c	1-1-c	0,081	0,080	0,081	0,074			**1,880**	92,4	77,9	85,1	75,610			**16,9**
	Sampling 2	Paralel 2a	2-1-a	0,340	0,364	0,352			**1,137**	**6,776**	498,0	418,2	458,1			**1,144**	**17,4**
		Paralel 2b	2-1-b	0,016	0,016	0,016			**0,741**	**2,107**	17,8	16,1	16,9			**0,709**	**10,1**
		Paralel 2c	2-1-c	0,074	0,081	0,078	0,149	0,111	**0,396**	**8,527**	88,7	75,6	82,1	185,705	130,658	**0,435**	**16,0**
Fish Pond	Sampling 1	Parallel 1b	C-1-7-b	0,243	0,255	0,249				**4,591**	262,5	251,6	257,0				**4,2**
		Parallel 1c	C-1-7-c	0,142	0,140	0,141	0,195			**0,987**	164,9	163,3	164,1	210,568			**0,9**
	Sampling 2	Parallel 2a	C-2-7-a	0,228	0,224	0,226			**0,951**	**2,023**	277,4	264,7	271,0			**0,915**	**4,7**
		Parallel 2b	C-2-7-b	0,192	0,204	0,198			**0,092**	**5,836**	234,6	229,6	232,1			**0,152**	**2,2**
		Parallel 2c	C-2-7-c	0,151	0,171	0,161	0,195	0,195	**1,043**	**11,932**	169,7	170,1	169,9	224,358	217,463	**1,067**	**0,2**
Abandoned Fish Pond	Sampling 1	Parallel 1b	1-7-b	0,596	0,596	0,596				**0,014**	621,0	600,8	610,9				**3,3**
		Parallel 1c	1-7-c	0,539	0,528	0,533	0,565			**2,005**	575,6	528,2	551,9	581,365			**8,6**
	Sampling 2	Parallel 2a	2-7-a	0,315	0,314	0,315			**0,924**	**0,554**	356,9	350,2	353,6			**0,928**	**1,9**
		Parallel 2b	2-7-b	0,541	0,596	0,568			**1,062**	**9,694**	663,9	644,2	654,1			**1,059**	**3,0**
		Parallel 2c	2-7-c	0,407	0,423	0,415	0,433	0,499	**0,138**	**3,997**	480,6	467,9	474,2	493,952	537,658	**0,131**	**2,7**
Yuqiao Reservoir	Upper Depth	Parallel 1a	D-1-a	0,001	0,004	0,003			**0,845**	**151,456**	2,4	8,1	5,3			**0,565**	**107,8**
		Parallel 1b	D-1-b	0,004	0,009	0,006			**0,260**	**70,046**	2,1	8,3	5,2			**0,590**	**118,1**

		Parallel 1c	D-1-c	0,018	0,013	0,015	0,008		**1,104**	**36,225**	7,9	15,8	11,9	7,449		**1,155**	**66,9**
	Middle Depth	Parallel 2a	D-2-a	0,012	0,012	0,012			**1,047**	**2,478**	11,9	17,5	14,7			**0,986**	**38,7**
		Parallel 2b	D-2-b	0,020	0,024	0,022			**0,101**	**16,292**	21,2	25,9	23,5			**0,028**	**20,1**
		Parallel 2c	D-2-c	0,030		0,030	0,021		**0,946**	**200,000**	29,9	36,4	33,2	23,802		**1,014**	**19,4**
	Deeper Depth	Parallel 3a	D-3-a	0,003	0,002	0,003			**0,251**	**69,896**	-0,5	5,0	2,2			**0,789**	**242,9**
		Parallel 3b	D-3-b	0,002	0,006	0,004			**1,102**	**112,420**	-0,8	4,7	1,9			**0,335**	**286,5**
		Parallel 3c	D-3-c	-0,003	0,002	0,002	0,003		**0,850**	**-1379,948**	-3,1	5,1	1,0	1,723		**1,125**	**835,6**